

# UC Riverside

## UC Riverside Electronic Theses and Dissertations

### Title

Characterizing the Molecular Arsenal of Insect-Parasitic Nematodes

### Permalink

<https://escholarship.org/uc/item/6hj593g2>

### Author

Chang, Dennis Zaaj

### Publication Date

2019

### Copyright Information

This work is made available under the terms of a Creative Commons Attribution-NonCommercial-NoDerivatives License, available at <https://creativecommons.org/licenses/by-nc-nd/4.0/>

Peer reviewed|Thesis/dissertation

UNIVERSITY OF CALIFORNIA  
RIVERSIDE

Characterizing the Molecular Arsenal of Insect-Parasitic Nematodes

A Dissertation submitted in partial satisfaction  
of the requirements for the degree of

Doctor of Philosophy

in

Cell, Molecular, and Developmental Biology

by

Dennis Chang

December 2019

Dissertation Committee:

Dr. Adler R. Dillman, Chairperson

Dr. Michael E. Adams

Dr. Sarjeet Gill

Copyright by  
Dennis Chang  
2019

The Dissertation of Dennis Chang is approved:

---

---

---

Committee Chairperson

University of California, Riverside

## **Acknowledgments**

The text of this dissertation, in part or in full, is a reprint of the material as it appears in Chang Dennis Z., Serra Lorraine, Lu Dihong, Mortazavi Ali, Dillman Adler R., May 1st, 2019. The co-author Adler R. Dillman listed in that publication directed and supervised the research which forms the basis for this dissertation.

Co-authors contributions:

Lorraine Serra: Conceptualization, Data curation, Formal analysis, Investigation, Methodology, Writing – original draft

Dihong Lue: Conceptualization, Formal analysis, Investigation, Methodology, Supervision, Writing – original draft, Writing – review & editing

Ali Mortazavi: Conceptualization, Formal analysis, Investigation, Methodology, Project administration, Supervision, Writing – original draft, Writing – review & editing

Adler R. Dillman: Conceptualization, Data curation, Formal analysis, Funding acquisition, Investigation, Methodology, Project administration, Supervision, Writing – original draft, Writing – review & editing

## ABSTRACT OF THE DISSERTATION

Characterizing the Molecular Arsenal of Insect-Parasitic Nematodes

by

Dennis Chang

Doctor of Philosophy, Graduate Program in Cell, Molecular, and Developmental  
Biology

University of California, Riverside, December 2019

Dr. Adler R. Dillman, Chairperson

Entomopathogenic nematodes (EPNs) are insect-parasitic nematodes that rapidly kill insects and have been used for biocontrol of insect pests. The symbiotic bacteria that these EPNs carry have traditionally been thought to be the only source of virulence, however, we have shown substantial proof that these nematodes do actively contribute to killing the insect-host. We show that EPNs from the genus *Steinernema* release excreted-secreted proteins (ESPs) at the early stages of infecting a host and these ESPs are toxic to insects. This paradigm shift in the EPN field merited further exploration into the mechanisms of toxicity of the nematode derived ESPs. Profiling of the ESPs revealed a complex mixture of proteins predicted to be involved in tissue damage and host immune modulation. Many of these proteins were also found to be highly similar to proteins used by vertebrate parasites. We found a core suite of proteins utilized by two *Steinernema* species of EPNs at the early stages of infection indicating these proteins have a central and important role in insect-parasitology and potentially vertebrate-parasitology as well. We continue to identify candidate

active proteins in the ESPs of *Steinernema feltiae* and produce these proteins for characterization.

## I. TABLE OF CONTENTS

Abstract.....	
I Table of contents.....	
II List of Figures.....	
III List of Tables.....	
IV Abbreviations.....	

### CHAPTER 1

<b>Introduction to EPNs and .....</b>	<b>1</b>
Crops loss and Bt .....	1
EPN classification & life-process .....	1
Bacterial symbiosis.....	3
EPNs as active contributors.....	3
References .....	5

### CHAPTER 2

<b>A core set of venom proteins is released by entomopathogenic nematodes in the genus <i>Steinernema</i>.....</b>	<b>9</b>
Abstract .....	10
Introduction.....	11
Results.....	14
<i>Steinernematids initiate active parasitism when exposed to host tissue.....</i>	<i>14</i>
<i>Activated Steinernema IJs release toxic proteins into their hosts.....</i>	<i>17</i>
<i>Comparative transcriptome analysis of in vitro and in vivo activated S. feltiae IJs reveals a core set of genes expressed at 6 hours after activation.....</i>	<i>20</i>
<i>Protein components of Steinernema ESPs .....</i>	<i>24</i>
<i>Comparison of S. feltiae and S. carpocapsae secreted venom proteins reveals a small set of conserved catalytic enzymes .....</i>	<i>27</i>
Discussion .....	31
Methods.....	44
References .....	61

### CHAPTER 3

<b>Identification, production, and characterization of <i>S. feltiae</i> individual candidate active proteins.....</b>	<b>72</b>
Introduction.....	72
Results.....	74
<i>ESP components are more than just toxic.....</i>	<i>74</i>
<i>Separation of crude ESPs reveals a complex toxic fraction.....</i>	<i>76</i>
<i>Enriched proteins as candidates.....</i>	<i>76</i>
<i>Expression of EPN proteins in a bacterial system.....</i>	<i>78</i>
<i>A serine protease highly enriched in the ESP of S. feltiae.....</i>	<i>70</i>
Discussion .....	83
Methods.....	86

Supplemental Information/Figures .....	91
References .....	92
<b>CHAPTER 4</b>	
<b>Adapting the Smart-seq2 Protocol for Robust Single Worm RNA-seq.....</b>	<b>95</b>
Abstract .....	96
Introduction.....	96
Materials .....	104
Methods.....	108
References .....	126
<b>CHAPTER 5</b>	
<b>Conclusions and Final Remarks .....</b>	<b>129</b>
<i>Steinernema</i> IJs actively contribute to host-killing .....	129
A core suite of ESP components shared by Steinernematids .....	130
<i>Steinernema</i> ESPs are both toxic and immunomodulatory.....	132
EPN virulence molecules and implications in agricultural pest control .....	133
References .....	134

## II. LIST OF FIGURES

<b>CHAPTER 1</b>	
Figure 1. The EPN life process.....	2
<b>CHAPTER 2</b>	
Figure 2. Activation of <i>S. feltiae</i> IJs .....	16
<b>CHAPTER 2</b>	
Figure 3. <i>Steinernema</i> IJs release toxic proteins.....	18
<b>CHAPTER 2</b>	
Figure 4. Genes differentially expressed during <i>in vitro</i> and <i>in vivo</i> IJ activation .....	21
<b>CHAPTER 2</b>	
Figure 5. Protein components of <i>S. feltiae</i> and <i>S. carpocapsae</i> .....	25
<b>CHAPTER 2</b>	
Figure 6. Gene expression of <i>S. feltiae</i> venom proteins <i>in vitro</i> and <i>in vivo</i> and comparison with <i>S. carpocapsae</i> .....	29
<b>CHAPTER 3</b>	
Figure 7. Fractionation of crude ESP from <i>S. feltiae</i> and toxic fractions.....	75
<b>CHAPTER 3</b>	
Figure 8. Protein composition of the toxic fraction compared to crude .....	77
<b>CHAPTER 3</b>	
Figure 9. Expression of candidate active proteins .....	79
<b>CHAPTER 3</b>	
Figure 10. Washing of inclusion bodies and Activity of serine protease Sf-Tryp .....	82
<b>CHAPTER 3</b>	
Figure 11. Supplemental: Optimization of protein expression induction time. .	91
<b>CHAPTER 4</b>	
Figure 12. SMART-Seq2 principles and workflow .....	98
<b>CHAPTER 4</b>	
Figure 13. Isolation and cutting of individual nematodes. ....	110
<b>CHAPTER 4</b>	
Figure 14. Example bioanalyzer profiles of amplified DNA quality.....	115
<b>CHAPTER 4</b>	
Figure 15. Example BioAnalyzer profiles of DNA library quality. ....	120
<b>CHAPTER 4</b>	
Figure 16. Galaxy web-interface displaying RNA-seq analysis.....	123

### III. LIST OF TABLES

#### CHAPTER 3

Table 1. Enrichment of protein in the toxic fraction compared to crude ..... 78

#### CHAPTER 4

Table 2. Indexing Primers..... 107

#### IV. ABBREVIATIONS

**(EPN)** Entomopathogenic nematodes

**(IJ)** Infective juvenile

**(Bt)** *Bacillus thuringiensis*

**(ESP)** Excreted-Secreted Proteins

**(M, mM or  $\mu$ M)** Molar, Millimolar, or micromolar respectively

**(g, mg,  $\mu$ g, or ng)** Gram, Milligram, Microgram, or Nanogram

**(L, mL or  $\mu$ L)** Liter, milliliter, and microliter respectively

**(ANOVA)** Analysis of Variance- a statistical test

**(PCR)** polymerase chain reaction

**(ns)** not significant

## CHAPTER 1

### Introduction

Estimates of worldwide crop loss due to arthropod pests range from 15-26% exceeding \$470 billion [1-3] and even with increased use of pesticides in the last 40 years crop loss as not significantly reduced [2]. Along with this, the increase in understanding of the dangers of many traditional synthetic pesticides on the environment and health of non-target animals, including humans, there is a need to look for safer alternative pest control. Genetic engineering including the advent of Bt-crops (crops genetically modified to produce the toxin from *Bacillus thuringiensis* bacteria) [4] has helped reduce the use of pesticides by about 35% [2]. However, resistance to the Bt toxin has already been reported and is expected to increase over time [5-7]. Research to improve the efficacy of current Bt toxins are underway [8, 9] however it is also important to continue developing pest control technologies and new molecules as alternatives or to work in adjunct with Bt.

EPNs (entomopathogenic nematodes) are insect-killing parasites that have been utilized for biocontrol of insect pests and can serve as a potential source of virulent molecules for development of insect pest-killing/deterrent technologies. EPNs are named for their entomopathogenic life-style (killing of the insect host by introduction of insect-pathogenic bacteria) contrasting other forms of nematode-arthropod associations such as phoretic (transport of the nematode by

the insect), necromenic (waiting until the host dies to feed/reproduce), and larval parasitic (a larval form of the nematode feeds on the host eventually causing death)[10, 11]. Nematodes generally can be classified as EPNs if they satisfy these criteria: 1) host of entomopathogenic bacteria by the alternative 3rd larval stage called the infective juvenile (IJ), 2) active host-seeking and infection into the host by the IJ, 3) release of the pathogenic bacteria, 4) death of the host within 5 days and reproduction of the nematode, 5) reassociation of the bacteria with the nematode, and 6) emergence of the nematode to seek out a new host [11-13]. Figure 1 illustrates the propagation of EPNs [14].

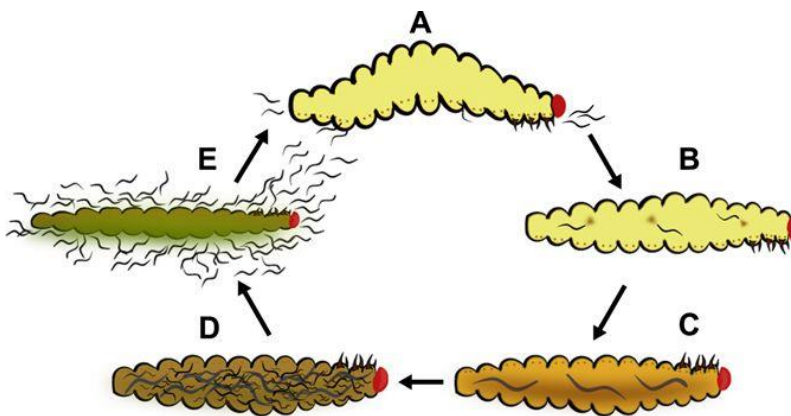


**Figure 1: The EPN life cycle.** (A) An insect host, typically a larva is infected. (B) Once inside the the EPNs release their symbiotic bacteria. (C) The host dies while the nematodes develop. (D) The nematodes will reproduce and feed on the cadaver for multiple generations until resources run out and nematodes will emerge (E) to seek out a new host.

There are at least 3 genera of EPNs; 1) *Steinernema* 2) *Heterorhabditis* and 3) *Oscheius*. Certain nematodes from the genus *Oscheisu* have only been recently described as potential EPNs while *Steinernema* (first described as early as the 1920s [15, 16]) and *Heterorhabditis* (first described in the 1970s [17, 18]) have been called 'entomopathogenic nematodes' since the early 1980s [19-21].

*Steinernema* and *Heterorhabditis* nematodes have been favored for study/use in biological control due to their general wide range of hosts, short time to death (typically within 48 hours), and scalability in mass production [11, 13, 22-27]. Though EPNs have been developed and commercialized in both large-scale agriculture and home gardening settings their lack of consistent efficacy has limited their wide adaptation [23, 28-30]. Further study into the mechanisms of EPN-derived pathogenicity may increase the potential to improve EPN efficacy in biocontrol of pests.

*Steinernema* nematodes generally associate with bacteria from the genus *Xenorhabdus* [18] and *Heterorhabditis* nematodes generally associate with bacteria from the genus *Photorhabdus* [17]. A wide assumption in the field of EPNs is that bacteria are the only source of virulence and cause of host, death while the nematode simply vectors the bacteria [13, 22, 31]. While this seems applicable to *Heterorhabditis* [32], there is growing evidence that *Steinernema* nematodes may contribute some level of virulence against the insect host. Part of this data includes a study reporting that an individual *S. carpocapsae* IJ was able to kill a pine weevil (*Hylobius abietis*) larva [33]. This is interesting in the fact that *S. carpocapsae* IJs typically carry only 20-200 cells of its bacterial symbiont (*Xenorhabdus nematophila*) and the LD50 of *X. nematophila* in the pine weevil is around 3500 cells [33]. Other studies have reported that axenic *S. carpocapsae*

IJs were able to infect and kill insect hosts [32, 34, 35]. Lastly, cell-free culture media used to grow *S. carpocapsae* exhibited toxicity effects in insects [36-38].

These reports merit the idea that EPN IJs from the genus *Steinernema* could potentially be more than just vectors and actively contribute to virulence against the insect host. In this dissertation, I will be describing my work on characterizing the molecular arsenal of EPNs from the genus *Steinernema*. This work will hopefully provide new information and insight to support the development of biocontrol and biotechnology for agricultural pest control.

## References

1. Culliney TW. Crop Losses to Arthropods. In: Pimentel D, Peshin R, editors. *Integrated Pest Management: Pesticide Problems, Vol3*. Dordrecht: Springer Netherlands; 2014. p. 201-25.
2. Oerke EC. Crop losses to pests. *The Journal of Agricultural Science*. 2006;144(1):31-43. Epub 2005/12/09. doi: 10.1017/S0021859605005708.
3. Mitchell C, Brennan RM, Graham J, Karley AJ. Plant Defense against Herbivorous Pests: Exploiting Resistance and Tolerance Traits for Sustainable Crop Protection. *Frontiers in Plant Science*. 2016;7(1132). doi: 10.3389/fpls.2016.01132.
4. Vaeck M, Reynaerts A, Höfte H, Jansens S, De Beuckeleer M, Dean C, et al. Transgenic plants protected from insect attack. *Nature*. 1987;328(6125):33-7. doi: 10.1038/328033a0.
5. Tabashnik BE, Brevault T, Carriere Y. Insect resistance to Bt crops: lessons from the first billion acres. *Nat Biotechnol*. 2013;31(6):510-21. doi: 10.1038/nbt.2597. PubMed PMID: WOS:000320113200022.
6. Ferre J, Van Rie J. Biochemistry and genetics of insect resistance to *Bacillus thuringiensis*. *Annu Rev Entomol*. 2002;47:501-33. doi: 10.1146/annurev.ento.47.091201.145234. PubMed PMID: WOS:000173421900017.
7. Wei JZ, Zhang YL, An SH. The progress in insect cross-resistance among *Bacillus thuringiensis* toxins. *Arch Insect Biochem Physiol*. 2019;102(3):15. doi: 10.1002/arch.21547. PubMed PMID: WOS:000490165800005.
8. Deist BR, Rausch MA, Fernandez-Luna MT, Adang MJ, Bonning BC. Bt toxin modification for enhanced efficacy. *Toxins (Basel)*. 2014;6(10):3005-27. doi: 10.3390/toxins6103005. PubMed PMID: 25340556.
9. Marques LH, Santos AC, Castro BA, Moscardini VF, Rosseto J, Silva OABN, et al. Assessing the Efficacy of *Bacillus thuringiensis* (Bt) Pyramided Proteins Cry1F, Cry1A.105, Cry2Ab2, and Vip3Aa20 Expressed in Bt Maize Against Lepidopteran Pests in Brazil. *Journal of Economic Entomology*. 2018;112(2):803-11. doi: 10.1093/jee/toy380.
10. Sudhaus W. Evolution of insect parasitism in rhabditid and diplogastrid nematodes. *Advances in Arachnology and Developmental Biology*. 2008:143-61.

11. Dillman AR, Chaston JM, Adams BJ, Ciche TA, Goodrich-Blair H, Stock SP, et al. An Entomopathogenic Nematode by Any Other Name. PLoS Pathog. 2012;8(3):4. doi: 10.1371/journal.ppat.1002527. PubMed PMID: WOS:000302225600003.
12. Chaston J, Goodrich-Blair H. Common trends in mutualism revealed by model associations between invertebrates and bacteria. FEMS Microbiology Reviews. 2010;34(1):41-58. doi: 10.1111/j.1574-6976.2009.00193.x.
13. Kaya HK, Gaugler R. Entomopathogenic Nematodes. Annu Rev Entomol. 1993;38:181-206. doi: 10.1146/annurev.en.38.010193.001145. PubMed PMID: WOS:A1993KF69700009.
14. Baiocchi T, Lee G, Choe D-H, Dillman AR. Host seeking parasitic nematodes use specific odors to assess host resources. Sci Rep. 2017;7(1):6270. doi: 10.1038/s41598-017-06620-2.
15. Poinar GO, Jr., Grewal PS. History of entomopathogenic nematology. J Nematol. 2012;44(2):153-61. PubMed PMID: 23482453.
16. Steiner G. *Neoaplectana glaseri*, n.g., n.sp. (Oxyuridae), a new nematode parasite of the Japanese beetle (*Popillia japonica* Newm.). Journal of the Washington Academy of Sciences. 1929;19(19):436-40.
17. George OP. Description and Biology of a New Insect Parasitic Rhabditoid, *Heterorhabditis* Bacteriophora N. Gen., N. Sp. (Rhabditida; Heterorhabditidae N. Fam.). Nematologica. 1975;21(4):463-70. doi: <https://doi.org/10.1163/187529275X00239>.
18. THOMAS GM, POINAR GO. *Xenorhabdus* gen. nov., a Genus of Entomopathogenic, Nematophilic Bacteria of the Family Enterobacteriaceae. International Journal of Systematic and Evolutionary Microbiology. 1979;29(4):352-60. doi: <https://doi.org/10.1099/00207713-29-4-352>.
19. Spiridonov SE. Auxiliary excretory system of an entomopathogenic nematode *Heterorhabditis* bacteriophora (Rhabditida). Zoologicheskii zhurnal. 1981;v. 60(12).
20. Akhurst RJ. *Xenorhabdus* nematophilus subsp. beddingii (Enterobacteriaceae): A New Subspecies of Bacteria Mutualistically Associated with Entomopathogenic Nematodes. International Journal of Systematic and Evolutionary Microbiology. 1986;36(3):454-7. doi: <https://doi.org/10.1099/00207713-36-3-454>.

21. Gaugler R. Ecological considerations in the biological control of soil-inhabiting insects with entomopathogenic nematodes. *Agriculture, Ecosystems & Environment*. 1988;24(1):351-60. doi: [https://doi.org/10.1016/0167-8809\(88\)90078-3](https://doi.org/10.1016/0167-8809(88)90078-3).
22. Grewal PS, Lewis EE, Gaugler R. Response of infective stage parasites (Nematoda: *Steinernematidae*) to volatile cues from infected hosts. *J Chem Ecol*. 1997;23(2):503-15. doi: Doi 10.1023/B:Joec.0000006374.95624.7e. PubMed PMID: ISI:A1997WR84600018.
23. Georgis R, Koppenhofer AM, Lacey LA, Belair G, Duncan LW, Grewal PS, et al. Successes and failures in the use of parasitic nematodes for pest control. *Biol Control*. 2006;38(1):103-23. doi: 10.1016/j.biocontrol.2005.11.005. PubMed PMID: WOS:000238596600008.
24. Stock SP, Koppenhofer AM. *Steinernema scarabaei* n. sp (Rhabditida : *Steinernematidae*), a natural pathogen of scarab beetle larvae (Coleoptera : Scarabaeidae) from New Jersey, USA. *Nematology*. 2003;5:191-204. doi: 10.1163/156854103767139680. PubMed PMID: WOS:000184809500004.
25. Shapiro-Ilan D. Entomopathogenic nematology: CABI; 2002. Available from: <https://www.cabi.org/cabebooks/ebook/20023023458>.
26. Andrea T-B, Weimin Y, Yasmin C. *Oscheius carolinensis* n. sp. (Nematoda: Rhabditidae), a potential entomopathogenic nematode from vermicompost. *Nematology*. 2010;12(1):121-35. doi: <https://doi.org/10.1163/156854109X458464>.
27. Stock SP, Goodrich-Blair H. Chapter XII - Nematode parasites, pathogens and associates of insects and invertebrates of economic importance. In: Lacey LA, editor. *Manual of Techniques in Invertebrate Pathology (Second Edition)*. San Diego: Academic Press; 2012. p. 373-426.
28. Nguyen KB, Smart GC. PRELIMINARY STUDIES ON SURVIVAL OF *STEINERNEMA-SCAPTERISCI* IN SOIL. *Soil Crop Sci Soc Fla Proc*. 1990;49:230-3. PubMed PMID: WOS:A1990DU57400056.
29. Parkman JP, Frank JH, Nguyen KB, Smart GCJ. Inoculative Release of *Steinernema scapterisci* (Rhabditida: *Steinernematidae*) to Suppress Pest Mole Crickets (Orthoptera: Gryllotalpidae) on Golf Courses. *Environmental Entomology*. 1994;23(5):1331-7. doi: 10.1093/ee/23.5.1331.

30. Shapiro-Ilan DI, Gouge D, Koppenhofer AM. Factors affecting commercial success: case studies in cotton, turf, and citrus. *Entomopathogenic Nematology*. 2002;333-55.
31. Goodrich-Blair H. They've got a ticket to ride: *Xenorhabdus nematophila*-*Steinernema carpocapsae* symbiosis. *Curr Opin Microbiol*. 2007;10(3):225-30. doi: 10.1016/j.mib.2007.05.006. PubMed PMID: WOS:000248036200005.
32. Han RC, Ehlers RU. Pathogenicity, development, and reproduction of *Heterorhabditis bacteriophora* and *Steinernema carpocapsae* under axenic *in vivo* conditions. *J Invertebr Pathol*. 2000;75(1):55-8. doi: 10.1006/jipa.1999.4900. PubMed PMID: WOS:000085395100009.
33. Pye AE, Burman M. *Neoaplectana carpocapsae*: infection and reproduction in large pine weevil larvae, *Hylobius abietis*. *Exp Parasitol*. 1978;46(1):1-11. doi: 10.1016/0014-4894(78)90151-0. PubMed PMID: WOS:A1978FY72800001.
34. Poinar GO, Thomas GM. Significance of *Achromobacter nematophilus* Poinar and Thomas (Achromobacteraceae - Eubacteriales) in Development of Nematode DD-136 (*Neoaplectana* sp *Steinernematidae*). *Parasitology*. 1966;56:385-&. PubMed PMID: WOS:A19667764600015.
35. Sicard M, Le Brun N, Pages S, Godelle B, Boemare N, Moullia C. Effect of native *Xenorhabdus* on the fitness of their *Steinernema* hosts: contrasting types of interaction. *Parasitol Res*. 2003;91(6):520-4. doi: 10.1007/s00436-003-0998-z. PubMed PMID: WOS:000187993700016.
36. Burman M. *Neoaplectana carpocapsae*: Toxin production by axenic Insect Parasitic Nematodes. *Nematologica*. 1982;28(1):62-70. PubMed PMID: WOS:A1982PU84500006.
37. Walter TN, Dunphy GB, Mandato CA. *Steinernema carpocapsae* DD136: Metabolites limit the non-self adhesion responses of haemocytes of two lepidopteran larvae, *Galleria mellonella* (*F. Pyralidae*) and *Malacosoma disstria* (*F. Lasiocampidae*). *Exp Parasitol*. 2008;120(2):161-74. doi: 10.1016/j.exppara.2008.07.001. PubMed PMID: WOS:000259659600006.
38. Lu DH, Macchietto M, Chang D, Barros MM, Baldwin J, Mortazavi A, et al. Activated entomopathogenic nematode infective juveniles release lethal venom proteins. *PLoS Pathog*. 2017;13(4):31. doi: 10.1371/journal.ppat.1006302. PubMed PMID: WOS:000402555700018.

## CHAPTER 2

### **A core set of venom proteins is released by entomopathogenic nematodes in the genus *Steinernema***

Dennis Z. Chang<sup>1</sup>, Lorryne Serra<sup>2</sup>, Dihong Lu<sup>1</sup>, Ali Mortazavi<sup>2</sup>, and Adler R. Dillman<sup>1\*</sup>

<sup>1</sup>Department of Nematology, University of California, Riverside, California 92521, USA

<sup>2</sup>Department of Entomology, University of California, Riverside, California 92521, USA

\*Correspondence to [adlerd@ucr.edu](mailto:adlerd@ucr.edu)

A version of this chapter is available online where supplemental figures and tables can be found.

Chang DZ, Serra L, Lu D, Mortazavi A, Dillman AR. A core set of venom proteins is released by entomopathogenic nematodes in the genus *Steinernema*. PLoS Pathog. 2019;15(5):e1007626. doi: 10.1371/journal.ppat.1007626.

## Abstract

Parasitic helminths release molecular effectors into their hosts and these effectors can directly damage host tissue and modulate host immunity. Excreted/secreted proteins (ESPs) are one category of parasite molecular effectors that are critical to their success within the host. However, most studies of nematode ESPs rely on *in vitro* stimulation or culture conditions to collect the ESPs, operating under the assumption that *in vitro* conditions mimic actual *in vivo* infection. This assumption is rarely if ever validated. Entomopathogenic nematodes (EPNs) are lethal parasites of insects that produce and release toxins into their insect hosts and are a powerful model parasite system. We compared transcriptional profiles of individual *Steinernema feltiae* nematodes at different time points of activation under *in vitro* and *in vivo* conditions and found that some but not all time points during *in vitro* parasite activation have similar transcriptional profiles with nematodes from *in vivo* infections. These findings highlight the importance of experimental validation of ESP collection conditions. Additionally, we found that a suite of genes in the neuropeptide pathway were downregulated as nematodes activated and infection progressed *in vivo*, suggesting that these genes are involved in host-seeking behavior and are less important during active infection. We then characterized the ESPs of activated *S. feltiae* infective juveniles (IJs) using mass spectrometry and identified 266 proteins that are released by these nematodes. In comparing these ESPs with

those previously identified in activated *S. carpocapsae* IJs, we identified a core set of 52 proteins that are conserved and present in the ESPs of activated IJs of both species. These core venom proteins include both tissue-damaging and immune-modulating proteins, suggesting that the ESPs of these parasites include both a core set of effectors as well as a specialized set, more adapted to the particular hosts they infect.

## **Introduction**

Parasitic nematodes continue to be a major source of mortality and morbidity worldwide, infecting nearly 25% of the global population [1, 2]. The molecules that are released by these parasites, including the excreted/secreted proteins (ESPs), represent the major interface between hosts and parasites, and directly influence the survival and health of the parasites as well as the pathology they cause to the hosts [3, 4]. Despite an abundance of studies addressing mechanistic aspects of host immune response to nematode parasites, there is a distinct paucity of molecular information about most parasitic nematodes, where few secreted molecules have been studied in detail. Further, the role of the parasite ESP composition in determining host specificity is unknown. What is known relies largely on ESP studies where release of the ESPs is stimulated and collected *in vitro*. An underlying assumption is that the ESPs collected under these conditions are relevant and similar to the ESPs released in *in vivo* infections, though this assumption has not been experimentally validated for

most if not all such studies [3]. Obtaining enough ESPs from nematodes that are actively involved in a host infection for subsequent analysis is difficult if not impossible. However, sequencing the transcriptomes of individual nematodes [5, 6], provides a way of comparing transcriptional profiles of parasites undergoing *in vitro* activation and *in vivo* infection.

Entomopathogenic nematodes (EPNs) are parasites of insects that rapidly kill their hosts. When EPNs deplete host nutrients the developing generation emerges from the cadaver as infective juveniles (IJs), an alternative third-stage larval form (L3) that is developmentally arrested, similar to the dauer juvenile stage in *C. elegans* [7]. The IJs are the only free-living stage of these nematodes, and they actively seek hosts to infect [8, 9]. Upon entering a new host, the IJs undergo the process of activation, or recovery from dauer, which entails resumption of growth and development, along with changes in morphology and gene expression that facilitate transition from a free-living form to an actively parasitic form [5, 10–12].

EPNs are being used as models for host-parasite interactions including ecology [13, 14], host-seeking behavior [9, 15], neurobiology [8], parasite activation [5, 16, 17], and the role of secreted products in parasitism [5, 18, 19]. There are more than 70 described species of EPNs in the genus *Steinernema*, and these vary in their host range and specificity [20, 21], making these nematodes a

potential model for understanding the evolution of ESPs and their role in niche partitioning among parasites. For example, *S. carpocapsae* is a generalist parasite capable of infecting more than 250 different species of insects from at least 13 orders [22, 23], while other species such as *S. scapterisci* and *S. scarabaei* are specialist parasites infecting a much narrower range of species [24, 25]. A recent study of the *S. carpocapsae* secretome found that this generalist parasite releases more than 450 different proteins when initiating active parasitism. Many of these proteins were hypothesized to be involved in tissue damage and immunosuppression of the host [5]. *S. feltiae* is another generalist EPN parasite but with a more limited host range than *S. carpocapsae* and in a different clade within *Steinernema* [26, 27]. Several studies have shown that *S. feltiae* IJs use their cuticle to suppress and evade host immunity [28–30]. It has even been postulated that unlike *S. carpocapsae*, *S. feltiae* does not use secretion processes or secreted proteins to induce host immunosuppression [31].

Here we utilized RNA-seq from individual *S. feltiae* nematodes throughout a time course of *in vitro* and *in vivo* activation to compare the induction of ESPs under these different conditions. We reported the secretome of *S. feltiae* and tested its activity *in vivo*. We showed that activated *S. feltiae* IJs release a variety of proteins likely involved in tissue damage as well as immune modulation. By analyzing the *in vivo* time course of activation, we identified putative neuropeptide pathway genes likely to be involved in host-seeking behavior as the

expression of these genes decreased as the nematodes is activated. Further, using comparative analysis we identified a core suite of 52 ESPs released by both *S. feltiae* and *S. carpocapsae* during active parasitism, indicating that despite differences in host range and specificity, some proteins may be broadly useful in parasitizing insect hosts. Most of these core proteins are conserved in nematode parasites of mammals, suggesting that they have an important and conserved role in parasitism.

## Results

### ***Steinernematids* initiate active parasitism when exposed to host tissue**

We utilized an *in vitro* activation method previously used for *S. carpocapsae* and *S. scapterisci* [5, 17] to determine how *S. feltiae* IJs activate. We exposed *S. feltiae* IJs to insect homogenate and found that they activated in a manner similar to what has been described for *S. carpocapsae* and *S. scapterisci* (Fig 2).

Expansion of the pharyngeal bulb was found to be a reliable indicator of IJ activation [5, 16, 17] and this feature was used to quantify activation. In naïve IJs (IJs not exposed to host tissue) the pharyngeal bulb is often difficult to observe at 400x magnification (Fig 2A). At 1000x magnification (Fig 2B) the pharyngeal bulb can be seen, however the bulb is typically more compressed, seemingly deflated, when compared to activated nematodes. As IJs are exposed to host tissue over time they begin exhibiting partially-activated morphology characterized by partial expansion of the pharyngeal bulb (Fig 2D) which, in contrast to naïve IJs, is more

expanded and can be readily observed at 400x (Fig 2C). These differences allow us to quickly and efficiently differentiate between non-activated and activated IJs under 400x magnification. After 6 hours of exposure to insect tissue, approximately 25% of IJs exhibit fully activated morphology with full expansion of the pharyngeal bulb, which is wider and appears rounder than the oval shape of partially activated nematodes (Fig 2F and 2D). Similar to what was observed for *S. carpocapsae*, *S. feltiae* exhibits high levels of activation (combined partial and full activation) after only 6 hours of exposure to host tissues (Fig 2G). However, *S. feltiae* IJs exhibited a higher percentage of fully activated morphology (approx. 25%) compared to *S. carpocapsae* (approx. 15%) at 6 hours. And while both species displayed time-dependent increase in activation rates, *S. feltiae* activation rates were often higher than *S. carpocapsae* with significantly higher full activation rates after 6, 24, and 30 hours of exposure (Fig 2G, S1 Table).

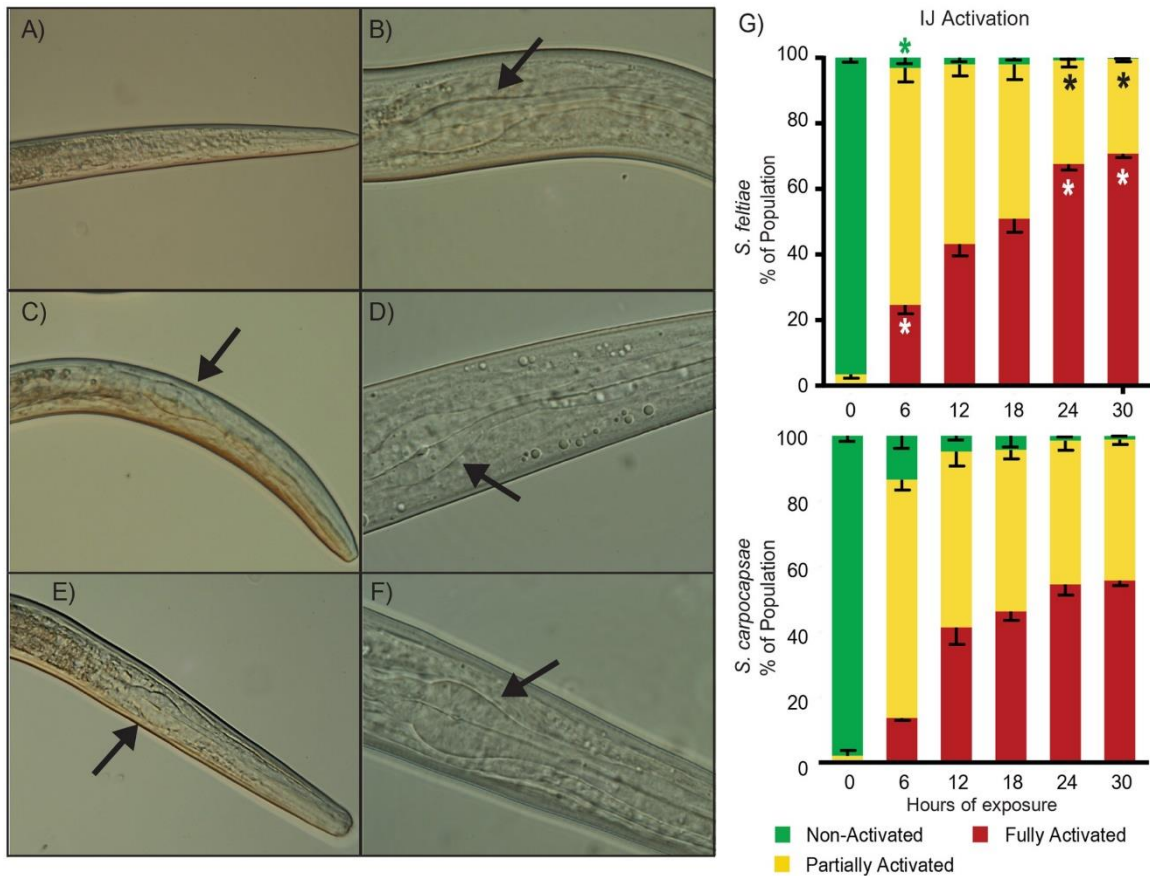


**Figure 2. Activation of *S. feltiae* IJs.** The left panel images are representative images of the head region of *S. feltiae* IJs exhibiting (A) naïve, (C) partially activated, and (E) fully activated morphology (400x). The pharyngeal bulb, if observable, is indicated by a black arrow. The right panel images are 1000x representative images of the *S. feltiae* IJs exhibiting activation morphology corresponding to the left panel images with (B) naïve, (D) partially activated, and (F) fully activated. (G) Time course activation rates based on activation morphology of IJs exposed to insect homogenate for 0, 6, 12, 18, 24, and 30 hours. All activation rate data was taken from IJs observed under 400x. The top graph is of *S. feltiae* activation and bottom graph is of *S. carpocapsae* activation (*S. carpocapsae* activation was reproduced from Lu. et al, 2017 with the addition of a 0-hour time point). Stars in the columns of the *S. feltiae* activation graph indicates a significant difference with  $p < 0.05$  between *S. feltiae* and *S. carpocapsae* rates of the same category (e.g. *S. feltiae* 6 hr full activation compared to *S. carpocapsae* 6 hr full activation, data in S1 Table). Column bars represent the mean with error bars representing standard deviation. Statistical analysis was done using a repeated measures two-way ANOVA with Sidak's multiple comparisons test.

### **Activated *Steinernema* IJs release toxic proteins into their hosts**

After determining the activation dynamics of *S. feltiae* IJs, we collected the ESPs of activated *S. feltiae* IJs to determine their effect in insects. *S. feltiae* IJs were activated in insect homogenate for 0, 6, 12, 18, 24, or 30 hours, washed to remove the insect homogenate, and incubated in PBS for 3 hours where they continued releasing ESPs. The PBS (with accumulated ESPs) was then filtered through a 0.22  $\mu\text{m}$  filter to remove the IJs and concentrated for further experiments. The relative age of all the ESPs were the same; at most, they were 3 hours old. We found that the profile of *S. feltiae* ESPs changed over time with proteins between 25 and 37 kDa being consistently present from 6–30 hours while proteins between 37–75 kDa peaked at 12 hours and diminished in abundance thereafter (Fig 3A). There was an overall time-dependent decrease in proteins released by *S. feltiae* (S1 Fig). Comparing the protein band profiles of *S. feltiae* and *S. carpocapsae* ESPs side-by-side shows that the majority of *S. feltiae* ESPs are between 25 and 75 kDa while *S. carpocapsae* ESPs are more concentrated in a narrower size range, between 25 and 50 kDa (Fig 3B). Naïve *S. feltiae* IJs produced a relatively large amount of ESPs, with most of these proteins below 37 kDa (Fig 3A and 2B) while naïve *S. carpocapsae* IJs produced undetectable levels of ESPs (Fig 3B).

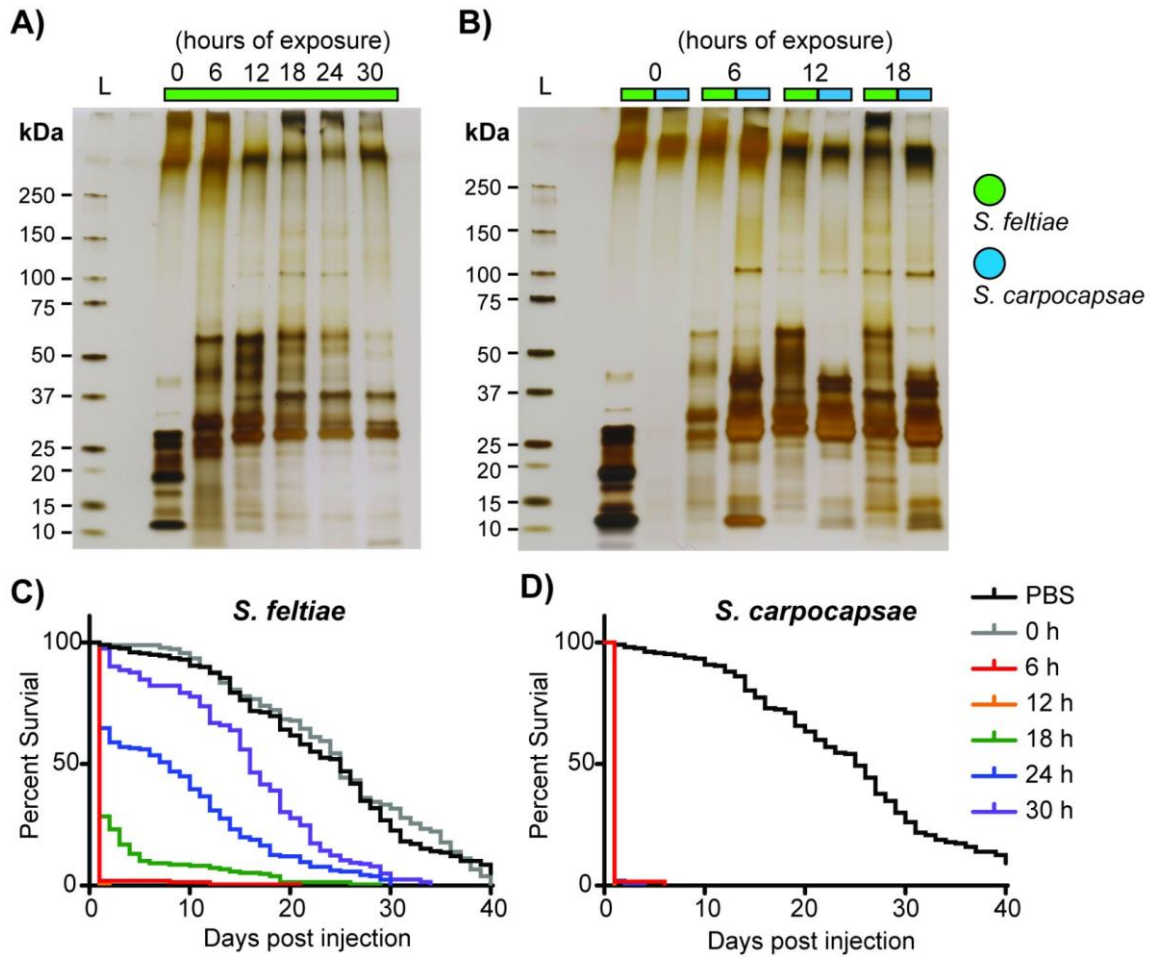


**Figure 3. *Steinerinema* IJs release toxic proteins.** (A) Silver stained protein gel of whole ESPs collected from *S. feltiae* IJs activated for 0 (non-exposed), 6, 12, 18, 24, and 30 hours in insect homogenate. All time course activations were done with approximately 2.5 million IJs and the collected ESPs were concentrated to the same volume (300  $\mu$ l) and the same volume (3  $\mu$ l) was loaded to each lane. (B) Silver stained protein gel of whole ESPs (1  $\mu$ g) from *S. feltiae* (green) and *S. carpocapsae* (blue) activated for 0, 6, 12, and 18 hours. (C) Survival curves of flies injected with 20 ng of whole ESPs from *S. feltiae*. (D) Survival curves of flies injected with 20 ng of whole ESPs from *S. carpocapsae* (*S. carpocapsae* survival curve was recapitulated from Lu. et al, 2017). Each survival curve includes 3 or more biological replicates totaling at least 180 flies.

Next, we tested the activity of *S. feltiae* ESPs in insect hosts. We injected 20 ng of *S. feltiae* ESPs into *Drosophila melanogaster* adults and monitored their survival. We found that the ESPs from naïve (0 hour) IJs were not toxic (Fig 3C). ESPs collected from the early activation time points (6 and 12 hours) exhibited the highest toxicity while ESPs from later activation time points (18, 24, and 30 hours) decreased in toxicity (Fig 3C). This activation-dependent toxicity is in stark contrast with *S. carpocapsae* ESPs, which maintained consistently high toxicity levels, even for ESPs collected after 30 hours of activation (Fig 3D). Late stage L4 and early adults were present at the later time points (24 and 30 hours) and since the more developed nematodes are fragile it was possible that some of these nematodes were damaged and unable to continue producing ESPs or were producing different ESPs. To address this possibility, we quantified the number of damaged nematodes throughout activation using a vital stain (0.2% trypan blue). Since it was the later time points (18, 24, and 30 hours) that exhibited notable decreases in ESP amount and toxicity we compared the number of damaged nematodes in these groups to that found among the 6-hour activated nematodes. The number of damaged nematodes did increase at the later time points (as expected) but the only group that exhibited a significantly higher percentage of damaged nematodes was the 30-hour time point, which accounted for less than 5% of the population (S2 Fig and S2 Table). Further, to simulate harsh experimental handling of the nematodes we repeated the activation time course but applied manual crushing/pressing of the activation

sponge before washing the nematodes out for staining and observation. We found that manual crushing/pressing of the sponge caused significant increases in the percentages of damaged nematodes, with the highest average just below 12% at the 30-hour time point (S2 Fig and S2 Table). We also evaluated whether the toxicity we observed was primarily from nematode-derived ESPs or contamination from its symbiotic bacteria, *Xenorhabdus bovienii*. We compared ESPs from axenic *S. feltiae* IJs activated for 6 hours and found that the profile of ESPs and the toxicity (S3 Fig) were similar to those of symbiotic IJs (Fig 3A–C), leading us to conclude that the toxicity in these experiments is a result of nematode-derived ESPs.

**Comparative transcriptome analysis of *in vitro* and *in vivo* activated *S. feltiae* IJs reveals a core set of genes expressed at 6 hours after activation**

We performed single-nematode RNA-seq analysis [6] in order to identify the similarities and differences between the activation of *S. feltiae* *in vivo* and *in vitro*. We collected RNA from 3 individual nematodes activated *in vitro* for 3, 6, and 9 hours and from nematodes dissected out of infected waxworms (*in vivo*) at 3, 6, 9, 12, and 15 hours. We performed differential expression (DE) analysis using edgeR [32] and found 5670 genes to be differentially expressed between 6 hours *in vitro* activated IJs and naïve IJs (Fig 4A). Among these genes, 3 general gene expression patterns were observed: Increasing expression over time, increasing

first and then decreasing over time, and high levels of expression in naïve IJs with expression decreasing over time (Fig 4A).

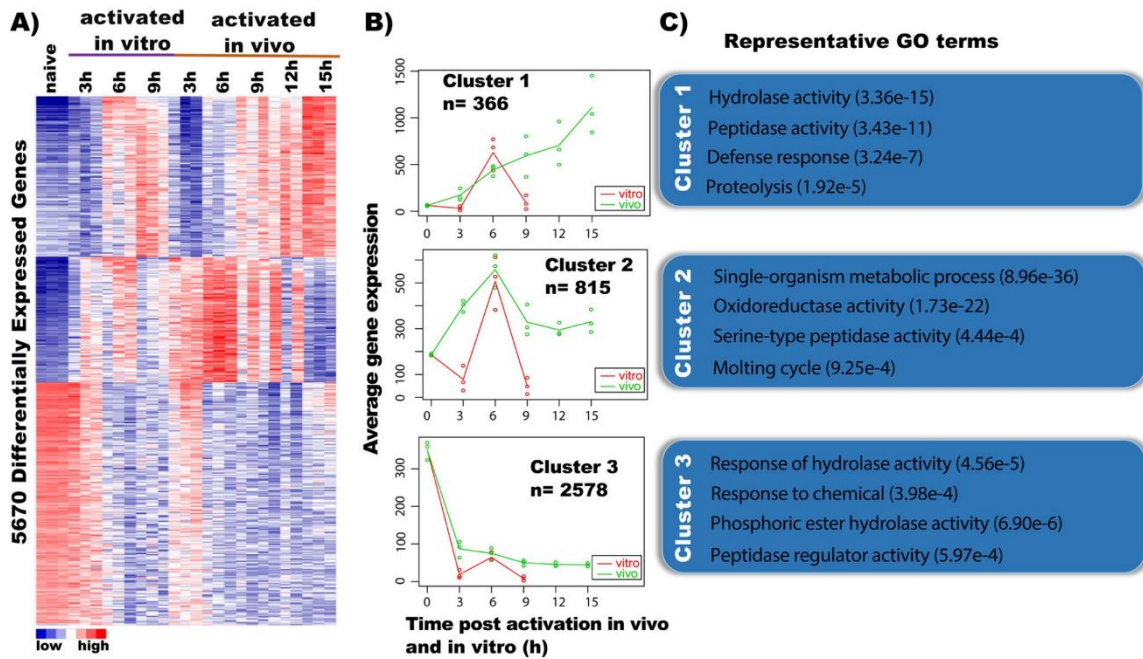


**Figure 4. Genes differentially expressed during in vitro and in vivo IJ activation.** (A) Heatmap showing the K-means of 5670 differentially expressed genes (FDR < 0.05) in activated IJs in vitro and in vivo using K = 3. (B) MaSigPro profiles of gene clusters during the time course (in vitro red, in vivo green). (C) Representative GO terms for each MaSigPro cluster.

With the 5670 differentially expressed genes between 6-hour *in vitro* activated IJs and naïve IJs, we then used MaSigPro to identify genes with significant expression differences and similarities between *in vitro* and *in vivo* time courses and identified 3 major clusters (Fig 4B), similar to the result from edgeR analysis (Fig 4A) [33]. Cluster 1 consists of 366 genes that demonstrate a distinct profile between *in vitro* (red) and *in vivo* (green) conditions (Fig 4B). While the 6-hour *in*

*vitro* and 6-hour *in vivo* samples had similar gene expression levels, many of these genes showed increasing expression up to 15 hours *in vivo*, whereas they showed decreasing expression by 9 hours *in vitro*. GO terms for defense response (p-value 3.24e-7), proteolysis (p-value 1.92e-5) as well as enzymatic activities such as peptidase (p-value 3.43e-11) and hydrolase (p-value 3.36e-15) are enriched in cluster 1 (Fig 4C). Enzymatic activity is also a feature of cluster 2 (815 genes) with enzymes such as oxidoreductase (p-value 1.73e-22) and serine-type peptidase (p-value 4.44e-4) reaching a peak of expression at 6 hours *in vitro* and *in vivo*. Lastly, cluster 3 consists of 2578 genes that decrease within 3 hours of activation. GO analysis of cluster 3 genes found enrichments in terms involved with response to hydrolase activity (p-value 4.56e-5), response to chemical (p-value 3.98e-4) and enzyme activity such as phosphoric ester hydrolase activity (p-value 6.90e-6) and peptidase regulator activity (p-value 5.97e-4) (Fig 4C).

An analysis of changes in gene expression over the time course (3, 6, 9, 12, and 15 hours post infection) of *in vivo* activation also identified 3 major patterns of expression or clusters (S4 Fig). Cluster 1 has 286 genes and GO terms for defense response (p-value 1.44e-5) and enzymatic activity such as hydrolase (p-value 4.01e-9) and peptidase (p-value 6.49e-9) (S4 Fig). Cluster 3 consists of 1,153 genes and GO analysis found enrichments in terms involved in enzymatic regulation such as negative regulation of catalytic activity (p-value 4.71e-4),

regulation of serine kinase activity (p-value 2.21e-4) and regulation of protein phosphorylation (pvalue 2.18e-5). Cluster 2 has 1,353 genes which have a high expression in IJs and a sharp decrease in gene expression by 3 hours with a minor peak at 6 hours (S4 Fig). GO analysis reveals enzymatic activity is also a feature of cluster 2 with enzymes such as kinase (p-value 7.89e-5) and phosphoprotein phosphatase (p-value 5.8e-4). Interestingly, the GO analysis is also enriched for neuropeptide signaling pathway (p-value 4.18e-10) (S4 Fig, Cluster 2). We investigated further into the neuropeptide pathway genes and found that L889\_g32029 (*Sf-flp-21*), which is orthologous to *C. elegans flp-21* and is a neuropeptide important for host-seeking behavior [34], decreases 8-fold in expression (S4 Fig). Similarly, L889\_g7374 (*Sf-flp-11*), which is an ortholog of *C. elegans flp-11*, demonstrates strong expression at the IJ stage but has the sharpest decrease by 15 hours (S4 Fig). Other neuropeptides such as L889\_g30047 (orthologous to *C. elegans flp-3*), L889\_g15885 (orthologous to *C. elegans flp-18*), L889\_g27993 (orthologous to *C. elegans flp-14*) and L889\_g32992 (orthologous to *C. elegans flp-7*) are highly expressed at the IJ stage and progressively decrease by 15 hours post infection (S4 Fig).

Overall, both *in vivo* and *in vitro* time courses showed significant downregulation of a set of naïve IJ genes within 3 hours as well as equivalent activation of another set of genes by 6 hours and differentially express similar sets of genes associated with proteolytic enzymes (peptidases). The *in vivo*-only analysis is

similar to the *in vivo* and *in vitro* DE analyses for both clusters 1 and 3 but have a different profile for cluster 2. In cluster 2 of the *in vivo*-only time course there is a decrease in the expression of neuropeptides (including ones thought to function in host-seeking behavior) at the later time points, which is likely correlated with reduction of host-seeking sensory functions after successful infection of a host.

### **Protein components of *Steinernema* ESPs**

Because of the high toxicity of the ESPs collected at the 6-hour time point and the similarity in gene expression between 6-hour *in vitro* and *in vivo* activated IJs, we chose to primarily focus on the 6-hour ESPs along with further analysis of ESPs from naïve IJs. Using mass spectrometry, we identified 266 proteins (False Discovery Rate, FDR < 5%, S3 Table). To determine the level of correlation between gene expression and relative protein abundance, an mRNA abundance (TPM, transcripts per million) to protein abundance (emPAI, exponentially modified protein abundance index) correlation analysis of the 266 proteins was performed. We found a weak positive correlation between mRNA and protein abundance with Pearson's correlation value of 0.452 and Spearman's rank value of 0.438 (S5 Fig).

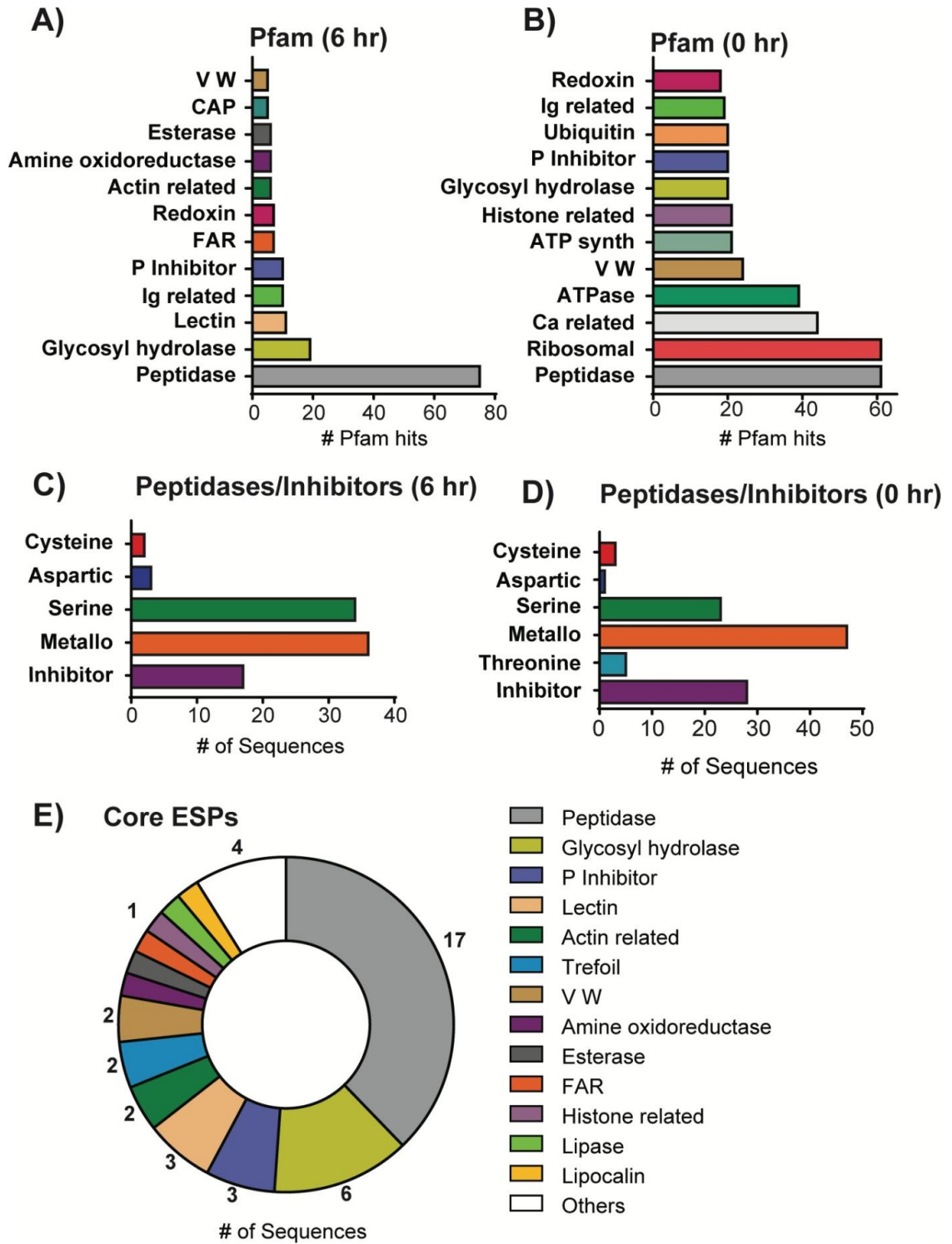


**Figure 5. Protein components of *S. feltiae* and *S. carpocapsae*.** Top 12 most abundant Pfam protein domains (E-value < 10<sup>-5</sup>) detected in ESPs of (A) *S. feltiae* activated for 6 hours and (B) *S. feltiae* naïve (0 hr) IJs. Peptidases and inhibitors detected using the MEROPS peptidase database for (C) *S. feltiae* activated for 6 hours and (D) *S. feltiae* naïve IJs (E-value < 10<sup>-5</sup>). (E) Pfam domains of core ESPs released by both *S. feltiae* and *S. carpocapsae* (E-value < 10<sup>-5</sup>).

We then analyzed the protein sequences for protein domains using Pfam, an online database of protein families [35]. Fig 5A lists the 12 most abundant Pfam domains in *S. feltiae* ESPs with peptidase domains being the highest in abundance followed by glycosyl hydrolases, lectins, Ig-related (Immunoglobulin like), and peptidase inhibitors. VW (Von Willebrand) domains and FAR domains were also found in relatively higher abundance (Fig 5A). A Merops (peptidase and peptidase inhibitor database) analysis detected 92 peptidases and 17 peptidase inhibitors with metallo and serine peptidase being the highest in abundance (Fig 5C). In analyzing the ESPs of naïve IJs we identified 682 proteins (FDR < 5%, S3 Table Sheet 2). Peptidase domains were also the highest in abundance in the ESPs from naïve IJs, followed closely by ribosomal, Ca-related (calcium interacting/regulating proteins) and ATPases (Fig 5B). A Merops analysis detected 79 peptidases and 28 inhibitors with both metallo and serine peptidases in high abundance; with the number of metallo peptidases more than double of serine peptidases (Fig 5D).

### **Comparison of *S. feltiae* and *S. carpocapsae* secreted venom proteins reveals a small set of conserved catalytic enzymes**

We confirmed that the mRNA of the 266 *S. feltiae* ESPs were detected at the 6-hour *in vitro* time point, and that these are expressed similarly at 6, 9, 12, and 15 hours *in vivo* (Fig 6A). We compared the gene expression of these 266 proteins between 6 hours *in vitro* and naïve IJs and found that 54 genes are

downregulated and 96 genes are upregulated upon activation (Fig 6B). Gene ontology terms (GO) for the 96 upregulated genes show strong enrichment for enzymes such as hydrolases (p-value  $2.63e-25$ ) and peptidases (p-value  $4.96e-18$ ) and endopeptidase (pvalue  $3.71e-8$ ), indicating that the activated nematodes increase the synthesis and release of enzymes to degrade host components, including proteins, at early stages of infection. In contrast, the 54 downregulated genes are related to muscle cell development (p-value  $3.09e-5$ ), protein complex assembly (p-value  $4.13e-5$ ) and morphogenesis (p-value  $2.96e-5$ ). These data suggest that at 6 hours *in vitro* the nematodes are at peak production of venom proteins.

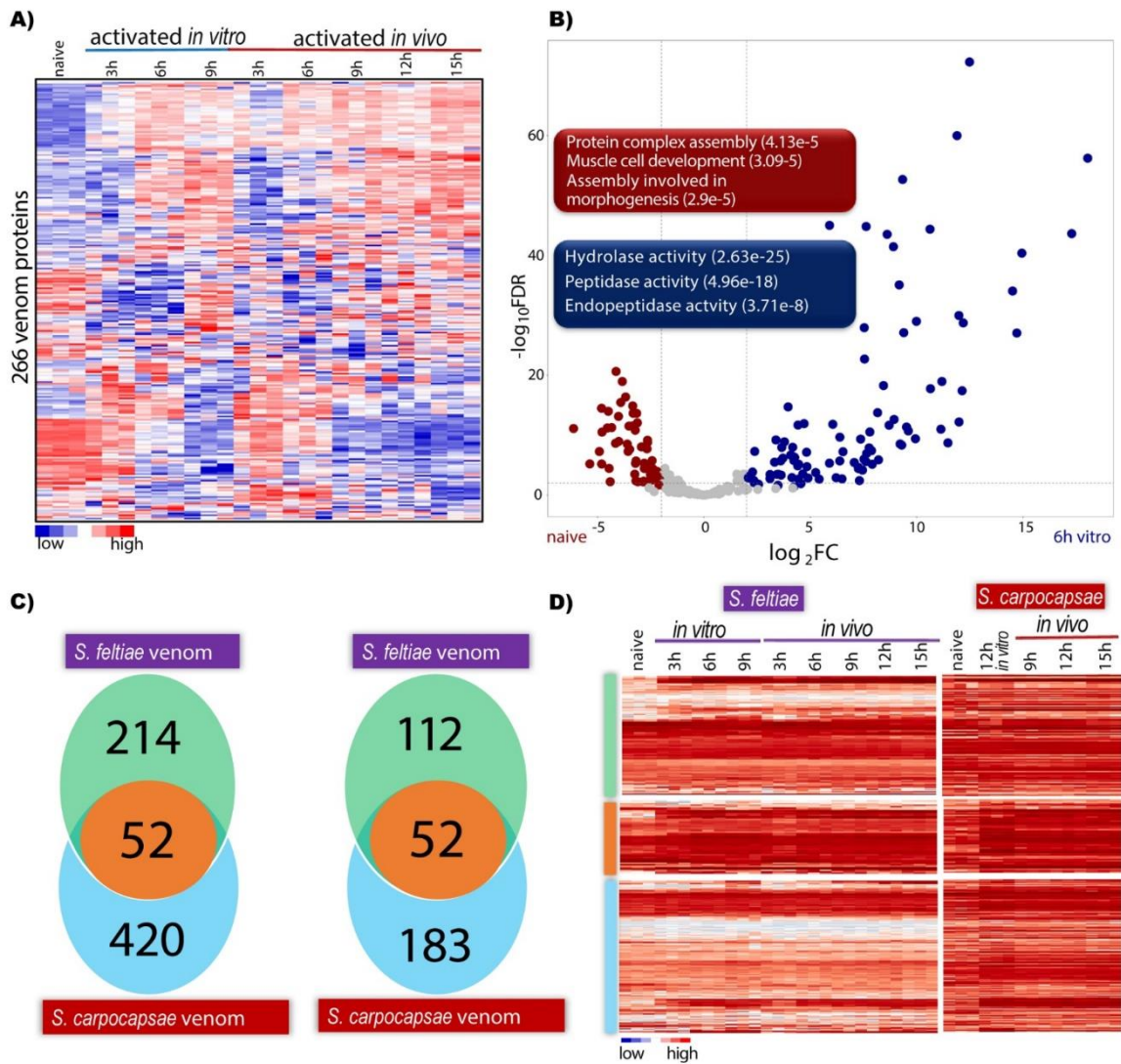


**Figure 6. Gene expression of *S. feltiae* venom proteins in vitro and in vivo and comparison with *S. carpocapsae*.** (A) Heatmap of the expression levels of 266 venom protein genes in both in vitro and in vivo activated IJs. (B) Volcano plot of 266 venom proteins showing the differentially expressed genes in non-activated and 6 hours in vitro activated IJs. Red and blue boxes are representative GO terms for significantly differentially expressed venom proteins. (C) Venn diagram illustrating the comparison of all *S. carpocapsae* venom proteins with *S. feltiae* venom proteins. (D) Venn diagram of conserved venom proteins with homologs in both species. 52 conserved proteins were detected in the venom of both species. (E) Heatmap of expression of the conserved homologs in panel D.

We then conducted a comparative gene expression analysis of ESPs from *S. feltiae* and *S. carpocapsae* to understand the similarities and differences of genes involved in killing hosts. Our orthology analysis between 266 ESPs in *S. feltiae* and 472 *S. carpocapsae* found 52 genes in common (Fig 6C, S4 Table). This is a lower number than expected, given that 112 of the 266 *S. feltiae* ESPs have homologs in *S. carpocapsae* (S5 Table) and 183 of 472 ESPs found in *S. carpocapsae* have homologs in *S. feltiae* (Fig 6D, S6 Table). However, most of these homologs are not detected in the ESPs of the other species even when they are expressed (Fig 6E) suggesting that these enzymes might have been coopted over time to become part of the venom of either species. Interestingly, both *S. feltiae* and *S. carpocapsae* have a high expression of the shared 52 genes. GO terms analysis of the 52 genes shows enrichment of peptidases (p-value 1.25e-7), hydrolases (p-value 6.71e-10) and alpha-glucosidase activity (p-value 2.36e-5) (S7 Table). These results correlate with Pfam domains found in common between *S. feltiae* and *S. carpocapsae* (Fig 5E and [5]). We conclude that this small set of proteins form part of a core of venom proteins within *Steinernema*. Next, we wanted to determine whether these 52 ESPs from insect-parasitic nematodes were conserved in nematode parasites of vertebrates. We ran blastp on the 52 proteins (E-value < 1e-3) and compiled the best non-*Steinernema* hits for each protein. More than half (31 out of 52) of these genes have orthologs in mammalian-parasitic nematodes (S6 Fig) that include *Strongyloides ratti*, *Toxocara canis*, and *Ancylostoma duodenale* (S4 Table). The

prevalence of these proteins in both insect- and vertebrate-parasitic nematode species leads us to speculate that these proteins may play critical roles during host infection and survival within the host for parasites in general.

## **Discussion**

### **Activation of infective juveniles**

Many nematodes have an alternate L3 stage of development, known as the dauer juvenile in free-living and necromenic species, or the infective juvenile for parasitic species [10, 36, 37]. The transition that parasitic IJs make when they enter a host and become actively parasitic and resume development is known as dauer recovery or activation. For parasitic nematodes, successful activation is critical to establishing a successful infection and reproduction in their hosts [5, 11, 38, 39]. Similar to other EPNs, *S. feltiae* activation rates increased in a time dependent manner after exposure to insect tissue *in vitro* [5, 17]. After 30 hours of exposure to host tissue, essentially all the nematodes displayed some level of activation with non-activation rates being an average of 0.3% (S1 Table).

Although *S. feltiae* and *S. carpocapsae* are in the same genus, they are members of different clades within the genus [27, 40, 41]. The fact that these EPNs display similar behavior and morphology during activation when exposed to insect tissue demonstrates that the *in vitro* model of activation we used is a consistent and robust model of activation. We found that when activated *in vitro*, the *S. feltiae* population does not exhibit synchronous activation. Some

individuals are fully activated, some are partially activated, and a small number are not activated at all. We found this resolution of activation quantification to be reliable and consistent however we do note that these 3 categories of activation are broad; encompassing different degrees of pharyngeal bulb expansion, and that the resolution could have been increased by including other factors such as active pumping of the pharyngeal bulb or expansion of the anterior gut. Along with this phased activation, the full activation rates seem to taper off when the nematodes are activated for a long time (Fig 2G). Similar observations have been made for *S. carpocapsae* and *S. scapterisci* activation [5, 17]. The phenomenon of non-synchronous activation is similar to the phased infectivity reported in *in vivo* infections, wherein a certain percentage of an IJ population is unable to infect insect hosts or displays reduced infectivity, but over time more individuals become infectious [42, 43]. This characteristic is believed to be inherent to the IJ itself and does not seem to be significantly affected by factors such as IJ population or host population density. Studies have shown that phased infectivity correlates well with *Heterorhabditis* EPNs but not as well with *Steinernema* EPNs [44, 45]. In contrast to *H. bacteriophora*, where the infectious percentage of the population seems to start out low, previous research suggests that a large percentage of a *Steinernema* IJ population is typically infectious [44]. It has been suggested that the phased infectivity hypothesis is incomplete, and many other factors, such as genetic/physical damage, attraction to infected vs non-infected hosts, and survival of the IJ within the host, could affect population

infectivity [46]. The age of the IJs could also be a contributing factor and was previously shown to affect activation rates in *Steinernematids* [16]. In our *in vitro* model, the IJs do not actually infect a host, but rather are exposed to host tissue as if they had already infected the host. In this context, all the IJs are exposed to host tissue at the same time and though the majority of the population activate to some degree some individuals seem to respond faster and become fully activated early on while another portion of the population activates slower. We did not test whether population density was a factor, nor did we strictly control for age (IJs were between 2 weeks and 2 months post collection) but our findings are consistent with previous studies of phased infectivity. Thus *in vitro* activation may be a useful tool in further exploring the potential relationship between infectivity and activation.

### **Using *in vitro* activation to study *in vivo* infection**

It is widely recognized that helminths modulate host immune system and cause pathology mainly through the release of proteins and small molecules that interact with host cells and tissues, and that these molecules are key factors in disease pathology and parasite fitness [47, 48]. However, nearly all previous and current helminth secretome and ESP studies have been done *in vitro*, due to the difficulty of detecting ESPs from helminth parasites in their hosts. Additionally, there has been little if any experimental validation that the *in vitro* induction of ESPs from various parasitic helminths accurately mimics *in vivo* conditions.

Here, we utilized single-nematode RNA-seq to compare the transcriptomes of nematodes dissected out of waxworms after infection for 3, 6, 9, 12, and 15 hours and those of nematodes activated *in vitro* for 3, 6, and 9 hours. We found that the transcriptional profiles of nematodes activated *in vitro* were generally similar to those of nematodes from *in vivo* infections at each time point (Fig 4A) however some time points were more similar than others. We identified three major clusters of genes among the 5670 differentially expressed genes between activated and naïve IJs and within these three clusters the transcriptome profiles of the 6 h *in vitro* and 6 h *in vivo* activated nematodes exhibited the most consistent correlation (Fig 4B). In contrast, the gene expression profiles of nematodes activated *in vitro* and *in vivo* at 3h and 9h had significantly different profiles and did not correlate consistently (Fig 4B). Therefore, 3h and 9h *in vitro* are not representative of their *in vivo* counterparts. These data suggest that (1) activation of IJs *in vitro* can mimic *in vivo* infection and yield physiologically relevant results; (2) the fidelity of the *in vitro* results needs to be experimentally validated rather than simply assumed; and (3) selection of the timing of ESP collection should be based on the experimental evidence of when the *in vitro* system best mimics the natural process. It is important to determine the similarity of expression profiles for other parasites such as mammalian-parasitic nematodes freshly dissected from hosts compared to those stimulated under *in vitro* ESP collection conditions [49–51]. RNA-seq of individual nematodes, as we

have done in this study, can be used to determine the similarity in the nematodes' response to *in vitro* and *in vivo* conditions in order to optimize experimental *in vitro* conditions. This method is especially beneficial in parasitic studies where low parasite yield is a limiting factor. In addition, gene expression similarity should be optimized when using non-natural hosts, which are often used due to the difficulty of obtaining or maintaining natural hosts or lack of tools and techniques in non-model hosts compared to a model hosts such as a mouse.

### **EPNs release lethal venom during infection**

In EPN research, the nematode has been traditionally assumed to act primarily as a vector for the pathogenic bacterial symbiont. Once the bacterial pathogen is inside the host, it will kill the host while multiplying and providing nourishment (the bacteria itself and the insect tissue) for the nematode [10, 20, 52]. However, there is a growing body of research establishing the nematode as an active contributor to pathogenesis, and in some cases such as with *S. scapterisci*, the nematode may be the main driver of virulence [53]. It is clear that aside from serving as a vector for the bacteria they carry, EPNs contribute to pathogenesis in two ways: They directly damage host tissue and they dampen host immunity, acquiring more time for themselves and the bacteria they carry to overcome and kill the host. Past studies have shown that axenic *S. carpocapsae* IJs can kill and reproduce in insect hosts [54–56] and individual effector molecules from *Steinernematids* have been characterized and shown to function in host immune

suppression and tissue damage [18, 19, 57–61]. More recently the secretome of *S. carpocapsae* was shown to be a complex mixture containing many proteins and that collectively, this venom is toxic to insects. ESPs collected from axenic *S. carpocapsae* IJs had similar protein profiles as those from IJs associated with their bacterial symbiont, and the ESPs from both populations were similarly toxic [5]. We have shown these findings to also be true for *S. feltiae*, where *S. feltiae* IJs exposed to insect tissue become activated and produce ESPs (Fig 2A) that are toxic to insects (Fig 2C). ESPs collected from axenic *S. feltiae* IJs also displayed similar protein profiles and toxicity (Fig 3A and 3C; S3 Fig) compared to their symbiotic counterparts. For EPNs in the genus *Steinernema*, the nematodes seem to play a much more active role in contributing to pathogenicity during infection than previously thought.

We found that there are notable differences in ESP production and content among *Steinernematids*. Whereas the protein profiles of *S. carpocapsae* ESPs were previously shown to be fairly constant after 6 to 30 hours of exposure to insect tissue [5] we found that the protein profiles and protein amount of *S. feltiae* ESPs change from 6 hours to 30 hours of exposure to host tissue (Fig 3A; S1 Fig). Comparing the profiles of ESPs from *S. feltiae* and *S. carpocapsae* side by side (Fig 3B), both have bands that are similar in size however the majority of intense *S. carpocapsae* bands are concentrated between 25–50 kDa while the majority of intense *S. feltiae* bands are not as concentrated and distinctly more

spread out between 25–75 kDa. We found that there is a core suite of proteins found in the ESPs of both species (Fig 5E, 6C) and the differences in the protein profiles could be a result of adaptation to different bacterial symbionts or perhaps a result of host specialization. Another striking difference in ESP production between the two species is that when measuring ESPs from naïve IJs, *S. carpocapsae* was shown to produce few if any ESPs (not detectable by Bradford assay nor any notable bands by silver-staining (Fig 3B)) while naïve *S. feltiae* IJs produce a relatively large quantity of ESPs (Fig 3B). ESPs from naïve *S. feltiae* IJs shared some similarities with those from 6-hour activated IJs; namely that they were produced in relatively large quantities and included peptidases, peptidase inhibitors, and glycosyl hydrolases (Fig 5B). However, the protein profiles are different from each other (Fig 3A) where ESPs from naïve IJs contain a more diverse array of proteins (S3 Table sheet 2) and there were generally more peptides detected for each protein domain (Fig 5B). Further, the ESPs of naïve IJs were not toxic unlike their activated counterparts (Fig 3C).

The release of ESPs from naïve *S. feltiae* IJs without any stimulation from host cues seems metabolically wasteful. We evaluated the possibility that the ESPs from naïve IJs we collected were a result of damage from experimental handling rather than active release by the nematodes. We concluded that the contribution of ESPs from damaged nematodes is likely minimal for the following reasons: (1) *S. feltiae* IJs were treated exactly as *S. carpocapsae* IJs in a previous report [5],

yet naïve *S. carpocapsae* IJs did not release detectable amounts of protein. (2) The nematodes in these experiments, if exposed to host tissue, began producing ESPs with a considerably different composition than naïve IJs (Figs 2B, 4A and 4B). (3) If allowed, the nematodes continued to develop into healthy, reproductive adults. Instead, our data reveals that naïve *S. feltiae* IJs are capable of producing a different set of ESPs, which could be involved with survival strategies including stress tolerance, lubrication and avoidance of desiccation, or maintaining the cuticle and other bodily structures. These strategies may be more pertinent to *S. feltiae* as it is categorized as more of a cruiser where it actively migrates in the soil seeking new hosts, while ambushers like *S. carpocapsae* tend to wait in epigeal habitats [13, 15]. Another possibility for the role of naïve *S. feltiae* IJ ESPs is preparation of the IJ cuticle for host infection since the cuticle of *S. feltiae* IJs has suppressive effects against host immune responses [28, 30, 31]. Peptidases, peptidase inhibitors, and immunoglobulin-like proteins are detected in high abundance in the ESPs and they can be produced to potentially coat/adhere to the cuticle. The production of ESPs from naïve *S. feltiae* IJs is an interesting find that differentiates *S. feltiae* from *S. carpocapsae* and merits further study to understand the biology of this parasite.

The toxicity of activated *S. feltiae* ESPs was highest at the earliest time points tested (6 and 12 hours of exposure) and toxic activity decreased in a time-dependent manner with those collected after 24 and 30 hours of exposure being

significantly less toxic (Fig 3C). The change in protein profiles (Fig 3A) and the reduced protein levels (S1 Fig) in *S. feltiae* ESPs over time seem to be correlated with the time-dependent toxicity decrease. However, it is unlikely that the reduction of toxicity is due to the decreasing abundance of total ESPs since the flies were exposed to the same amount of ESPs (20 ng per fly); instead, it is more likely that some low abundance toxin(s) in the mixture decrease(s) over time, resulting in lower toxic activity. The correlation between protein profiles/abundance and toxicity was not observed for *S. carpocapsae* ESPs: Later time points (42 and 54 hours of exposure) had similar protein profiles and protein abundance compared to earlier time points (6–30 hours of exposure), but were significantly reduced in toxicity or were not toxic at all [5]. This suggests that the toxic activity is due to low abundance proteins. Therefore, the toxins of both species are likely low abundance proteins and not the most abundant ones (Fig 3A and 3B). Other proteins found in the ESPs likely have non-toxic functions during infection such as immunosuppression or immune evasion.

We considered the possibility that damaged nematodes could be an explanation for the time-dependent decrease in ESP amount or toxicity and upon evaluation found a time correlated increase in the number of damaged nematodes.

However, the highest level of damage we observed was less than 5% of the total population (S2 Fig). Even manually crushing the activation arena to simulate excessive force averaged less than 12% of the nematodes being damaged. We

believe that the percentage of damaged nematodes from our experimental handling alone is insufficient to explain the dramatic changes we see in *S. feltiae* IJ ESP production and activity. It could also be argued that instead of (or in conjunction with) the nematodes being significantly damaged, they become unhealthy at the later time points due to various factors such as depletion of resources. We acknowledge this possibility however, it is unlikely the limiting factor as this was not observed in *S. carpocapsae* [5]. Instead, the time-dependent decrease in toxicity and amount of *S. feltiae* ESPs compared to the much slower decrease in toxicity and amount of *S. carpocapsae* ESPs suggests that these nematodes utilize different strategies in establishing themselves as parasites. *S. feltiae* may have a stronger reliance on its bacterial symbiont, *X. bovienii*, in order to overcome and kill the host. Soon after activation and release of bacterial symbionts, the IJs may switch their priority from killing the host to survival, feeding, and development. Axenic *S. feltiae* IJs have been shown to be capable of killing insect hosts, however the studies are limited compared to studies of *S. carpocapsae* and they generally report reduced efficiencies [62, 63]. We found no difference in activity between ESPs from axenic compared with symbiotic *S. feltiae* IJs, however we tested the activity of the ESPs alone and did not examine the larger context of an actual insect infection. It is possible that differences in ESP profiles between *S. carpocapsae* and *S. feltiae* are involved in niche partitioning and differences in host range and specificity.

### **Core EPN venom proteins**

We found 266 proteins in *S. feltiae* ESPs which is significantly fewer than the 472 proteins that were detected in *S. carpocapsae* ESPs [5]. However, this difference may be due to the more fragmented nature of the available *S. feltiae* genome, which has an N50 of 47.5kb compared to the 300kb N50 of the *S. carpocapsae* genome [40] that was used in the previous study (N50 is the length of the shortest contig that together with all the longer contigs cover 50% of the genome assembly). Although it is likely that the ESPs from EPNs are complex mixtures containing many different classes of molecules, we focused on analyzing the proteins. The most abundant group of proteins in activated *S. feltiae* venom are peptidases with a high proportion of serine and metallopeptidases (Fig 5A and 4C). This is similar to what was previously reported in *S. carpocapsae* ESPs [5]. However, *S. carpocapsae* ESPs contained fewer metallopeptidases and significantly more serine peptidases. The high abundance of peptidases and peptidase inhibitors in the ESPs of both species illustrate the importance of these enzymes for EPNs as well as other parasites. Many studies have implicated their potential use in vaccine development and treatment [64–67]. Peptidases and peptidase inhibitors have been shown to have multiple functions in parasite pathogenesis including suppressing/evading host immune systems, host tissue damage, and parasite development [68]. Serine peptidases in particular have been suggested to be used by many parasites including *Trichinella spiralis*, *Ascaris suum*, and *Brugia malayi*, among others [69–71]. Some specific

characterizations of nematode serine peptidase functions include collagen degradation, suppression of melanization, inhibition of blood clotting, and parasite sperm activation [72–74].

We analyzed the protein domains in the ESPs to determine the potential molecular functions of the proteins. For *S. feltiae*, the second most abundant protein domain after peptidases were domains associated with hydrolysis of glycosidic bonds. These enzymes are hypothesized to have many potential functions, including cleavage of glycosylated proteins and breakdown of structural components that contain glycosidic bonds, with many similarities to peptidases. Some of the other protein domains detected in higher abundance in both *S. feltiae* and *S. carpocapsae* ESPs are Ig (immunoglobulin) or Ig-like, Von Willebrand, and FAR (fatty acid/retinol binding protein). The fact that both EPN species have high representation of these domains in their ESPs suggests their importance for EPN success. It is likely that some of these proteins are involved in immunomodulation. For example, it has been hypothesized that FAR proteins affect immune signaling [75], and while this has been experimentally demonstrated in plants [76–78], it has yet to be shown in an animal system. *S. feltiae* has been shown to modulate insect immunity using its cuticle but the use of specific excreted/secreted proteins in immune modulation by *S. feltiae* would be a novel finding [28, 31].

Additionally, we evaluated the correlation between mRNA abundance and protein abundance for these ESPs. The correlation was weak but positive with a Pearson's correlation of 0.452 and Spearman's rank correlation of 0.438 (S5 Fig). mRNA-protein abundance correlations have consistently been weak in various studies including those involving nematodes [79, 80] and our data support this trend. The discrepancies between mRNA and protein abundance is likely due to post-transcriptional regulating systems that can include small non-coding RNAs and microRNAs which has been postulated before [79]. It has been pointed out that most studies of mRNA-protein abundance correlation have been focused on transcriptome-wide data and a study specifically focused on upregulated transcripts resulted in a higher distribution of strong correlations, but we did not evaluate this in the present study [81].

In examining the 266 ESPs released by *S. feltiae* and the 472 ESPs released by *S. carpocapsae*, we found 52 proteins conserved in the ESPs of both species (Fig 5E, 6C). This was unexpectedly low since 112 of the 266 *S. feltiae* ESPs have homologs in *S. carpocapsae* and 184 of the 472 *S. carpocapsae* ESPs have homologs in *S. feltiae* (Fig 6D). Both *S. feltiae* and *S. carpocapsae* have a high expression of the shared 52 venom genes, representing a core of effector proteins shared by these EPNs. Within this core set of ESPs there are peptidases, glycosyl hydrolases, lectins as well as proteins likely to be involved in immune modulation such as FAR proteins, immunoglobulins, and

immunoglobulin-like proteins. The specific functions of these core venom proteins are yet unknown, but their conservation between *S. carpocapsae* and *S. feltiae*, which are in different clades within the genus, suggests that they are important effectors of parasitism and function in a variety of insect hosts. The genus *Steinernema* is the oldest known lineage of EPNs, potentially coevolving with their insect hosts for ~350 million years [26]. Determining the functions of the proteins in this core suite of ESPs may elucidate important steps in the evolution of EPNs and even more broadly parasitic nematodes in general.

## **Materials and Methods**

### **Insects**

*Galleria mellonella* (waxworms) were purchased from CritterGrub ([www.crittergrub.com](http://www.crittergrub.com)). Oregon-R *Drosophila melanogaster* flies were reared in round bottom 8 oz bottles with food medium (129.4 g/L dextrose, 7.4 g/L agar, 61.2 g/L corn meal, 32.4 g/L yeast, and 2.7 g/L tegosept). The bottles were kept at 25°C with 60% relative humidity on a 12 hr light/dark cycle.

### **Nematodes**

*S. feltiae* IJs were cultured and propagated *in vivo* using waxworms as previously described [5]. Briefly, 15 wax worms were placed into a 10 cm petri dish with filter paper pressed to the bottom and 1 ml of tap water containing 750 *S. feltiae* IJs (50 IJs/worm) was dispersed onto the filter paper. The infection plates were

incubated at 25°C with 60% humidity in the dark for 10 days. Then, the waxworm cadavers were transferred to White traps [82]. After 2–3 days (depending on IJ density) the IJs were collected and washed using a glass vacuum filter holder (Fisher Scientific, 09-753-1C) with an 11 µm nylon mesh filter (Millipore, NY1104700). The IJs were stored at 15°C at a density of 7–10 IJs/µl.

### **Waxworm homogenate preparation**

Insect homogenate was prepared as previously described [5]. Briefly, 25 g of waxworms were frozen and grounded in liquid nitrogen with a mortar and pestle into a fine powder. The waxworm powder was then transferred quickly into a glass beaker and resuspended in 100 mL of Phosphate Buffered Saline (PBS, 137 mM NaCl, 2.7 mM KCl, 10 mM Na<sub>2</sub>HPO<sub>4</sub>, 1.8 mM KH<sub>2</sub>PO<sub>4</sub>, pH 7.4). The mixture was then microwaved to a boil 7–8 times with stirring in between. The homogenate was then aliquoted into 50 mL conical tubes and centrifuged for 5 minutes at 3200 rcf to pellet the solid debris of the waxworm. The supernatant, including the top oil layer were transferred into a new container. PBS was then added to the 50 mL conical tubes containing the waxworm pellets, mixed, centrifuged, and the supernatant was collected. This was repeated until the desired volume and percent extract was reached. In this case, 25g of waxworm was used to make 100 ml of 25% waxworm homogenate. The waxworm homogenate extract was used immediately or aliquoted and stored at -20°C.

### **Activation of IJs**

IJ activation was done as previously described [5]. 100 mL of 25% waxworm homogenate was thawed and supplemented with 1x triple antibiotic Pen/Strep/Neo (P4083, Sigma-Aldrich). The homogenate was soaked into 8.2 g of autoclaved cut sponge pieces (approximately 3x3x10 mm). 2.5 million *S. feltiae* IJs were washed 4 times with autoclaved 0.8% NaCl solution and excess liquid was removed from the washed IJs before gentle Pasteur pipette transferring/mixing into the homogenate-soaked sponge. The container was covered with aluminum foil and incubated in the dark at 25°C with 60% relative humidity for a specified amount of time. For most of the contents of this study, the IJs were incubated in waxworm homogenate for 6 hours. The IJs were then washed out of the sponge with 6–8 rounds of autoclaved 0.8% NaCl solution and once separated from the sponge, further washed with 4–5 rounds of 0.8% NaCl solution. Activations were replicated at least 3 times for each experiment.

### **Quantification of activation rates**

IJ activation quantification was done as described [5, 16, 17]. Briefly, activated IJs were observed under 400x magnification on a compound light microscope and scored for the activation phenotype based on expansions of the pharyngeal bulb. Fully activated phenotypes (see Fig 2E), partially activated phenotypes (Fig 2 image C), and Non-activated phenotypes (see Fig 2A) were scored. The difference between non-activated IJs from those that have been partially or fully

activated is easily visualized as the absence of a visible pharyngeal bulb at 400x magnification. Differentiating between partially and fully activated IJs relies on the relative size and shape of the pharyngeal bulb; fully activated IJs have a wider, round-shaped bulb whereas partially activated IJs have a narrower, oval-shaped bulb. To minimize bias and double scoring the same nematode, scoring started with viewing IJs at one corner of the coverslip. All IJs with anterior/head region in view were scored before shifting the slide to view the next adjacent region. This was repeated until all regions of the coverslip was viewed without viewing the same region twice. Activations were done in 3 replicates for each time point (naïve/0 hr, 6 hr, 12 hr, 18 hr, 24 hr, and 30 hr) and each replicate was scored 3 times to obtain averages. Significant differences between *S. feltiae* and *S. carpocapsae* IJ activations were determined using the Prism 8 by paired two-way ANOVA with (Prism recommended) Sidak's multiple comparisons between related groups (i.e. rates of partially activated *S. feltiae* IJs at 30 hrs of exposure compared to rates of partially activated *S. carpocapsae* IJs at 30 hrs of exposure).

### **ESP collection**

ESP collection from the EPN was done as previously described [5]. After IJs were activated and thoroughly washed, they were transferred into a 1 L Erlenmeyer flask containing 100 mL of autoclaved PBS supplemented with 1x triple antibiotic Pen/Strep/Neo. The flask was shaken at 220 rpm in the dark for 3

hours and the nematodes were then centrifuged (700–800 rcf for 1 minute) in 15 mL conical tubes to preliminarily separate the majority of the nematodes from the PBS. The PBS supernatant was then collected and filtered through a 0.22 µm syringe filter (Fisher Scientific, 9719001) and concentrated to approximately 300 µL using a 3 kD cut-off centrifuge column (Millipore, UFC900308). The protein concentration of the venom was quantified using a Bradford assay (Bio-Rad, 500–0006).

### **Protein gel electrophoresis and silver staining**

*S. feltiae* ESPs were prepared for gel electrophoresis by boiling for 5–10 minutes in 1x Laemmli sample buffer supplemented with 50mM Dithiothreitol (DTT) (Bio-Rad, 1610747). The denatured proteins were loaded into a Mini-PROTEAN TGX precast gels (Bio-Rad, 4561086) and electrophoresed at 100 V for 60–90 minutes. Silver staining was done following the manufacturer's protocol (Pierce, # 24600).

### **Testing *S. feltiae* IJ venom toxicity**

*S. feltiae* ESPs toxicity was tested *in vivo* on *Drosophila melanogaster* flies as previously described [5, 83]. Adult male flies 5–6 days old were anesthetized with CO<sub>2</sub> and injected with 20 ng of ESPs in a volume of 50 nl using pulled glass needles and a highspeed pneumatic microinjector (Tritech Research, MINJ-FLY). PBS was injected as a negative control. After injection the flies were transferred

to new vials containing food and stored at 25°C with 60% relative humidity on a 12hr light/dark cycle. Survival of the flies was recorded over 40 days or until all the flies had died. ESP collection and toxicity testing were done in 3 biological replicates for each time point (PBS, 0 hr, 6 hr, 12 hr, 18 hr, 24 hr, 34 hr) with 3 technical replicates of each biological replicate. At least 60 flies were used for each technical replicate totaling at least 180 flies for each biological replicate.

### **Vital staining for nematode damage assay**

Nematodes were activated *in vitro* as described in the “Activation of IJs” section of the methods however scaled down to fit a 9 cm petri dish (0.082 g of sponge, 1 mL of 25% insect homogenate, and approximately 25,000 *S. feltiae* IJs). The sponge pieces were each pressed down 5 times before the nematodes were washed out and rinsed with 4 rounds of autoclaved PBS. The nematodes were then stained by mixing an equal volume of nematodes with an equal volume of 0.4% trypan blue (Sigma-Aldrich) to give a final dye concentration of 0.2%. The mixture was allowed to sit for 5 minutes before transferring the nematodes to a microscope slide for viewing and counting. This was replicated 3 times for each time point (6, 12, 18, 24, 30 hours of activation) with approximately 5000 counts each replicate (15,000 total counts for each time point) Representative images are in S2 Fig and raw counts in S2 Table.

### **Axenic nematode production and assay**

Axenic nematode production and assaying was done as previously described [5] with some slight modifications. Axenic *S. feltiae* IJs were produced *in vitro* by growing bleach sterilized *S. feltiae* eggs on the colonizing defective mutant bacterial strain of *Xenorhabdus nematophila*, HGB315 [84]. HGB315 is unable to colonize the nematodes however can still be a food source. Phase I of the HGB315 bacteria colonies (blue) were obtained and verified using NBTA agar plates (40 mg/L 2,3,5-triphenyltetrazolium, 25 mg/L bromothymol blue, 8 g/L nutrient agar, supplemented with 0.1% (w/v) sodium pyruvate) and double checked with MacConkey Agar plates (reddish brown) (Difco MacConkey Agar, #212123, supplemented with 0.1% (w/v) sodium pyruvate). HGB315 was cultured in LB broth supplemented with 0.1% (w/v) sodium pyruvate over night at 28°C and shaking at 220 rpm. 100–150 µl of overnight HGB315 liquid culture was spread on lipid agar plates (4 ml/L corn oil, 7 ml/L of corn syrup, 5 g/L of yeast extract, 2 g/L MgCl<sub>2</sub>, 8 g/L of nutrient broth, 15 g/L of Bacto Agar, supplemented with 0.1% (w/v) sodium pyruvate) and incubated at 28°C overnight to form a thin layer of bacterial lawn. Surface sterilized *S. feltiae* eggs in a minimal volume of sterile Ringer's solution (172 mM KCl, 68 mM NaCl, 5 mM NaHCO<sub>3</sub>, pH 6.1) was dropped onto the lipid agar plates and allowed to develop into gravid females. This is the first round pass to produce F1 generations of *S. feltiae* nematodes that were exposed only to the non-colonizing HGB315. HGB315 is a strain of *X. nematophila* which is not the native symbiotic bacteria of *S. feltiae* (*Xenorhabdus*

*bovieni*), therefore these nematodes develop and become gravid much slower at approximately 5–6 days (versus ~4 days on *X. bovieni*) post seeding. To obtain axenic eggs, gravid females were rinsed in autoclaved 0.8% NaCl solution for 3 times followed with rocking in axenizing solution (0.7% NaOCl (bleach)/0.5 M NaOH) for 7.5 minutes for 3 times. Brief vortexing was applied 2–3 times in the first two rounds of axenizing to ensure mixing and degradation of adult nematode tissue. After the axenizing treatment, the eggs were rinsed in autoclaved Ringer's solution for 3 times followed by incubation in a triple antibiotic solution (Penicillin, Neomycin, Streptomycin) for 30–45 minutes. The eggs were then rinsed with autoclaved Ringer's solution for 3 times and centrifuged at 700 rcf for 1 min and the supernatant was removed to create a highly dense egg suspension with minimal liquid volume. Approximately 500,000 eggs were gently dispersed onto the lipid agar plates containing the HGB315 bacteria. When the bacteria were depleted, the nematodes were washed off and split into 3–5 new HGB315 bacteria plates. The *S. feltiae* nematodes were kept on the plates until they reached a high density and IJs can be seen crawling up the sides of the plates. At this point the population was still a mix of different life stages so the nematodes were transferred to White traps to collect axenic IJs.

### **Axenic assay**

To assay for non-colonization of bacteria inside *S. feltiae* IJs: approximately 1000 IJs were rinsed 3 times with autoclaved Ringer's solution, followed by surface

sterilization with 4 mM Hyamine 1622 solution (Sigma, 51126) for 30 minutes, and rinsed 3 times with Ringer's solution. The IJs were then concentrated to a volume of 50  $\mu$ l and homogenized with a tissue grinder (Fisher Scientific, 12-141-363). The homogenate was then plated onto LB plates (supplemented with 0.1% (w/v) sodium pyruvate) and incubated at 28°C in the dark. The plates were checked for bacterial growth for 5 days (S3 Fig). This was replicated 3 times for each batch of axenic *S. feltiae* IJs.

### **Mass spectrometry of *S. feltiae* ESPs**

To prepare *S. feltiae* ESPs for mass spectrometry analysis, the proteins were first precipitated with 80% acetone (-20°C pre-chilled) at 4:1 acetone to sample volume. The mixture was vortexed for 5 seconds 3 times and stored at -20°C overnight. The mixture was then centrifuged at 15,000 rcf for 10 minutes at 4°C to pellet the precipitated proteins. The supernatant was carefully removed, followed by addition of fresh -20°C chilled 80% acetone, and mixing by pipetting. The mixture was then centrifuged at 15,000 rcf for another 10 minutes. This process was repeated one more time and after removal of the 2nd 80% acetone wash the protein pellet was allowed to air dry for 5 minutes. The protein pellet was then digested using the Trypsin/Lys-C, Mass Spec Grade kit (Promega, V5071) following the manufacturer's Two-Step In-Solution Digestion protocol. Briefly, the protein pellet was suspended in 7 M urea/50 mM Tris-HCl (pH 8), followed by addition of DTT to a final concentration of 5 mM, and incubated at

37°C for 30 minutes. Iodoacetamide was then added to a final concentration of 15 mM, and incubated at room temperature for 30 minutes in the dark. The Trypsin/Lys-C protease mix was added at a ratio of 25:1 (protein: protease (w/w)) and incubated at 37°C for 4 hours. The mixture was then diluted with 50 mM Tris-HCl (pH 8) to reduce the urea concentration to approximately 0.5 M and continued incubation at 37°C overnight. Trifluoroacetic acid (TFA) was added to a final concentration of 0.5–1% to terminate digestion and the mixture was centrifuged at 15,000 rcf for 10 minutes to pellet particulate matter. The supernatant containing digested protein was cleaned using a C18 spin column (Pierce, 89873) following the manufacturer's protocol.

### **Mass spectrometry**

Online 2D-nano LC/MS/MS was used to perform MudPIT mass spec analysis of *S. feltiae* ESPs. The mass spec apparatus consisted of a 2D nanoAcquity UPLC (Waters, Milford, MA) configured with an Orbitrap Fusion MS (Thermo Scientific, San Jose, CA). LC solutions/fractionation and MS parameters were as previously described [5]. The raw mass spec data was processed/analyzed with the Proteome Discoverer 2.2 software (Thermo Scientific, San Jose, CA) with the Sequest HT search engine running against the *S. feltiae* protein profile, *Steinernema\_feltiae*. PRJNA204661.WBPS11.protein.fa (Parasite.Wormbase.org). Duplicate genes were removed and only genes with FDR <5% were considered for further analysis. The raw mass spec data have

been uploaded to the ProteomeXchange repository and can be accessed with the following links.

0 hr: <ftp://massive.ucsd.edu/MSV000082993>

6 hr: <ftp://massive.ucsd.edu/MSV000082997>

### **Protein domain and peptidase analyses**

Protein/peptide sequences of *S. feltiae* ESPs obtained from mass spec and the protein domain families were analyzed using the Pfam database and the hmmscan program (E-value < 10<sup>-5</sup>) of the HMMER software 3.0 as described [85]. Peptidase types based on the catalytic center amino acid (Serine, Metallo, Aspartic, etc.) and peptidase inhibitors were identified by BLAST+ against the MEROPS Peptidase database [86] from <https://www.ebi.ac.uk/Tools/sss/ncbiblast/>. Only hits with an E-value of <10<sup>-5</sup> were further analyzed.

### **Single nematode transcriptome sequencing**

*S.feltiae* single nematode transcriptome sequencing was done as previously described [5, 6]. *In vitro* activated IJs were activated as described in the Activation of IJs section of the methods but scaled down to fit in a 6 cm petri dish with 1 ml of insect homogenate, 0.08 g of sponge, and 25,000 IJs [16, 17]. The IJs were activated for time points 3, 6, and 9 hrs. After activation the IJs were washed out of the sponge with autoclaved 0.8% NaCl and transferred to 1.5 ml

ependorf tubes. The IJs were cleaned by spinning down and removing/replacing the NaCl supernatant 4 times. We used only IJs that displayed fully activated morphology (confirmed by microscope) for each time point. This method, though arguably not highly representative of the entire population, was used in order to consistently select for individuals that were activating the fastest for each time point and minimize variation from nematodes with different levels of activation. The IJs were then transferred to RNase-free water before lysis. Naïve (0 hr) IJs were not exposed to any insect tissue and washed before proceeding to lysis. *In vivo* activated *S. feltiae* IJs were activated by infecting live waxworms at 50 IJs/waxworm. After 30 minutes the waxworms were gently rinsed in autoclaved 0.8% NaCl to wash off IJs that were on the surface of the waxworms but had not entered the waxworm. The infected waxworms were then stored in the dark at 25°C with 60% relative humidity for 3, 6, 9, 12, or 15 hrs. After the specified hours, the waxworms were individually placed in 6 cm petri dishes with autoclaved 0.8% NaCl and the activated IJs were dissected out. The IJs were washed by transferring them to new 6 cm petri dishes with fresh autoclaved NaCl 5x until being transferred to RNase free water before lysis. Activated IJs for each time point/condition (6 hr *in vitro*, 12 hr *in vivo*, etc.) were individually isolated in RNase-free water, cut into 3–4 pieces, and immediately transferred to lysis buffer containing RNase inhibitor Proteinase K. The sample was placed on ice and observed periodically until the nematode tissue had been digested (typically 45–

60 minutes). The sample was then incubated in a thermocycler at 85°C for 3 minutes to deactivate proteinase K. dNTP/ Oligo-dT30VN- (50-AAGCAGTGGTATCAACGCAGAGTACT30VN-30) was added to the sample and poly-A RNA was reverse transcribed in a reaction solution of 100U Superscript II RT (Thermo Fisher Scientific, 18064014), 10 U RNase inhibitor (Promega, N2611), 1x Superscript II first-strand buffer, 5 mM DTT, 1 M Betaine, 6 mM MgCl<sub>2</sub>, 1 μM TSO- (LNA-modified TSO 50-AAGCAGTGGTATCAACGCAGAGTACATrGrG+G-30, Exiqon.com), and RNase-free water. The reverse transcription program was set to 1) 42°C 90 min, 2) 50°C 2 min, 42°C 2 min (repeat 14x), 3) 70°C 15 min, and 4) 4°C Hold. The cDNA was then added to a cDNA amplification mix with final concentrations of 1x KAPA HiFi HotStart ReadyMix (Kapa Biosystems, KK2602), 0.1 μM IS PCR primer (50-AAGCAGTGGTATCAACGCAGAGT-30, ordered from idtdna.com), and RNase-free water. The cDNA amplification program was set to 1) 98°C 3 min, 2) 98°C 20 sec, 67°C 15 sec, 72°C 6 min (repeat 17x), 3) 72°C 5 min, and 4) 4°C Hold. To clean the amplified cDNA, it was mixed with Ampure XP beads at a ratio of 1:1 (v/v). The mixture was then placed on a magnetic bead stand to magnetize the cDNA-bound beads to side-wall of the tube and washed with 3 rounds of 80% ethanol. After removal of the final ethanol wash the beads were air dried for 3–4 minutes and observed frequently under a microscope. At the first sign of a dry crack in the beads, 17.5 μl of elution Buffer (EB, 10 mM Tris-Cl, pH 8.5) was added, and incubated for 2 minutes. The sample was placed

back on the magnetic bead stand for 2–3 minutes to separate the beads from the EB solution (now containing clean cDNA) and the EB solution was collected. cDNA concentration was measured by Qubit Fluorometer (Thermo Fisher Scientific) and the quality was analyzed by BioAnalyzer (Agilent). The cDNA was tagmented using the Nextera DNA library prep kit (Illumina, FC-121-1030) following the protocol in L. Serra, et al 2018. Briefly, 20 ng of cDNA in 8  $\mu$ l was mixed with 10  $\mu$ l of Tagment DNA buffer and 2.2  $\mu$ l of Tagment DNA enzyme from the kit. The mixture was incubated at 55°C for 5 minutes and cleaned up using the QIAquick DNA cleanup column (QIAGEN, 28104). The tagmented cDNA was then amplified using the Phusion High Fidelity PCR master mix (New England Biolabs, M0531L) with 30  $\mu$ l of tagmented cDNA, 2.5  $\mu$ l of Primer-1 (Ad1\_no MX), 2.5  $\mu$ l of Primer-2(Ad2.#), and 35  $\mu$ l of Phusion High Fidelity PCR master mix buffer. The amplification program was set to 1) 72°C 5 min, 2) 98°C 30 sec, 3) 98°C 10 sec, 63°C 30 sec., 72°C 1 min (repeat 10x), and 4) 4°C Hold. The sample was then cleaned up with Ampure XP beads as described above except, scaling up to use 30  $\mu$ l of EB and collecting 27.5  $\mu$ l of the supernatant. Libraries were prepared and sequenced as paired-end, 43 base pair reads on the Illumina Nextseq 500.

### **Gene expression quantification**

Unstranded, paired-end 43 bp RNA-seq reads for each worm were mapped to the *S. feltiae* transcriptome downloaded from WormBase ParaSite (WS263)

using Bowtie 1.0.0 with the following options: -X 1500 -a -m 200—S—seedlen 25 -n 2—offrate 1 -p 64 -v 3 [87]. After Bowtie, gene expression was quantified with RSEM with the following options: rsem-calculate-expression—bam—paired-end. Gene expression for *S. carpocapsae* were performed as previously described [5] and reported in Transcripts Per Million (TPM). We used counts for differential gene expression analysis. Reads for single worm RNA-seq samples were submitted to Gene Expression Omnibus (GEO) under the accession number GSE119223.

### **Normalization and batch correction**

The Transcript per million (TPM) generated by rsem-calculate-expression for *S. feltiae* samples were normalized according to groups using the R package limma [88] because samples were collected, processed and sequenced in different batches. Samples were batched corrected between 3 and 9 hours *in vitro* to 6 hours *in vitro*, 3,6,9,12,15 hours *in vivo* with edgeR package removebatcheffects with log2 of TPM matrix. Normalization and batch correction for *S. carpocapsae* were done as previously described [5].

### **mRNA and protein correlation**

Log2 of the average TPM+1 (transcripts per million, relative RNA abundance) and Log2 of the emPAI (exponentially modified Protein Abundance Index, relative protein abundance) for the 266 genes of *S. feltiae* ESPs was plotted in

Rstudio using the package ggplot2 [89]. Pearson's correlation and Spearman's rank correlation values were calculated in Excel.

### **Gene expression analysis and GO enrichment analysis**

Differential gene expression was determined using edgeR [32]. Counts were normalized by library size using calcNormFactors. Genes were called differentially expressed if FDR < 0.05 and fold change > 2. The list of genes that were differentially expressed (DE) using edgeR were used to create a TPM matrix. Gene expression in TPM were clustered using Cluster 3.0 [90] with the following options: log transformed, mean centered, normalized. Then genes were hierarchically clustered with center correlation. Heatmap were visualized with Java TreeView [91]. Heatmap for Fig 6C were done using the R package heatmap.2 with centroid hierarchical clustering by row. MaSigPro was run as a two-time series to evaluate the differences and similarities of gene expression between *in vitro* and *in vivo* time course with 5670 differentially expressed genes found with edgeR between 6 hours *in vitro* activated and naïve IJs. Gene ontology enrichment analyses was calculated using Blast2GO Fisher's exact test and considered statistically significant if FDR < 0.05 [92]. List of genes used in Blast2GO were differentially expressed according to edgeR or dynamically expressed according to maSigPro.

## **Venom orthology analysis**

We obtained a list of N:N orthologs and paralogs between *S. feltiae* and *S. carpocapsae* from WormBase ParaSite Biomart. List were obtained by choosing *S. feltiae* genome as query to find orthologs and paralogs in *S. carpocapsae*. List of venom proteins for *S. carpocapsae* were obtained from Lu et al. 2017 and compared to list of *S. feltiae* venom proteins. Orthology analysis was done with edgeR with function “match”. In determining the orthology of *S. feltiae* L889\_g32029 (*Sf-flp-21*) to *C. elegans flp-21*, we relied on the predicted sequence of the mature peptide [34, 93]. Using this method, we determined that, similar to *Sc-flp-21*, *Sf-flp-21* has an identical predicted mature peptide as the *flp-21* from *C. elegans*.

## References

1. Hotez PJ, Alvarado M, Basanez MG, Bolliger I, Bourne R, Boussinesq M, et al. The global burden of disease study 2010: interpretation and implications for the neglected tropical diseases. *PLoS Negl Trop Dis*. 2014;8(7):e2865. doi: 10.1371/journal.pntd.0002865. PubMed PMID: 25058013; PubMed Central PMCID: PMCPMC4109880.
2. Pullan RL, Smith JL, Jasrasaria R, Brooker SJ. Global numbers of infection and disease burden of soil transmitted helminth infections in 2010. *Parasites & Vectors*. 2014;7:19. doi: 10.1186/1756-3305-7-37. PubMed PMID: WOS:000334641400001.
3. Cuesta-Astroz Y, de Oliveira FS, Nahum LA, Oliveira G. Helminth secretomes reflect different lifestyles and parasitized hosts. *International Journal for Parasitology*. 2017;47(9):529-44. doi: 10.1016/j.ijpara.2017.01.007. PubMed PMID: WOS:000408076200003.
4. Stoltzfus JD, Pilgrim AA, Herbert DR. Perusal of parasitic nematode 'omics in the post-genomic era. *Molecular and Biochemical Parasitology*. 2017;215:11-22. doi: 10.1016/j.molbiopara.2016.11.003. PubMed PMID: WOS:000405049100003.
5. Lu DH, Macchietto M, Chang D, Barros MM, Baldwin J, Mortazavi A, et al. Activated entomopathogenic nematode infective juveniles release lethal venom proteins. *Plos Pathogens*. 2017;13(4):31. doi: 10.1371/journal.ppat.1006302. PubMed PMID: WOS:000402555700018.
6. Serra L, Chang D, Macchietto M, Williams K, Murad R, Lu D, et al. Adapting the Smart-seq2 Protocol for Robust Single Worm RNA-seq. *Bio-protocol*. 2018;8(4):e2729. doi: 10.21769/BioProtoc.2729.
7. Cassada RC, Russell RL. The dauer larva, a post-embryonic developmental variant of the nematode *Caenorhabditis elegans*. *Developmental Biology*. 1975;46(2):326-42. doi: [https://doi.org/10.1016/0012-1606\(75\)90109-8](https://doi.org/10.1016/0012-1606(75)90109-8).
8. Hallem EA, Dillman AR, Hong AV, Zhang Y, Yano JM, DeMarco SF, et al. A sensory code for host seeking in parasitic nematodes. *Curr Biol*. 2011;21(5):377-83. doi: 10.1016/j.cub.2011.01.048. PubMed PMID: 21353558; PubMed Central PMCID: PMC3152378.
9. Dillman AR, Guillermin ML, Lee JH, Kim B, Sternberg PW, Hallem EA. Olfaction shapes host-parasite interactions in parasitic nematodes. 2012. doi: 10.1073/pnas.1211436109.

10. Kaya HK, Gaugler R. Entomopathogenic Nematodes. Annual Review of Entomology. 1993;38:181-206. doi: 10.1146/annurev.en.38.010193.001145. PubMed PMID: WOS:A1993KF69700009.
11. Crook M. The dauer hypothesis and the evolution of parasitism: 20 years on and still going strong. Int J Parasit. 2014;44(1):1-8. doi: 10.1016/j.ijpara.2013.08.004. PubMed PMID: WOS:000331415400001.
12. Hawdon JM, Jones BF, Perregaux MA, Hotez PJ. *Ancylostoma Caninum* - Metalloprotease Release Coincides with Activation of Infective Larvae in-Vitro. Experimental Parasitology. 1995;80(2):205-11. doi: DOI 10.1006/expr.1995.1025. PubMed PMID: ISI:A1995QP93400005.
13. Campos-Herrera R, Barbercheck M, Hoy CW, Stock SP. Entomopathogenic Nematodes as a Model System for Advancing the Frontiers of Ecology. Journal of Nematology. 2012;44(2):162-76. PubMed PMID: WOS:000320451700010.
14. Hodson AK, Siegel JP, Lewis EE. Ecological influence of the entomopathogenic nematode, *Steinernema carpocapsae*, on pistachio orchard soil arthropods. Pedobiologia. 2012;55(1):51-8. doi: 10.1016/j.pedobi.2011.10.005. PubMed PMID: WOS:000300211100007.
15. Lewis EE, Campbell J, Griffin C, Kaya H, Peters A. Behavioral ecology of entomopathogenic nematodes. Biological Control. 2006;38(1):66-79. doi: 10.1016/j.biocontrol.2005.11.007. PubMed PMID: WOS:000238596600006.
16. Alonso V, Nasrolahi S, Dillman A. Host-Specific Activation of Entomopathogenic Nematode Infective Juveniles. Insects. 2018;9(2):59. doi: 10.3390/insects9020059.
17. Lu DH, Sepulveda C, Dillman AR. Infective Juveniles of the Entomopathogenic Nematode *Steinernema scapterisci* Are Preferentially Activated by Cricket Tissue. Plos One. 2017;12(1):14. doi: 10.1371/journal.pone.0169410. PubMed PMID: WOS:000391612300184.
18. Balasubramanian N, Hao YJ, Toubarro D, Nascimento G, Simoes N. Purification, biochemical and molecular analysis of a chymotrypsin protease with prophenoloxidase suppression activity from the entomopathogenic nematode *Steinernema carpocapsae*. Int J Parasit. 2009;39(9):975-84. doi: 10.1016/j.ijpara.2009.01.012. PubMed PMID: ISI:000267569000004.

19. Toubarro D, Avila MM, Montiel R, Simoes N. A Pathogenic Nematode Targets Recognition Proteins to Avoid Insect Defenses. *Plos One*. 2013;8(9):13. doi: 10.1371/journal.pone.0075691. PubMed PMID: WOS:000325423500086.
20. Lewis EE, Clarke DJ. Nematode Parasites and Entomopathogens. In: Vega FE, Kaya HK, editors. *Insect Pathology*, 2nd Edition. San Diego: Elsevier Academic Press Inc; 2012. p. 395-424.
21. Hunt DJ, Nguyen KB, Spiridonov SE. *Steinernematidae*: species descriptions. *Advances in entomopathogenic nematode taxonomy and phylogeny*: Brill; 2016. p. 111.
22. Poinar GO, Jr. *Nematodes for biological control of insects*. 1979.
23. Hodson AK, Friedman ML, Wu LN, Lewis EE. European earwig (*Forficula auricularia*) as a novel host for the entomopathogenic nematode *Steinernema carpocapsae*. *Journal of Invertebrate Pathology*. 2011;107(1):60-4. doi: 10.1016/j.jip.2011.02.004. PubMed PMID: WOS:000289831300008.
24. Nguyen KB, Smart GC. *Steinernema scapterisci* n. sp. (Rhabditida, Steinernematidae). *Journal of Nematology*. 1990;22(2):187-99. PubMed PMID: WOS:A1990CY91100007.
25. Stock SP, Koppenhofer AM. *Steinernema scarabaei* n. sp (Rhabditida : Steinernematidae), a natural pathogen of scarab beetle larvae (Coleoptera : Scarabaeidae) from New Jersey, USA. *Nematology*. 2003;5:191-204. doi: 10.1163/156854103767139680. PubMed PMID: WOS:000184809500004.
26. Adams BJ, Peat SM, Dillman AR. Phylogeny and evolution. In: Nguyen KB, Hunt DJ, editors. *Entomopathogenic nematodes: Systematics, phylogeny, and bacterial symbionts*. *Nematology monographs and perspectives*. 5. Leiden-Boston: Brill; 2007. p. 693-733.
27. Spiridonov SE, Reid AP, Podrucka K, Subbotin SA, Moens M. Phylogenetic relationships within the genus *Steinernema* (Nematoda : Rhabditida) as inferred from analyses of sequences of the ITS1-5.8S-ITS2 region of rDNA and morphological features. *Nematology*. 2004;6:547-66. doi: Doi 10.1163/1568541042665304. PubMed PMID: ISI:000226415300008.
28. Dunphy GB, Webster JM. Partially characterized components of the epicuticle of dauer juveniles *Steinernema feltiae* and their influence on hemocyte activity in *Galleria mellonella*. *Journal of Parasitology*. 1987;73(3):584-8. doi: 10.2307/3282140. PubMed PMID: WOS:A1987J343300020.

29. Brivio MF, Pagani M, Restelli S. Immune suppression of *Galleria mellonella* (Insecta, Lepidoptera) humoral defenses induced by *Steinernema feltiae* (Nematoda, Rhabditida): involvement of the parasite cuticle. *Experimental Parasitology*. 2002;101(2-3):149-56. doi: 10.1016/s0014-4894(02)00111-x. PubMed PMID: WOS:000179436600009.
30. Brivio MF, Mastore M, Moro M. The role of *Steinernema feltiae* body-surface lipids in host-parasite immunological interactions. *Molecular and Biochemical Parasitology*. 2004;135(1):111-21. doi: 10.1016/j.molbiopara.2004.01.012. PubMed PMID: WOS:000221489500012.
31. Brivio M, Mastore M. Nematobacterial Complexes and Insect Hosts: Different Weapons for the Same War. *Insects*. 2018;9(3):117. PubMed PMID: doi:10.3390/insects9030117.
32. Robinson MD, McCarthy DJ, Smyth GK. edgeR: a Bioconductor package for differential expression analysis of digital gene expression data. *Bioinformatics*. 2010;26(1):139-40. doi: 10.1093/bioinformatics/btp616. PubMed PMID: 19910308; PubMed Central PMCID: PMC2796818.
33. Conesa and Nueda CA, Nueda J. maSigPro: Significant Gene Expression Profile Differences in Time Course Gene Expression Data. 1.52.0 ed: R package; 2018.
34. Morris R, Wilson L, Sturrock M, Warnock ND, Carrizo D, Cox D, et al. A neuropeptide modulates sensory perception in the entomopathogenic nematode *Steinernema carpocapsae*. *Plos Pathogens*. 2017;13(3):17. doi: 10.1371/journal.ppat.1006185. PubMed PMID: WOS:000398120300047.
35. Finn RD, Coghill P, Eberhardt RY, Eddy SR, Mistry J, Mitchell AL, et al. The Pfam protein families database: towards a more sustainable future. *Nucleic Acids Research*. 2016;44(D1):D279-D85. doi: 10.1093/nar/gkv1344. PubMed PMID: WOS:000371261700038.
36. Hu PJ. Dauer. *WormBook*. 2007. doi: 10.1895/wormbook.1.144.1.
37. Viney ME, Lok JB. The biology of *Strongyloides* spp. *WormBook*. 2015. doi: 10.1895/wormbook.1.141.2.
38. Bonner TP. Initiation of Development *In vitro* of Third-Stage *Nippostrongylus brasiliensis*. *The Journal of Parasitology*. 1979;65(1):74-8. doi: 10.2307/3280205.

39. Hawdon JM, Volk SW, Pritchard DI, Schad GA. Resumption of Feeding *In vitro* by Hookworm Third-Stage Larvae - a Comparative Study. *Journal of Parasitology*. 1992;78(6):1036-40. doi: Doi 10.2307/3283226. PubMed PMID: ISI:A1992KL32200013.
40. Dillman AR, Macchietto M, Porter CF, Rogers A, Williams B, Antoshechkin I, et al. Comparative genomics of *Steinernema* reveals deeply conserved gene regulatory networks. *Genome Biol*. 2015;16:200. doi: 10.1186/s13059-015-0746-6. PubMed PMID: 26392177; PubMed Central PMCID: PMC4578762.
41. Adams BJ, Peat SM, Dillman AR. Phylogeny and evolution. *Entomopathogenic Nematodes: Systematics, Phylogeny and Bacterial Symbionts*. 2007;5:693-733. PubMed PMID: ISI:000301864200007.
42. Hominick WM, Reid AP. Perspectives on entomopathogenic nematology. Boca Raton, FL 33431: CRC Press Inc.; 1990. p. 327-45.
43. Griffin CT. Effects of prior storage conditions on the infectivity of *Heterorhabditis* sp (Nematoda: Heterorhabditidae). *Fundamental and Applied Nematology*. 1996;19(1):95-102. PubMed PMID: ISI:A1996TP25100014.
44. Campbell JF, Koppenhofer AM, Kaya HK, Chinnasri B. Are there temporarily non-infectious dauer stages in entomopathogenic nematode populations: a test of the phased infectivity hypothesis. *Parasitology*. 1999;118 ( Pt 5):499-508. PubMed PMID: 10363283.
45. Dempsey CM, Griffin CT. Phased activity in *Heterorhabditis megidis* infective juveniles. *Parasitology*. 2002;124:605-13. doi: 10.1017/S0031182002001609. PubMed PMID: ISI:000177212400005.
46. Grewal PS, Lewis EE, Gaugler R. Response of infective stage parasites (Nematoda: Steinernematidae) to volatile cues from infected hosts. *Journal of Chemical Ecology*. 1997;23(2):503-15. doi: Doi 10.1023/B:Joec.0000006374.95624.7e. PubMed PMID: ISI:A1997WR84600018.
47. Hewitson JP, Grainger JR, Maizels RM. Helminth immunoregulation: The role of parasite secreted proteins in modulating host immunity. *Molecular and Biochemical Parasitology*. 2009;167(1):1-11. doi: 10.1016/j.molbiopara.2009.04.008. PubMed PMID: ISI:000268049600001.
48. Lightowlers MW, Rickard MD. Excretory Secretory Products of Helminth-Parasites - Effects on Host Immune-Responses. *Parasitology*. 1988;96:S123-S66. PubMed PMID: ISI:A1988M840500009.

49. Holland MJ, Harcus YM, Riches PL, Maizels RM. Proteins secreted by the parasitic nematode *Nippostrongylus brasiliensis* act as adjuvants for Th2 responses. *European Journal of Immunology*. 2000;30(7):1977-87. doi: Doi 10.1002/1521-4141(200007)30:7<1977::Aid-Immu1977>3.0.Co;2-3. PubMed PMID: ISI:000088262300020.
50. Healer J, Ashall F, Maizels RM. Characterization of Proteolytic Enzymes from Larval and Adult *Nippostrongylus brasiliensis*. *Parasitology*. 1991;103:305-14. doi: Doi 10.1017/S0031182000059588. PubMed PMID: ISI:A1991GH06800016.
51. Hewitson JR, Harcus YM, Curwenb RS, Dowle AA, Atmadja AK, Ashton PD, et al. The secretome of the filarial parasite, *Brugia malayi*: Proteomic profile of adult excretory-secretory products. *Molecular and Biochemical Parasitology*. 2008;160(1):8-21. doi: 10.1016/j.molbiopara.2008.02.007. PubMed PMID: ISI:000257024600002.
52. Dillman AR, Chaston JM, Adams BJ, Ciche TA, Goodrich-Blair H, Stock SP, et al. An Entomopathogenic Nematode by Any Other Name. *Plos Pathogens*. 2012;8(3):4. doi: 10.1371/journal.ppat.1002527. PubMed PMID: WOS:000302225600003.
53. Aryal SK, Lu D, Le K, Allison L, Gerke C, Dillman AR. Sand crickets (*Gryllus firmus*) have low susceptibility to entomopathogenic nematodes and their pathogenic bacteria. *J Invertebr Pathol*. 2019;160:54-60. Epub 2018/12/12. doi: 10.1016/j.jip.2018.12.002. PubMed PMID: 30528638.
54. Han RC, Ehlers RU. Pathogenicity, development, and reproduction of *Heterorhabditis bacteriophora* and *Steinernema carpocapsae* under axenic *in vivo* conditions. *Journal of Invertebrate Pathology*. 2000;75(1):55-8. doi: 10.1006/jipa.1999.4900. PubMed PMID: WOS:000085395100009.
55. Poinar GO, Thomas GM. Significance of *Achromobacter nematophilus* Poinar and Thomas (Achromobacteraceae - Eubacteriales) in Development of Nematode DD-136 (*Neoaplectana* sp Steinernematidae). *Parasitology*. 1966;56:385-&. PubMed PMID: WOS:A19667764600015.
56. Sicard M, Le Brun N, Pages S, Godelle B, Boemare N, Moullia C. Effect of native *Xenorhabdus* on the fitness of their *Steinernema* hosts: Contrasting types of interaction. *Parasitology Research*. 2003;91(6):520-4. doi: 10.1007/s00436-003-0998-z. PubMed PMID: WOS:000187993700016.

57. Burman M. *Neoplectana carpocapsae*: Toxin production by axenic Insect Parasitic Nematodes. *Nematologica*. 1982;28(1):62-70. PubMed PMID: WOS:A1982PU84500006.
58. Walter TN, Dunphy GB, Mandato CA. *Steinernema carpocapsae* DD136: Metabolites limit the non-self adhesion responses of haemocytes of two lepidopteran larvae, *Galleria mellonella* (*F. Pyralidae*) and *Malacosoma disstria* (*F. Lasiocampidae*). *Experimental Parasitology*. 2008;120(2):161-74. doi: 10.1016/j.exppara.2008.07.001. PubMed PMID: WOS:000259659600006.
59. Hao YJ, Montiel R, Nascimento G, Toubarro D, Simoes N. Identification and expression analysis of the *Steinernema carpocapsae* elastase-like serine protease gene during the parasitic stage. *Exp Parasitol*. 2009;122(1):51-60. doi: 10.1016/j.exppara.2009.01.014. PubMed PMID: WOS:000265463600009.
60. Jing YJ, Toubarro D, Hao YJ, Simoes N. Cloning, characterisation and heterologous expression of an astacin metalloprotease, Sc-AST, from the entomoparasitic nematode *Steinernema carpocapsae*. *Molecular and Biochemical Parasitology*. 2010;174(2):101-8. doi: 10.1016/j.molbiopara.2010.07.004. PubMed PMID: WOS:000283697900002.
61. Toubarro D, Avila MM, Hao YJ, Balasubramanian N, Jing YJ, Montiel R, et al. A Serpin Released by an Entomopathogen Impairs Clot Formation in Insect Defense System. *Plos One*. 2013;8(7):12. doi: 10.1371/journal.pone.0069161. PubMed PMID: WOS:000322064300088.
62. Ehlers RU, Wulff A, Peters A. Pathogenicity of axenic *Steinernema feltiae*, *Xenorhabdus bovienii*, and the bacto-helminthic complex to larvae of *Tipula oleracea* (Diptera) and *Galleria mellonella* (Lepidoptera). *Journal of Invertebrate Pathology*. 1997;69(3):212-7. doi: 10.1006/jipa.1996.4647. PubMed PMID: WOS:A1997WZ20900003.
63. Dunphy GB, Webster JM. Influence of *Steinernema feltiae* (Filipjev) Wouts, Mracek, Gerdin and Bedding DD136 strain on the humoral and haemocytic responses of *Galleria mellonella* (L.) larvae to selected bacteria. *Parasitology*. 1985;91(2):369-80. Epub 2009/04/01. doi: Doi: 10.1017/s0031182000057437.
64. Odaly JA, Cabrera Z. Immunization of hamsters with TLCK-killed parasites induces protection against *Leishmania* infection. *Acta Tropica*. 1986;43(3):225-36. PubMed PMID: WOS:A1986E140800004.
65. Redmond DL, Knox DP. Protection studies in sheep using affinity-purified and recombinant cysteine proteinases of adult *Haemonchus contortus*. *Vaccine*.

2004;22(31-32):4252-61. doi: 10.1016/j.vaccine.2004.04.028. PubMed PMID: WOS:000224758200016.

66. Ruiz A, Molina JM, Gonzalez JF, Conde MM, Martin S, Hernandez YI. Immunoprotection in goats against *Haemonchus contortus* after immunization with cysteine protease enriched protein fractions. *Veterinary Research*. 2004;35(5):565-72. doi: 10.1051/vetres:2004032. PubMed PMID: WOS:000224585800005.

67. Knox D. Proteases in blood-feeding nematodes and their potential as vaccine candidates. In: Robinson MW, Dalton JP, editors. *Cysteine Proteases of Pathogenic Organisms. Advances in Experimental Medicine and Biology*. 712. Berlin: Springer-Verlag Berlin; 2011. p. 155-76.

68. McKerrow JH, Caffrey C, Kelly B, Loke P, Sajid M. Proteases in parasitic diseases. *Annual Review of Pathology-Mechanisms of Disease. Annual Review of Pathology-Mechanisms of Disease*. 1. Palo Alto: Annual Reviews; 2006. p. 497-536.

69. Todorova VK, Stoyanov DI. Partial characterization of serine proteinases secreted by adult *Trichinella spiralis*. *Parasitology Research*. 2000;86(8):684-7. doi: 10.1007/pl00008552. PubMed PMID: WOS:000088738100013.

70. Cwiklinski K, Meskill D, Robinson MW, Pozio E, Appleton JA, Connolly B. Cloning and analysis of a *Trichinella pseudospiralis* muscle larva secreted serine protease gene. *Veterinary Parasitology*. 2009;159(3-4):268-71. doi: 10.1016/j.vetpar.2008.10.036. PubMed PMID: WOS:000264038400019.

71. Rees-Roberts D, Mullen LM, Gounaris K, Selkirk ME. Inactivation of the complement anaphylatoxin C5a by secreted products of parasitic nematodes. *International Journal for Parasitology*. 2010;40(5):527-32. doi: 10.1016/j.ijpara.2009.10.006. PubMed PMID: WOS:000277107400004.

72. Zhao YM, Sun W, Zhang P, Chi H, Zhang MJ, Song CQ, et al. Nematode sperm maturation triggered by protease involves sperm-secreted serine protease inhibitor (Serpin). *Proceedings of the National Academy of Sciences of the United States of America*. 2012;109(5):1542-7. doi: 10.1073/pnas.1109912109. PubMed PMID: WOS:000299731400044.

73. Drake LJ, Bianco AE, Bundy DAP, Ashall F. Characterization of peptidases of adult *Trichuris muris*. *Parasitology*. 1994;109:623-30. doi: 10.1017/s0031182000076502. PubMed PMID: WOS:A1994PV35900010.

74. Hotez PJ, Cerami A. Secretion of a proteolytic anticoagulant by *Ancylostoma* hookworms. *Journal of Experimental Medicine*. 1983;157(5):1594-603. doi: 10.1084/jem.157.5.1594. PubMed PMID: WOS:A1983QQ38700018.
75. Kennedy MW, Corsico B, Cooper A, Smith BO. The Unusual Lipid-binding Proteins of Nematodes: NPAs, nemFABPs and FARs. In: Kennedy MW, Harnett W, editors. *Parasitic Nematodes: Molecular Biology, Biochemistry and Immunology*, 2nd Edition. Wallingford: Cabi Publishing-C a B Int; 2013. p. 397-412.
76. Iberkleid I, Vieira P, Engler JD, Firester K, Spiegel Y, Horowitz SB. Fatty Acid-and Retinol-Binding Protein, Mj-FAR-1 Induces Tomato Host Susceptibility to Root-Knot Nematodes. *Plos One*. 2013;8(5):14. doi: 10.1371/journal.pone.0064586. PubMed PMID: WOS:000320362700159.
77. Vieira P, Kamo K, Eisenback JD. Characterization and silencing of the fatty acid- and retinol-binding Pp-far-1 gene in *Pratylenchus penetrans*. *Plant Pathology*. 2017;66(7):1214-24. doi: 10.1111/ppa.12664. PubMed PMID: ISI:000409374900017.
78. Phani V, Shivakumara TN, Davies KG, Rao U. *Meloidogyne incognita* Fatty Acid- and Retinol- Binding Protein (Mi-FAR-1) Affects Nematode Infection of Plant Roots and the Attachment of *Pasteuria penetrans* Endospores. *Frontiers in Microbiology*. 2017;8. doi:10.3389/Fmicb.2017.02122. PubMed PMID: ISI:000414123500001.
79. Abreu RD, Penalva LO, Marcotte EM, Vogel C. Global signatures of protein and mRNA expression levels. *Molecular Biosystems*. 2009;5(12):1512-26. doi: 10.1039/b908315d. PubMed PMID: WOS:000271727600013.
80. Grun D, Kirchner M, Thierfelder N, Stoeckius M, Selbach M, Rajewsky N. Conservation of mRNA and Protein Expression during Development of *C.elegans*. *Cell Reports*. 2014;6(3):565-77. doi: 10.1016/j.celrep.2014.01.001. PubMed PMID: WOS:000331168400014.
81. Koussounadis A, Langdon SP, Um IH, Harrison DJ, Smith VA. Relationship between differentially expressed mRNA and mRNA-protein correlations in a xenograft model system. *Scientific Reports*. 2015;5:9. doi: 10.1038/srep10775. PubMed PMID: WOS:000356137300001.
82. White GF. A method for obtaining infective nematode larvae from cultures. *Science*. 1927;66(1709):302-3. PubMed PMID: 17749713.

83. Pham LN, Dionne MS, Shirasu-Hiza M, Schneider DS. A specific primed immune response in *Drosophila* is dependent on phagocytes. *Plos Pathogens*. 2007;3(3):8. doi: 10.1371/journal.ppat.0030026. PubMed PMID: WOS:000248495200006.
84. Heungens K, Cowles CE, Goodrich-Blair H. Identification of *Xenorhabdus nematophila* genes required for mutualistic colonization of *Steinernema carpocapsae* nematodes. *Molecular Microbiology*. 2002;45(5):1337-53. doi: DOI 10.1046/j.1365-2958.2002.03100.x. PubMed PMID: WOS:000177750400015.
85. Finn RD, Clements J, Eddy SR. HMMER web server: interactive sequence similarity searching. *Nucleic Acids Research*. 2011;39:W29-W37. doi: 10.1093/nar/gkr367. PubMed PMID: ISI:000292325300006.
86. Rawlings ND, Waller M, Barrett AJ, Bateman A. MEROPS: the database of proteolytic enzymes, their substrates and inhibitors. *Nucleic Acids Research*. 2014;42(D1):D503-D9. doi: 10.1093/nar/gkt953. PubMed PMID: WOS:000331139800075.
87. Langmead B, Trapnell C, Pop M, Salzberg SL. Ultrafast and memory-efficient alignment of short DNA sequences to the human genome. *Genome Biology*. 2009;10(3):10. doi: 10.1186/gb-2009-10-3-r25. PubMed PMID: WOS:000266544500005.
88. Ritchie ME, Phipson B, Wu D, Hu YF, Law CW, Shi W, et al. limma powers differential expression analyses for RNA-sequencing and microarray studies. *Nucleic Acids Research*. 2015;43(7):13. doi: 10.1093/nar/gkv007. PubMed PMID: WOS:000354722500005.
89. Wickham H. ggplot2: Elegant Graphics for Data Analysis. *Ggplot2: Elegant Graphics for Data Analysis*. 2009:1-212. doi: 10.1007/978-0-387-98141-3. PubMed PMID: WOS:000269437100014.
90. de Hoon MJL, Imoto S, Nolan J, Miyano S. Open source clustering software. *Bioinformatics*. 2004;20(9):1453-4. doi: 10.1093/bioinformatics/bth078. PubMed PMID: WOS:000222125600013.
91. Saldanha AJ. Java Treeview-extensible visualization of microarray data. *Bioinformatics*. 2004;20(17):3246-8. doi: DOI 10.1093/bioinformatics/bth349. PubMed PMID: WOS:000225361400039.
92. Conesa A, Gotz S, Garcia-Gomez JM, Terol J, Talon M, Robles M. Blast2GO: a universal tool for annotation, visualization and analysis in functional

genomics research. *Bioinformatics*. 2005;21(18):3674-6. doi: 10.1093/bioinformatics/bti610. PubMed PMID: 16081474.

93. Li C, Kim K. Family of FLP peptides in *Caenorhabditis elegans* and related nematodes. *Frontiers in Endocrinology*. 2014;5. doi: 10.3389/fendo.2014.00150. PubMed PMID: WOS:000209749800149.

## CHAPTER 3

### **Identification, production, and characterization of *S. feltiae* individual candidate active proteins.**

Dennis Z. Chang, Alireza S. Hamidzad, Martin Lopez, Adler R. Dillman

#### **Introduction**

In the field of entomopathogenic nematodes (EPNs), we have recently provided data that substantially shows the nematode in the EPN-bacteria duo complex is not simply the vector, actively contributes to host killing and likely host immune suppression. Crude ESP from the entomopathogenic nematodes *Steinernema carpocapsae* and *Steinernema feltiae* were shown to be toxic to insects [1, 2], which merits further exploration into the mechanism of toxicity for potential applications in EPN-derived pest control. Along with the availability of assembled genomes of multiple *Steinernema* EPNs [3], improved gene expression profiling methods of nematodes [4], and continual improvements to protein separation and mass spectrometry technologies, we are in a more favorable situation than ever before to explore the question of how nematodes contribute to killing of the host in the EPN-bacteria duo complex. To decipher the mechanism, however, we will first need to identify and characterize individual components of the ESPs responsible for toxicity.

While multiple studies of individual ESP components from entomopathogenic nematodes have been performed, they have exclusively been derived from *S. carpocapsae* [5-14]. This is not surprising, as *S. carpocapsae* is the most widely used and studied EPN due to its wide range of hosts, scalability of mass production, and ability to formulate for long-term shelf-life [15, 16]. However, narrowing the majority of studies to one species can be detrimental, as these EPNs have their limits in terms of pest control efficacy due to both host-specificity and environmental factors. *S. feltiae*, although having been considered a generalist, has a more limited host-range than *S. carpocapsae*, but it has been consistently effective against various Dipteran larvae (flies). It is one of the few EPNs that can maintain infectivity at lower temperatures (10°C), whereas *S. carpocapsae* lose infectivity below 22°C [16]. In addition, *S. feltiae* produces on average double the amount ( $\mu\text{g}$ ) of ESP than *S. carpocapsae* [1, 2]. This does not clearly translate to more toxicity per nematode *S. feltiae* over *S. carpocapsae* in our studies, however it does allow more efficient production of ESPs to work with. After profiling the components and biological activity of crude ESPs from these two species [1, 2], we move further into identifying and characterizing the individual active proteins found in the ESPs of *S. feltiae*. We do this to shed light on the important proteins utilized by other EPNs with the goal of providing knowledge that can be used in studying EPN evolution, host-range and niche

specialization of different species, and most of all, an alternative source of virulence molecules for pest control research.

## **Results**

### **ESPs components are more than just toxic**

In elucidating the active proteins of interest in crude ESPs, anion-exchange FPLC (Fast Protein Liquid Chromatography) was utilized to separate the proteins by charge. 800 µg of crude ESPs from *S. feltiae* was separated on a 1 mL HiTrap Q FastFlow (GE, Life Sciences) strong anion exchange column using a gradient of 0 M NaCl to 1 M NaCl over 60 minutes at a rate of 0.5 mL/min. The flow-through was collected into 500 µL fractions and eluted protein was collected into 200 µL fractions. The FPLC chromatogram (Fig 7A) shows the fractions that were desalted and concentrated down to 20-30 µL volumes (red circles), of which 50 nL was injected into each of 10-15 adult *D. melanogaster* flies. Approximately 15 ng of protein from each tested fraction was injected into the individual flies. We found that fractions 42 and 37 showed high toxicity, killing the flies within 24 hours (Fig 7B) similar to the toxicity levels of crude ESPs (Chapter 2, Fig 3D). Fraction 27 exhibited some toxicity but relatively less than 37 or 42. The other fractions that were tested were less toxic than fractions 37 or 42, with fractions 14 and 55 showing toxicity levels more similar to PBS control (Fig 7B). The initial flow-through was also tested but no toxicity was observed (Data not shown).

Both fractions 42 and 37 were of interest due to their high toxicity, but an additional observation was made regarding the injection of fraction 42; flies injected with fraction 42 exhibited strong dark coloration indicative of melanization (Fig 7C). This whole-body darkening is not typically seen when injecting the flies with crude ESPs, suggesting that the crude ESPs contained molecules that suppressed melanization, leading us to hypothesize that fraction 42 contains active toxins without the melanization inhibitors. For this reason,

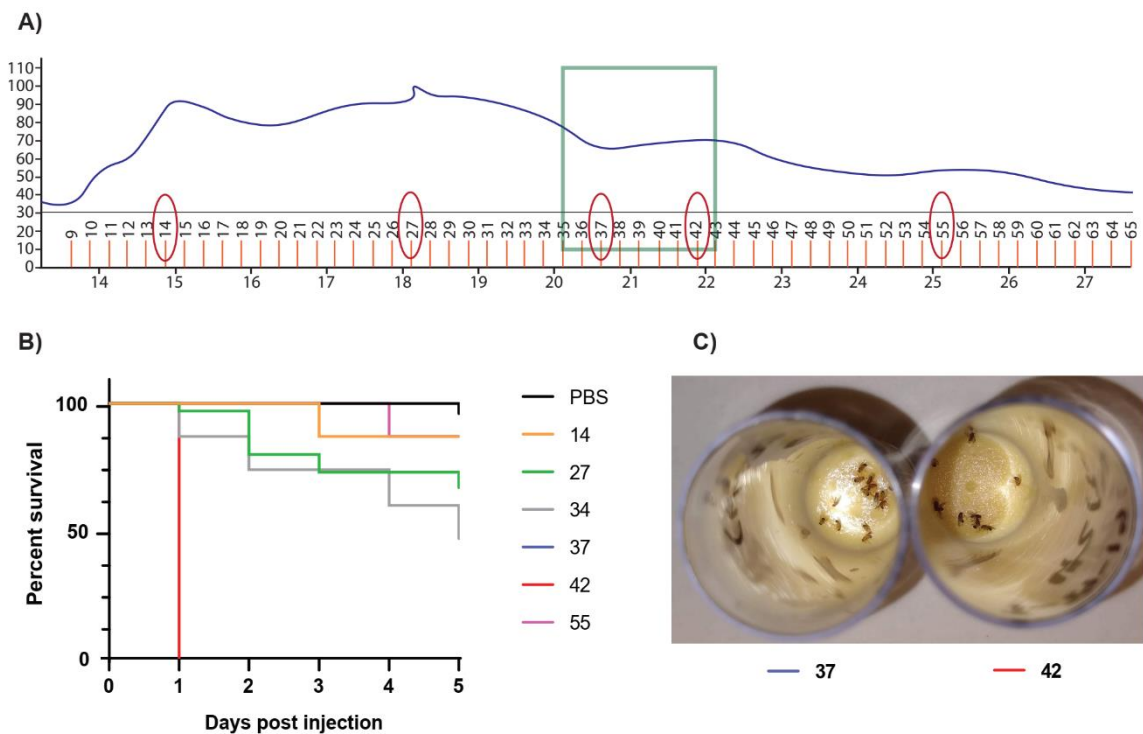


**Figure 7. Fractionation of crude ESPs from *S. feltiae* and toxic fractions.** (A) The FPLC chromatogram of 800  $\mu$ g of crude *S. feltiae* ESPs eluted off of a 1 mL strong anion exchange column. The y-axis represent relative UV absorbance readings and x-axis represents mLs of elution buffer with increasing NaCl molarity. The red bars and associated number represents each 200  $\mu$ L fraction collected. (B) Survival curve of adult *D. melanogaster* flies injected with approximately 15 ng of protein from their associated fraction number over 5 days after one initial injection. (C) Dead flies 24 hours post-injection with either fraction 37 (left) or 42 (right).

fraction 42 was prioritized for further investigation of the activity/toxins proteins in *S. feltiae* ESPs.

Although the FPLC chromatograms showed peaks that were not clean, single peaks, the data does show that protein bound to the column and eluted off based on the increasing salt gradient. This suggests that the active fractions consisted of the toxin proteins that have been at least somewhat separated from non-toxic proteins and therefore should be relatively enriched in quantity compared to the crude mixture. We therefore ran mass spectrometry on the original crude ESP and the toxic fraction to compare their protein composition in both protein identities and quantity.

### **Separation of crude ESPs reveals a complex toxic fraction**

Around 500 unique proteins were detected in both the crude ESP and the isolated toxic fraction. Comparing the most abundant proteins identified by mass spectrometry there are consistencies between the crude (Fig 8A) and the active fraction (Fig 8B) such as peptidases, EGF-like, protease inhibitors, and Allergen\_V5 proteins. Differences at the lower end include lysozyme-like proteins and ShKT domains higher in the crude ESPs and more Saposins and Ig-like domains in the fraction. To analyze protein enrichment directly, we compared the relative abundance of specific proteins found in both crude and fraction and focused on the proteins that increased dramatically in the toxic fraction (Table 1)

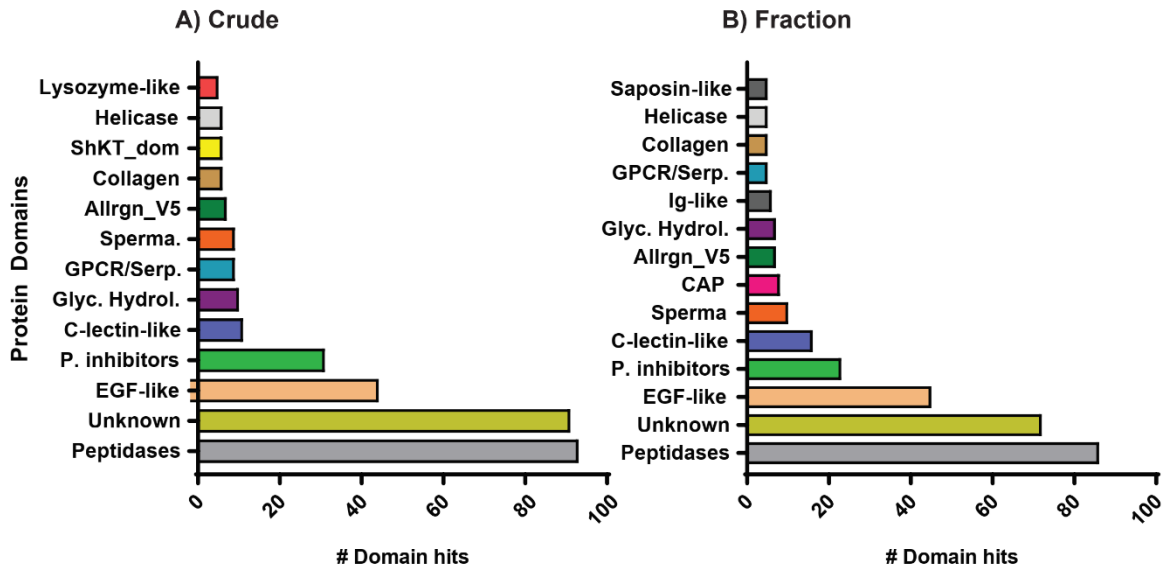


**Figure 8. Protein composition of the toxic fraction compared to crude.** Top protein domains (5 or more hits) detected by pFAM analysis in crude ESPs (A) and toxic fraction 42 (B). E-value <math><10e-5</math>. Terms: P. inhibitor = protease inhibitors, Glyc. Hydrol. = Glycosyl hydrolases, Sperma. = Spermadhesins.

Gene	Avg. Mass	Crude Area	Fraction Area	Enrichment Ratio	Domain
L889_g11860.t1	55868	2.70E+05	6.99E+07	<b>258.89</b>	Integrin
L889_g26971.t1	79875	4.90E+06	1.24E+09	<b>253.06</b>	C-type lectin
L889_g27103.t1	48374	4.92E+04	9.70E+06	<b>197.15</b>	SCOP
L889_g16874.t1	34570	7.75E+07	2.85E+09	<b>36.77</b>	Serine protease
L889_g16227.t1	49865	6.42E+06	2.10E+08	<b>32.71</b>	Metallo protease
L889_g10825.t1	105998	3.64E+07	1.00E+09	<b>27.47</b>	Glycosyl hydrolase
L889_g6506.t1	11865	5.25E+09	1.30E+11	<b>24.76</b>	SCP
L889_g12678.t1	154820	4.67E+06	1.07E+08	<b>22.91</b>	Metallo protease
L889_g27243.t1	30937	1.71E+08	3.84E+09	<b>22.46</b>	Serine protease
L889_g18285.t1	84022	7.05E+07	1.43E+09	<b>20.28</b>	C-type lectin
L889_g7998.t1	34924	9.31E+05	1.84E+07	<b>19.76</b>	Unknown
L889_g31534.t1	32394	3.09E+06	4.46E+07	<b>14.43</b>	Amino oxidase
L893_g13820.t2	39390	1.09E+06	1.56E+07	<b>14.31</b>	14-3-3
L889_g19899.t1	37106	5.17E+07	7.19E+08	<b>13.91</b>	Metallo protease
L889_g22646.t1	17269	2.81E+07	2.98E+08	<b>10.60</b>	PLA2/ Phospholipase
L889_g5185.t1	31934	7.54E+08	7.67E+09	<b>10.17</b>	Serine protease

**Table 1. Enrichment of proteins in the toxic fraction compared to crude.** A relative abundance enrichment ratio was calculated for proteins found in both crude and the toxic fraction. The enrichment ratio was calculated by dividing the relative abundance of the protein in the fraction by the relative abundance in the crude. Larger ratios indicate higher relative abundance enrichment after protein FPLC separation. Proteins indicated by green are the proteins which we have made the most progress.

## Expression of EPN proteins in a bacterial system

To express candidate active proteins, primers were designed for the genes Sf-PLA2 (a 17 kDa phospholipase), Sf-Tryp (a 35 kDa Trypsin-like serine protease, and Sf-GH (a 100 kDa glycosyl hydrolase). The genes were PCR amplified from *S. feltiae* cDNA, cloned into the pETDuet-1 E. coli vector (71146, EMD Millipore) and induced for protein expression at 20°C. 'Total' lysate and 'soluble' lysate samples were taken and screened for protein expression by SDS coomassie stained gel. 20- and 24-hour induction times resulted in similarly high expression of the candidate proteins in the total lysate (Fig 9A, indicated in white circles)

however expression was significantly lower in the soluble lysate (Fig 9C). To verify expression of the 6xHis-tag with the proteins the gels were His-tag stained before Coomassie staining (Fig 9B, indicated in red circles).

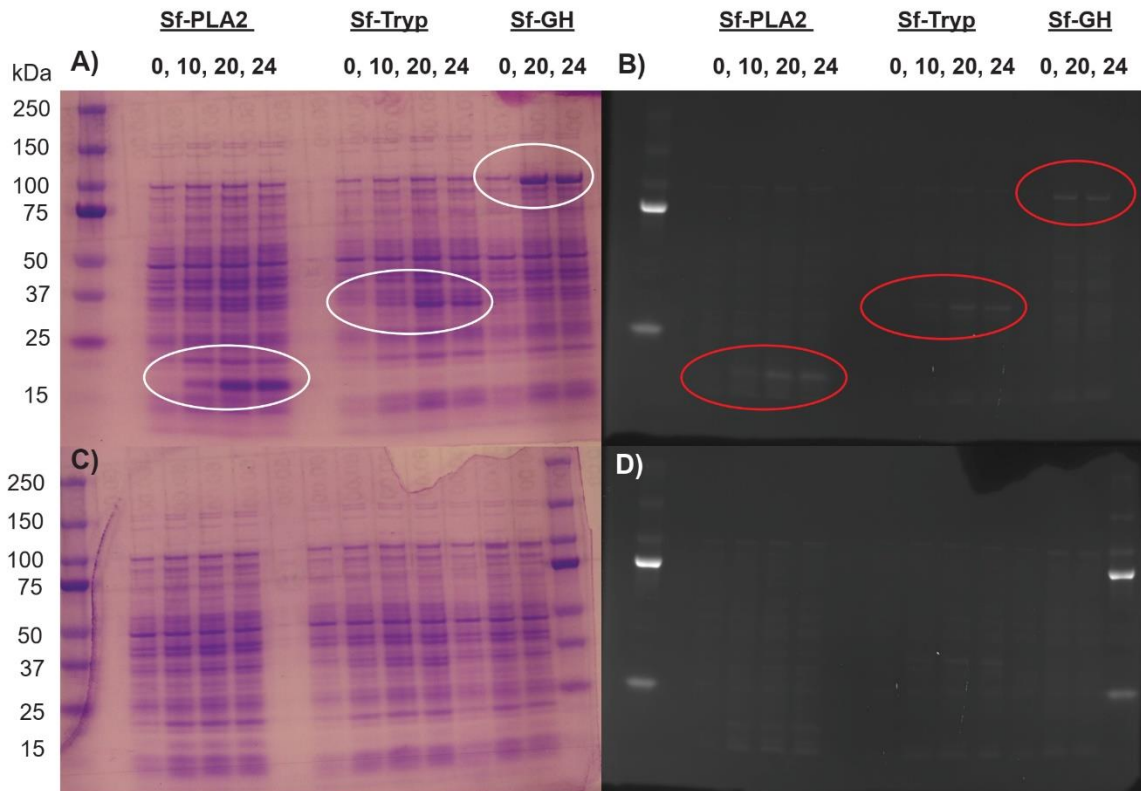


**Figure 9. Expression of candidate active proteins.** Shuffle T7 *E. coli* cells were transformed with the pETDUET-1 vector containing either genes Sf-PLA2 ( Phospholipase, 17 kDa), Sf-Tryp, Trypsin-like, 35 kDa), or Sf-GH (Glycosyl Hydrolase, 100 kDa). The bacteris was grown to 0.6 OD<sub>600</sub> and induced with 0.5 mM IPTG for either 0, 10, 20, or 24 hours before running the total lysate (A) and soluble lysate (C) on an SDS gel. Before Coomassie staining the gels were His-tag stained to check for 6x-his-tag expression of the proteins for the corresponding total lysate set (B) and soluble set (D).

Since expression in the soluble portion of the lysate was very low for all three proteins, we chose to focus on purification of the proteins from the total lysate. This meant that most of the proteins were aggregating into inclusion bodies and would require denaturation and refolding. In preparing the total lysate for denaturation the samples were initially sonicated to remove cell debris, followed by brief sonication with 1% Triton-X to wash the inclusion bodies. This resulted in removal of most of the excess protein while retaining the majority of the expressed proteins (Fig 10A). These samples were then solubilized in denaturing buffer (8 M Urea, 50 mM Tris) and refolded through dialysis in the refolding buffer (1 M Urea, 50 mM Tris, 3 mM L-glutathione reduced, 1 mM L-glutathione oxidized, 5 mM CaCl<sub>2</sub>) at 4°C overnight. The samples were then dialyzed into the final buffer (50 mM Tris, 5 mM CaCl<sub>2</sub>) to remove the urea. His-tag purification attempts have been made but have not been very successful. Along with this and time restraint, only the serine protease Sf-Tryp has been characterized for activity. Sf-PLA<sub>2</sub>, a phospholipase, will be characterized for lipid metabolism activity and Sf-GH, a glycosyl hydrolase, will be characterized for carbohydrate metabolism however that data will not be part of this dissertation.

### **A serine protease highly enriched in the ESP of *S. feltiae***

Since Sf-Tryp is predicted to be a trypsin-like protease we characterized it for protease activity on succinylated casein. 200 µg of succinylated casein was

mixed with 20  $\mu\text{g}$  of Sf-Tryp and TNBSA. This was compared to the control of 20  $\mu\text{g}$  of Sf-Tryp and TNBSA only (Fig 10B). If proteolytic activity occurred on the casein, its free amine groups would be exposed and the TNBSA will bind to the free amines allowing absorption readings at 250 nm. Fig 10B shows increased absorption readings of the Sf-Tryp + casein compared to the protease alone. Since his-tag purification has not been successful and 2 unknown protein bands consistently found between 32-46 kDa (Fig 10A) are still present in the sample we cannot be confident yet that the protease activity observed is strictly due to Sf-Tryp. To circumvent this, we assayed the Sf-PLA2 sample for protease activity. Sf-PLA2 is a phospholipase and should not have any proteolytic activity and the sample contains comparable amounts of the unknown proteins (Fig 10A). 20  $\mu\text{g}$  of the Sf-PLA2 sample was prepared as described previously and absorption readings were similar between the Sf-PLA2 only and the Sf-PLA2 + casein samples with no significant differences, indicating lack of proteolytic activity.

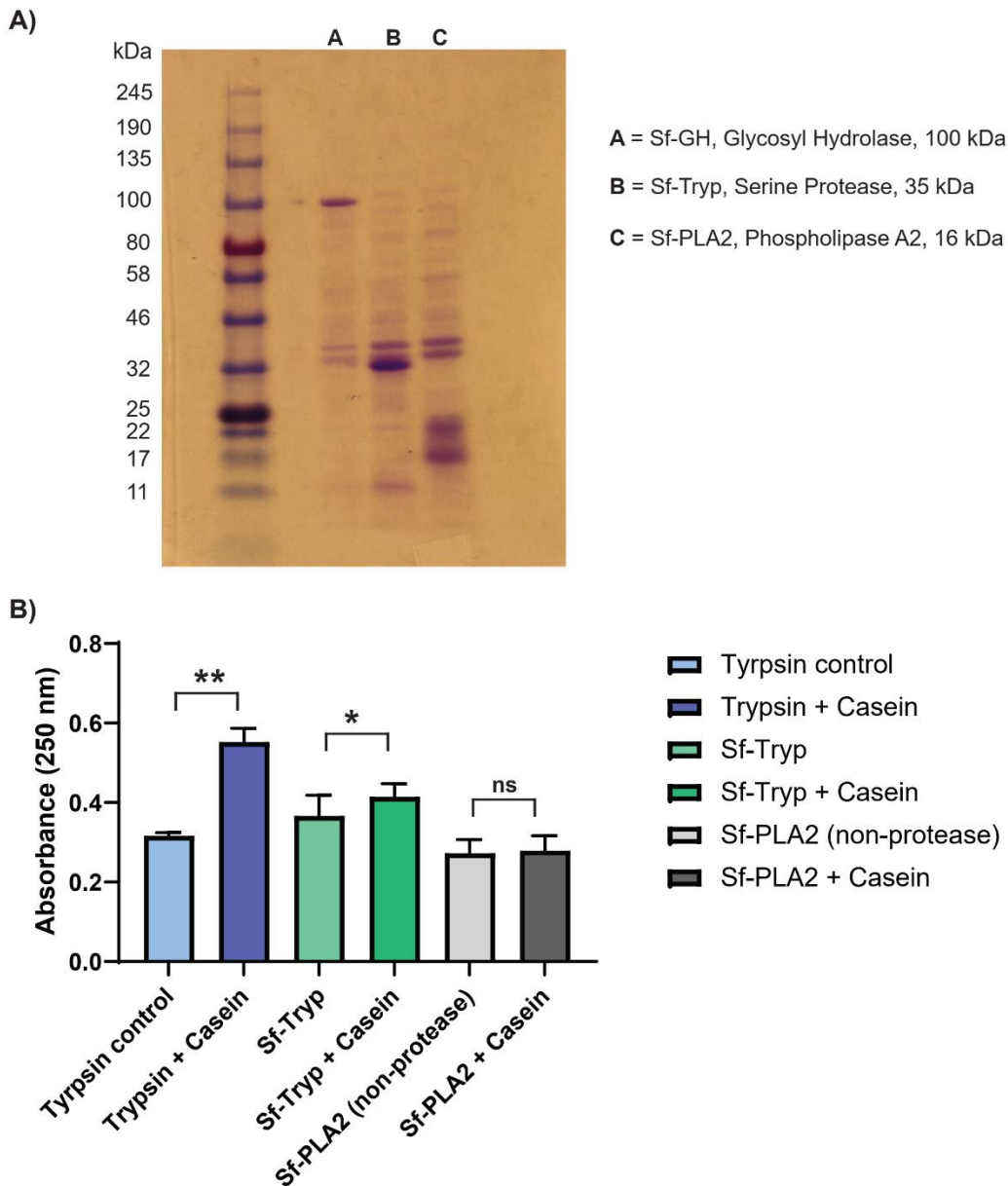


**Figure 10. Washing of inclusion bodies and Activity of serine protease Sf-Tryp.** The total cell lysate of *E. coli* cells expressing either (A-A) Sf-GH, 100 kDa glycol hydrolase, (A-B) Sf-Tryp, 35 kDa serine protease, or (A-C) Sf-PLA2, 17 kDa phospholipase. The totally lysate was sonicated initially to lyse the cells then sonicated a 2<sup>nd</sup> time with 1% triton-x. (B) Proteolytic activity assay of the samples containing Sf-Tryp and Sf-PLA2 (non-protease). Absorbion readings are of 3 technical replicates and paired T-test was used for the statistical analysis.

## Discussion

Fractionation of crude ESPs from *S. feltiae* and *in vivo* biological activity of those fractions reveals that the ESP components are likely more than just toxic. The active components of the ESPs are expected to be involved in both toxic [1, 2] and immunomodulatory mechanisms. Previous injections of crude ESPs into fruit flies have consistently shown flies dying without any change in overall color. However, injection of 15 ng of proteins from fraction 42 in this study resulted in dead flies exhibiting a dark color (Fig 9C). We think that this is the result of melanization, a form of quick-acting innate immune response, used by insects when wounded or when infected by pathogens. Since this response is typically not seen in flies injected with crude ESPs and was also not observed in other toxic fractions, we hypothesize that fraction 42 contains the toxic components without the melanization inhibitors. For these reasons, we focused on fraction 42 in our efforts to identify candidate toxic proteins. Comparisons of proteins found in toxic fractions (w/ melanization inhibitors) to toxic fractions (w/o melanization inhibitors) would be a very interesting direction of research. However, the scope of this study was on proteins found in fraction 42 (toxic fraction w/o melanization inhibitors) in order to focus on identifying the toxic components.

Since we were able to separate crude ESPs into toxic and non-toxic fractions, it is likely that the abundance of toxic components have increased/enriched in the toxic fractions relatively compared to the crude. We set 2 criteria in making our

list likely candidate active proteins 1) detected in both crude and the toxic fraction, and 2) relative abundance increased by a factor of 10 or more from the crude to the fraction (Table 1). From this list, two proteins have been successfully expressed in an *E. coli* expression system (Sf-PLA2, a predicted 17 kDa phospholipase, & Sf-GH, a 100 kDa, glycosyl hydrolase) and one (Sf-Tryp, a predicted 35 kDa trypsin-like serine protease) has been profiled for enzyme activity at the time of this dissertation (Fig 10A & 10B). Further purification of Sf-Tryp is required in order to better characterize the degree of proteolytic activity, however significant proteolytic activity compared to a non-protease protein (produced in the same type of plasmid vector and cell line) indicates proper expression/folding/function of this EPN protein. The possibility of this serine protease having toxic properties remains to be determined, but past studies of individual EPN proteases generally point towards immunomodulation, where they have been shown or at least implicated in impairing hemolymph clot formation [11], suppression of phenoloxidase activity [5], and inhibition of host hemolymph melanization [8].

### **Expression of EPN proteins in a bacterial system**

To express candidate active proteins, primers were designed for the genes Sf-PLA2 (a 17 kDa phospholipase), Sf-Tryp (a 35 kDa Trypsin-like serine protease, and Sf-GH (a 100 kDa glycosyl hydrolase). The genes were PCR amplified from *S. feltiae* cDNA, cloned into the pETDuet-1 *E. coli* vector (71146, EMD Millipore)

and induced for protein expression at 20°C. 'Total' lysate and 'soluble' lysate samples were taken and screened for protein expression by SDS coomassie stained gel. 20- and 24-hour induction times resulted in similarly high expression of the candidate proteins in the total lysate (Fig 9A, indicated in white circles) however expression was significantly lower in the soluble lysate (Fig 9C). To verify expression of the 6xHis-tag with the proteins the gels were His-tag stained before Coomassie staining (Fig 9B, indicated in red circles).

### **A serine protease highly enriched in the ESP of *S. feltiae***

This resulted in removal of the majority of excess protein while retaining the majority of the expressed proteins (Fig 10A). These samples were then solubilized in denaturing buffer (8 M Urea, 50 mM Tris) and refolded through dialysis in the refolding buffer (1 M Urea, 50 mM Tris, 3 mM L-glutathione reduced, 1 mM L-glutathione oxidized, 5 mM CaCl<sub>2</sub>) at 4°C overnight. The samples were then dialyzed into the final buffer (50 mM Tris, 5 mM CaCl<sub>2</sub>) to remove the urea. His-tag purification attempts have been made but have not been very successful. Along with this and time constraints, only the serine protease Sf-Tryp has been characterized for activity. Sf-PLA<sub>2</sub>, a phospholipase, will be characterized for lipid metabolism activity and Sf-GH, a glycosyl hydrolase, will be characterized for carbohydrate metabolism however that data will not be part of this dissertation,

Since Sf-Tryp predicted to be a trypsin-like protease we characterized it for protease activity on succinylated casein. 200 µg of succinylated casein was mixed with 20 µg of Sf-Tryp and TNBSA. This was compared to the control of 20 µ of Sf-Tryp and TNBSA only (Fig 10B). If proteolytic activity occurred on the casein, its free amine groups would be exposed and the TNBSA will bind to the free amines allowing absorption readings at 250 nm. Fig 10B shows increased absorption readings of the Sf-Tryp + casein compared to the protease alone. Since his-tag purification has not been successful and 2 unknown protein bands consistently found between 32-46 kDa (Fig 10A) are still present in the sample we cannot be confident yet that the protease activity observed is strictly due to Sf-Tryp. To circumvent this, we assayed the Sf-PLA2 sample for protease activity. Sf-PLA2 is a phospholipase and should not have any proteolytic activity and the sample contains comparable amounts of the unknown proteins (Fig 10A). 20 µg of the Sf-PLA2 sample was prepared as described previously and absorption readings were similar between the Sf-PLA2 only and the Sf-PLA2 + casein samples with no significant differences, indicating lack of proteolytic activity.

## **Methods**

### **Fast Protein Liquid Chromatography (FPLC)**

800 µg of crude *S. feltiae* ESPs was collected in PBS and verified for toxicity as previously described (chapter 2 methods). The collection was then buffer

exchanged into 1 mL of equilibration buffer (20 mM Tris-HCl, pH 8.5, 0 M NaCl). The crude ESP was bound to a HiTrap Q FF 1 mL anion exchange column (1750530, GE Life Science) and eluted at a rate of 0.5 mL/min with a gradient of 0 to 100% elution buffer (20 mM Tris-HCl, pH 8.5, 1 M NaCl) in 60 minutes. Protein elutions detected by UV absorbance were collected into 250  $\mu$ L fractions. FPLC was done using an Amersham Biosciences AKTA FPLC System (P-920 pump, UPC-900 monitor, Frac-920 fraction collector, and UNICORN 5.31 Workstation Software) graciously lent to us for use from Sarjeet S. Gill, Ph.D. University of California, Riverside.

### **Fruit fly injections**

Select fractions of crude ESPs were concentrated down to approximately 30  $\mu$ L using 3 kDa cut-off centrifugal filters (UFC500324, EMD Millipore) and desalted by 4-5 rounds of filtering with fresh 20 mM Tris buffer (no NaCl). The protein concentrations were quantified by Bradford assay. 15 ng was injected into each fly (see chapter 2 methods) and observed for 5 days post-injection.

### **Mass spectrometry and relative abundance enrichment analysis.**

Crude ESP proteins and proteins from the toxic fraction (derived from the same batch of crude ESP) were analyzed by mass spectrometry using the Orbitrap Fusion Lumos Tribrid system (Thermo Scientific) at the Biomolecular and Proteomics Mass Spectrometry Facility at the University of California, San Diego

(Funding source: NIH Grant S10 OD021724). The mass spectrometry analysis parameters were set as previously described (chapter 2 methods [1, 2]) and protein relative abundance quantification was obtained using the Maxquant LFQ algorithm [3]. For the relative abundance enrichment analysis, a relative abundance enrichment ratio was obtained for each gene/protein by dividing the relative abundance of protein 'X' in the toxic fraction over the relative abundance of protein 'X' in the crude ESPs. Proteins with abundance enrichment ratios of 10 or higher were deemed significant and considered for further experimentation.

### **Gene cloning and protein expression in *E. coli***

The candidate active genes were PCR amplified from *S. feltiae* cDNA and cloned into the pETDuet-1 *E. coli* vector (71146, EMD Millipore) at the BamHI and HindIII restrictions sites using the NEBuilder HiFi DNA Assembly Cloning Kit (E5520, New England Biolabs). Sequence and orientation of the plasmid constructs were verified by sanger sequencing.

Primers list:

Gene	Protein		Primers
L889_g22646	Sf-PLA2	Fwd	accatcatcaccacagccagATCAGGAAGAACGTCTTCGC
		Rev	ttaagcattatgcgccgcaTTAGTTGTGAAATTGCAGTGGTTTCC
L889_g16874	Sf-Tryp	Fwd	accatcatcaccacagccagCATCCAGTCAAGGAACTCGTC
		Rev	ttaagcattatgcgccgcaTCAAAATGTTGTCAAATGTTCTTCAGAC
L889_g10825	Sf-GH	Fwd	accatcatcaccacagccagCGACTCGGTCCGACGG
		Rev	ttaagcattatgcgccgcaTCACTCATTCTGCCACTCAATCT

The plasmids were transformed into Shuffle T7 *E. coli* cells (C3026J, New England Biolabs) following the manufacturer's protocol and cultured at 30 °C.

The culture was diluted to OD<sub>600</sub> = 0.6 and protein expression was induced with 0.5 mM IPTG at 20°C for 10, 20, or 24 hours.

### **Protein lysate preparation and His-tag staining**

For small scale lysate preparation and protein expression screening; 1 mL of induced bacteria culture was spun down at 12,000 rpm for 5 minutes and the pellet was mixed with 600 µL of 50 mM Tris, pH = 8 buffer. The mixture was sonicated 2x at 50% power, 1 sec on, 1 sec off, for 1 minute (on ice). A sample was taken for 'Total' lysate screening before spinning down at 16,000 x g for 5 minutes to sample the supernatant for 'Soluble' lysate screening. Total and soluble lysate samples were mixed at a 1:3 ratio (4x Laemmli SDS buffer: Lysate) and heated at 95°C for 7 minutes before loading and running on an SDS protein electrophoresis gel. His-staining for the 6x-his tag on expressed proteins in the SDS gel was done using the InVision His-Tag In-Gel Stain (LC6030, ThermoFisher Scientific) following the manufacturer's protocol and visualized on a UV imager before moving on to Coomassie staining. For larger scale lysate preparation; 50 mL of induced bacteria was spun down at 5000 x g for 15 minutes and the pellet was mixed with 8 mL of 50 mM Tris, pH=8 buffer. The mixture was sonicated 3x at 50% power, 10 seconds on, 5 seconds off, for 5 minutes (on ice). The lysate was spun down at 16,000 x g for 10 minutes to pellet the protein debris and the supernatant was removed. The pellet material containing the protein inclusion bodies was washed by sonication 1x at 50%

power, 1 sec on, 1 sec off, for 1 minute in 5 mL of 1% triton-X. The samples were then spun down to pellet the inclusion bodies and washed with 50 mM Tris buffer. This was repeated 2 more times.

### **Protein Denaturation and Refolding**

Before protein denaturation, the washed protein inclusion bodies were assayed by Bradford for approximate protein concentration. The samples were then spun down at 16,000 x g to pellet the inclusion bodies and solubilized in denaturing buffer (8 M Urea, 20 mM DTT, 50 mM Tris, pH 8) to reach a final protein concentration of 200 µg/mL. The mixture was rotated at 4°C for 1-hour. For protein refolding we dialyzed (71509-3, EMD Millipore) the denatured proteins with the refolding buffer (1 M Urea, 3 mM L-glutathione reduced, 1 mM L-glutathione oxidized, 5 mM CaCl<sub>2</sub>, 50 mM Tris, pH 8) followed by further dialysis into the final buffer (50 mM CaCl<sub>2</sub>, 50 mM Tris, pH 8). All dialysis steps were done at 4°C.

### **Protease Assay**

Protease activity was profiled using the Pierce Colorimetric Protease Assay Kit (23263, ThermoFisher Scientific) following the manufacture's protocol. 20 µg of candidate proteins were assayed, and the activity was compared to 20 µg of the manufacturer provided Trypsin positive control. Statistical analysis was done with the Student's parametric T-test comparing enzyme/protein + substrate activity to

their enzyme/protein only controls using the GraphPad Prism 8 software. One significance star =  $p < 0.05$ .

### Supplemental Information/Figures

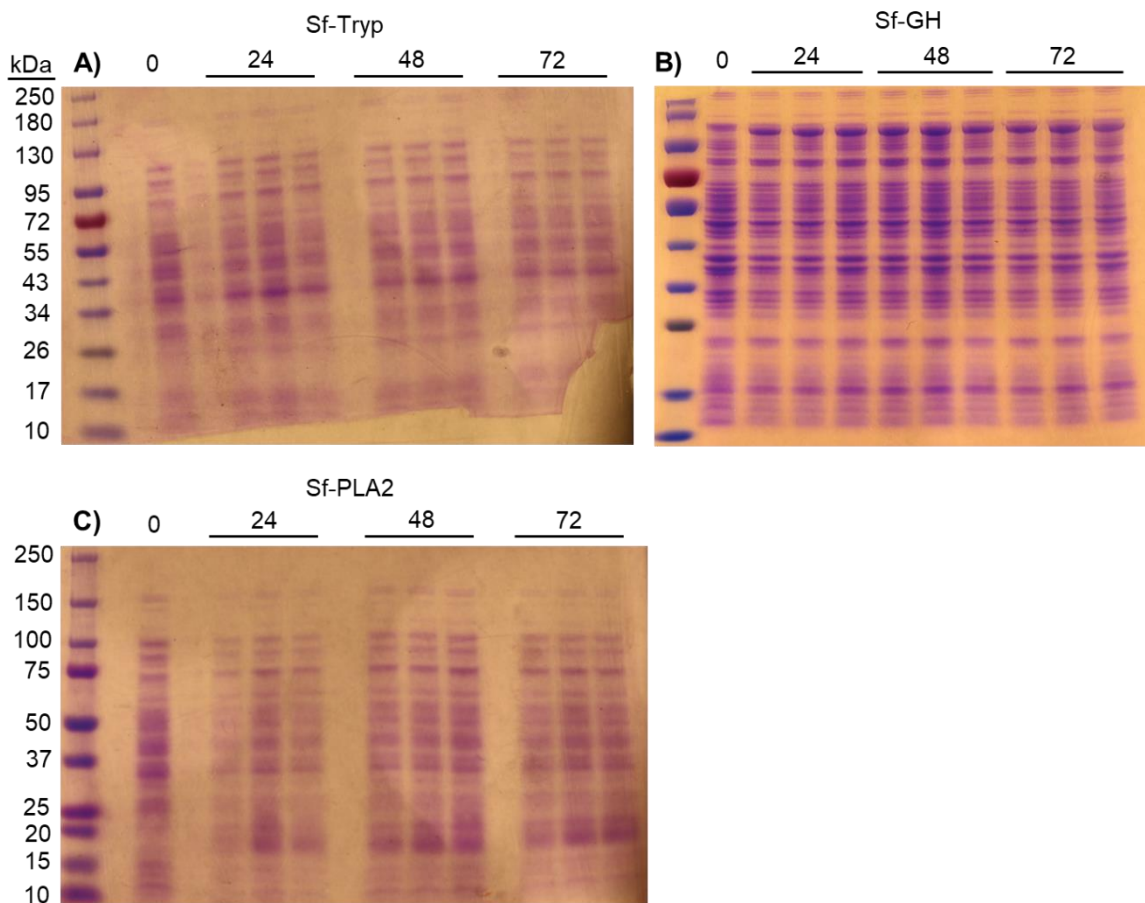


**Figure 11, Supplemental: Optimization of protein expression induction time.** The optimal time of protein expression induction for each gene was determined by inducing 3 replicates at time points 24, 48, or 72 hours of exposure to IPTG (Isopropyl  $\beta$ -d-1-thiogalactopyranoside). 1 mL of *E. coli* cells at  $OD_{600} = 0.6$  was induced with  $0.5 \mu\text{M}$  IPTG for the noted hours before lysis and prep for SDS-gel electrophoresis. Each time point consists of 3 biological replicates with 12  $\mu\text{L}$  of total cell lysate in each lane for (A) Sf-Tryp (35 kDa), (B) Sf-GH (100 kDa), and (C) Sf-PLA2 (17 kDa)

## References

1. Lu DH, Macchietto M, Chang D, Barros MM, Baldwin J, Mortazavi A, et al. Activated entomopathogenic nematode infective juveniles release lethal venom proteins. *PLoS Pathog.* 2017;13(4):31. doi: 10.1371/journal.ppat.1006302. PubMed PMID: WOS:000402555700018.
2. Chang DZ, Serra L, Lu D, Mortazavi A, Dillman AR. A core set of venom proteins is released by entomopathogenic nematodes in the genus *Steinernema*. *PLoS Pathog.* 2019;15(5):e1007626. doi: 10.1371/journal.ppat.1007626.
3. Dillman AR, Macchietto M, Porter CF, Rogers A, Williams B, Antoshechkin I, et al. Comparative genomics of *Steinernema* reveals deeply conserved gene regulatory networks. *Genome Biol.* 2015;16:200. doi: 10.1186/s13059-015-0746-6. PubMed PMID: 26392177; PubMed Central PMCID: PMC4578762.
4. Serra L, Chang D, Macchietto M, Williams K, Murad R, Lu D, et al. Adapting the Smart-seq2 Protocol for Robust Single Worm RNA-seq. *Bio-protocol.* 2018;8(4):e2729. doi: 10.21769/BioProtoc.2729.
5. Balasubramanian N, Hao YJ, Toubarro D, Nascimento G, Simoes N. Purification, biochemical and molecular analysis of a chymotrypsin protease with prophenoloxidase suppression activity from the entomopathogenic nematode *Steinernema carpocapsae*. *Int J Parasit.* 2009;39(9):975-84. doi: 10.1016/j.ijpara.2009.01.012. PubMed PMID: ISI:000267569000004.
6. Balasubramanian N, Nascimento G, Ferreira R, Martinez M, Simoes N. Pepsin-like aspartic protease (Sc-ASP155) cloning, molecular characterization and gene expression analysis in developmental stages of nematode *Steinernema carpocapsae*. *Gene.* 2012;500(2):164-71. doi: 10.1016/j.gene.2012.03.062. PubMed PMID: WOS:000304511300002.
7. Balasubramanian N, Toubarro D, Nascimento G, Ferreira R, Simoes N. Purification, molecular characterization and gene expression analysis of an aspartic protease (Sc-ASP113) from the nematode *Steinernema carpocapsae* during the parasitic stage. *Molecular and Biochemical Parasitology.* 2012;182(1-2):37-44. doi: 10.1016/j.molbiopara.2011.12.001. PubMed PMID: WOS:000301473400005.
8. Balasubramanian N, Toubarro D, Simoes N. Biochemical study and *in vitro* insect immune suppression by a trypsin-like secreted protease from the nematode *Steinernema carpocapsae*. *Parasite Immunol.* 2010;32(3):165-75. doi: 10.1111/j.1365-3024.2009.01172.x. PubMed PMID: WOS:000274412600001.

9. Hao YJ, Montiel R, Nascimento G, Toubarro D, Simoes N. Identification and expression analysis of the *Steinernema carpocapsae* elastase-like serine protease gene during the parasitic stage. *Exp Parasitol*. 2009;122(1):51-60. doi: 10.1016/j.exppara.2009.01.014. PubMed PMID: WOS:000265463600009.
10. Jing YJ, Toubarro D, Hao YJ, Simoes N. Cloning, characterisation and heterologous expression of an astacin metalloprotease, Sc-AST, from the entomoparasitic nematode *Steinernema carpocapsae*. *Molecular and Biochemical Parasitology*. 2010;174(2):101-8. doi: 10.1016/j.molbiopara.2010.07.004. PubMed PMID: WOS:000283697900002.
11. Toubarro D, Avila MM, Hao YJ, Balasubramanian N, Jing YJ, Montiel R, et al. A Serpin Released by an Entomopathogen Impairs Clot Formation in Insect Defense System. *Plos One*. 2013;8(7):12. doi: 10.1371/journal.pone.0069161. PubMed PMID: WOS:000322064300088.
12. Toubarro D, Avila MM, Montiel R, Simoes N. A Pathogenic Nematode Targets Recognition Proteins to Avoid Insect Defenses. *Plos One*. 2013;8(9):13. doi: 10.1371/journal.pone.0075691. PubMed PMID: WOS:000325423500086.
13. Toubarro D, Lucena-Robles M, Nascimento G, Costa G, Montiel R, Coelho AV, et al. An apoptosis-inducing serine protease secreted by the entomopathogenic nematode *Steinernema carpocapsae*. *Int J Parasit*. 2009;39(12):1319-30. doi: 10.1016/j.ijpara.2009.04.013. PubMed PMID: WOS:000269598100003.
14. Toubarro D, Lucena-Robles M, Nascimento G, Santos R, Montiel R, Verissimo P, et al. Serine Protease-mediated Host Invasion by the Parasitic Nematode *Steinernema carpocapsae*. *Journal of Biological Chemistry*. 2010;285(40):30666-75. doi: 10.1074/jbc.M110.129346. PubMed PMID: WOS:000282135500035.
15. Shapiro-Ilan DI, Gouge DH, Piggott SJ, Fife JP. Application technology and environmental considerations for use of entomopathogenic nematodes in biological control. *Biol Control*. 2006;38(1):124-33. doi: <https://doi.org/10.1016/j.biocontrol.2005.09.005>.
16. Shapiro-Ilan DI, Gaugler R. Rhabditida: *Steinernematidae* & *Heterorhabditidae* [Digital]. [cited 2019]. Available from: <https://biocontrol.entomology.cornell.edu/pathogens/nematodes.php>.
17. Cox J, Hein MY, Luber CA, Paron I, Nagaraj N, Mann M. Accurate proteome-wide label-free quantification by delayed normalization and maximal peptide ratio extraction, termed MaxLFQ. *Molecular & cellular proteomics : MCP*.

2014;13(9):2513-26. Epub 2014/06/17. doi: 10.1074/mcp.M113.031591. PubMed  
PMID: 24942700

## Chapter 4

### **A revised adaptation of the Smart-seq2 protocol for single nematode RNA-seq**

Dennis Z. Chang<sup>1†</sup>, Lorryne Serra<sup>2†</sup>, Dihong Lu<sup>1</sup>, Ali Mortazavi<sup>2\*</sup>, and Adler Dillman<sup>1\*</sup>

<sup>1</sup>Department of Nematology, University of California, Riverside, California, USA;

<sup>2</sup>Department of Developmental and Cell Biology, Center for Complex Biological Systems, University of California, Irvine, California, USA.

†Equal contribution.

\*For correspondence: [adlerd@ucr.edu](mailto:adlerd@ucr.edu), [ali.mortazavi@uci.edu](mailto:ali.mortazavi@uci.edu)

This chapter is an updated version of Serra, et al. *Bio-protocol*, 2018 and has been submitted for manuscript review/publication at the time of this dissertation.

Serra L, Chang D, Macchietto M, Williams K, Murad R, Lu D, et al. Adapting the Smart-seq2 Protocol for Robust Single Worm RNA-seq. *Bio-protocol*.

2018;8(4):e2729. doi: 10.21769/BioProtoc.2729.

## **Abstract**

The advancement of transcriptomic studies in plant-parasitic nematodes will greatly benefit from the development of single nematode RNA-seq methods. Since many plant-parasitic nematodes are obligate parasites, it is often difficult to obtain sufficient numbers of nematodes for transcriptomic studies. Here we have adapted SMART-Seq2 for single-nematode RNA-seq requiring only an individual nematode for a sample replicate. This protocol provides a detailed step-by-step procedure of the RNA-seq workflow starting from lysis of the nematode to quantification of transcripts using a user-friendly online platform.

## **Introduction**

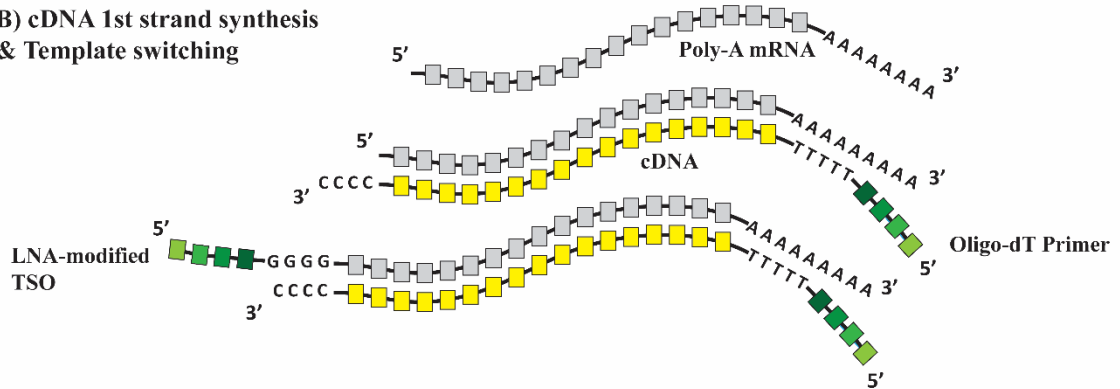
Studying the transcriptomic changes in organisms is becoming much more widespread and seemingly the standard as the molecular window to view the biology of organisms. RNA-seq methods and technology have been continually developed and improved. Current RNA-seq work-flows follow a few basic steps: 1) lysis of cells to access the RNA and often purification of the RNA, 2) cDNA synthesis using reverse transcriptase, typically a modified M-MLV (Moloney-Murine Leukemia Virus reverse transcriptase [1], 3) amplification of the cDNA by PCR, and 4) sequencing of the DNA. One of the more popular methods is known as the SMART-Seq (Switching Mechanism at the 5' end of the RNA transcript) [2, 3] with an updated iteration called SMART-Seq2 [4, 5]. M-MLV reverse transcriptase is known to add additional cytosines to the 3' end of the

synthesized cDNA after transcribing the template RNA and SMART-Seq targets these additional nucleotides using TSO (Template Switching Oligonucleotides) that allow the reverse transcriptase to switch from the RNA template to the TSO template. This allows the addition of specific sequences to the 3' of cDNA resulting in simple primer design and subsequent PCR amplification with increased coverage of the 5' end of RNA transcripts [2, 6], i.e. better generation of full-length transcripts. SMART-Seq2 has been optimized for single-cell or low RNA input samples by modifications including (but not limited to) the addition Betaine and MgCl<sub>2</sub> to increase reverse transcriptase processivity, LNA (locked nucleic-acid) [7] TSO to increase thermal stability and annealing to the additional cytosines at the 3' end of the synthesized cDNA, and use of reagents that result in overall increased transcript coverage and cDNA yield [8]. Low input and single-cell RNA-seq kits such as SMART-Seq v4 (Takara Bio USA, Inc) and NEBnext Single-cell/Low input (New England Biolabs, Inc) are just two examples of commercially available kits that utilize low input RNA optimized SMART-Seq and they demonstrate the value that scientists find in studying low input RNA systems.

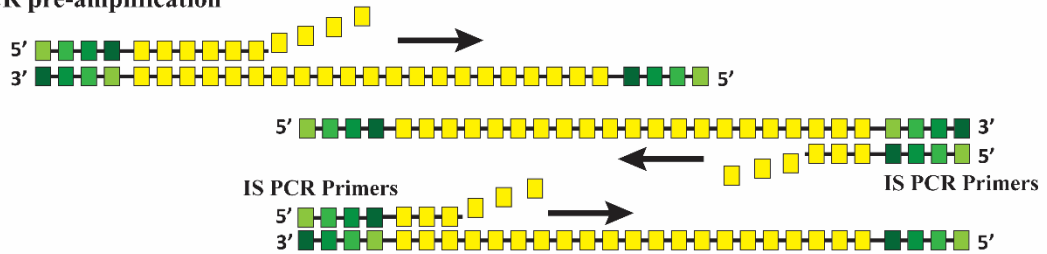
**A) Cutting and lysis of the nematode**



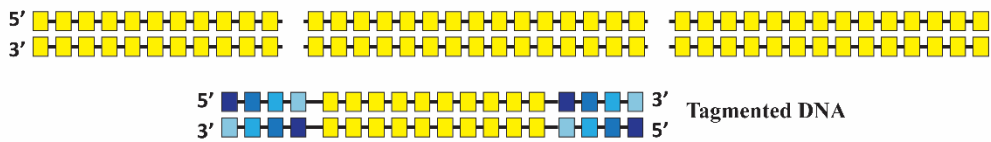
**B) cDNA 1st strand synthesis & Template switching**



**C) cDNA 2nd strand synthesis & PCR pre-amplification**



**D) Fragmentation & Tagmentation of DNA**



**E) Addition of index primers by PCR**

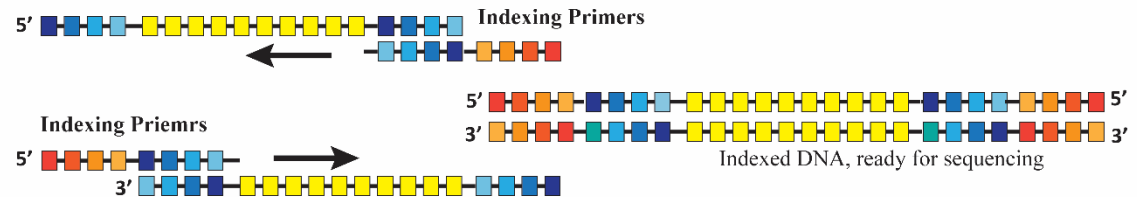


**Figure 12. SMART-Seq2 principles and workflow.** Adapted from Picelli, et al. 2013 [4] and Serra, et al. 2018 [20]. A) Cutting the nematode with a syringe needle and lysis of the tissue with lysis buffer and proteinase K to isolate mRNA. B) The 1<sup>st</sup> cDNA strand is synthesized by binding of the Oligo-dT<sub>30</sub>-VN primer to the poly-A tail of mRNA. The reverse transcriptase will use the mRNA as the template until it reaches the 5' end of the mRNA where it will add additional cytosines to the new cDNA strand. The LNA-modified TSO (Locked nucleic acid, Template switching oligonucleotide) will then anneal to the overhanging cytosines and the reverse transcriptase will switch from mRNA to the new TSO as the template for reverse transcription. C) cDNA is amplified by PCR. D) Amplified DNA getting fragmented and tagged by transposomes carrying the tag sequences (transposomes not shown). E) Indexes are added to the DNA fragments via PCR to prepare the library for sequencing. total cell lysate of *E. coli* cells expressing either (A-A) Sf-GH, 100 kDa glycol hydrolase, (A-B) Sf-Tryp, 35 kDa serine protease, or (A-C) Sf-PLA2, 17 kDa phospholipase. The totally lysate was sonicated initially to lyse the cells then sonicated a 2<sup>nd</sup> time with 1% triton-x. (B) Proteolytic activity assay of the samples containing Sf-Tryp and Sf-PLA2 (non-protease). Absorbance readings are of 3 technical replicates and paired T-test was used for the statistical analysis.

As single-cell and low input RNA-seq technology and methodology continue to advance, nematologists can adapt and improve these methods for single-nematode RNA-seq. Developing and advancing single-nematode RNA-seq methods would benefit the field of nematology (applicable to science in general) in 3 major ways: 1) it allows transcriptomic study of limited quantities of nematode samples, especially those from natural or agricultural environments; 2) it could obtain higher resolution transcriptomic data of developing nematodes by sampling individuals of different stages without the need to synchronize a population; and 3) it may better address research questions related to population/sample heterogeneity since individual nematodes are analyzed separately rather than being pooled.

RNA input from free-living nematode species such as *C. elegans* is typically not a limiting factor because they can generally be reared and studied in relatively large numbers. Parasitic nematodes and difficult to culture non-model species, on the other hand, are often limited in the number of nematodes obtainable and therefore limited in the RNA starting material. Plant-parasitic nematodes (PPNs) are obligate biotrophs and need to be cultured on plant hosts which presents the first hurdle for obtaining sufficient amounts of nematodes. RNA-seq studies of plant-parasitic nematodes still generally require a relatively high degree of processing to isolate PPNS from plants and generally entails blending of plant tissues (particularly root tissues) and filtering through sieves/meshes (typically in

series) [9-13]. These methods are currently the most efficient ways to obtain sufficient numbers of PPNs (or PPN eggs) to yield enough RNA material for traditional RNA-seq. Single-nematode RNA-seq requires minimal numbers of individuals and presents the opportunity to significantly reduce the time and effort put into isolating nematodes from plant hosts. Single-nematode RNA-seq would also benefit studies of rare or difficult to access PPNs which could be due to various factors such as low population density, limited host range, or seasonal variation.

A major aspect often studied in PPNs (and parasites in general) is gene expression throughout the different life stages. These life stages fulfill specific purposes for the nematodes and encompass different morphological and physiological changes [14, 15]. A single infested plant is expected to contain a population of PPNs with mixed life stages. So, extra care must be taken to assess and isolate the nematodes based on life-stages. Processing a relatively large number of nematodes can take more time and comes with an increased risk of contaminating nematodes of different life-stages. Single-nematode RNA-seq requires very few individuals thereby reducing the risk of contamination during processing. Additionally, the higher resolution of transcriptomic data will likely be obtained from sequencing individual nematodes leads to more efficient discovery of important gene expression differences/similarities between the life stages. Even in studies where life-stage is not considered, more specific factors

such as morphological, physiological, or behavioral changes of individuals can be more efficiently assessed and correlated with gene expression profiles of individual nematodes.

Heterogenous populations of some PPN species can be studied by isolating nematodes from specific plant tissues or parts. In the case of migratory endoparasitic PPNs, which feed while traveling through host tissue causing damage along the way, many species exhibit different life stages that can often be associated with specific parts of the plant [16]. Since this often results in low numbers of nematodes, traditional RNA-seq would require multiple plants to be processed taking up more time and effort. Single-nematode RNA-seq not only saves time and effort but it facilitates analysis of the heterogeneity of a population from a single host, therefore limiting the impact of host variance.

Another potential benefit of single-nematode RNA-seq is in its application to the issue of how PPNs react to different plant hosts. Some PPNs have very narrow host ranges such as *Ditylenchus africanus* which primarily targets peanuts while *Ditylenchus dipsaci* is known to infect more than 500 different plant species [17]. PPNs that target multiple plant species could be expected to utilize different strategies of infection and regulate gene expression in a host-specific manner; however, this topic is still underexplored [18]. Understanding whether a species of PPN uses only a specific set of genes to infect plants or whether different

genes are utilized based on the host could lead to improved targeting of essential infection genes controlling PPNs.

In our own need to circumvent the issue of low RNA input due to the limited number of parasitic nematodes from *in vivo* insect infections, we have adapted SMART-Seq2 protocols [5, 19] into a streamlined protocol for single-nematode RNA-seq [20]. While the protocol was originally adapted for insect-parasitic nematodes [21] and their embryos [22], it could easily be adapted to other nematodes. The protocol in this book chapter is an updated adaptation of the aforementioned protocol [20] covering nematode lysis, reverse transcription of RNA, amplification of cDNA, DNA library labeling/preparation for sequencing, and a basic description of how to use Galaxy [23] to quantify transcript abundance from raw RNA-seq data with the Salmon program [24]. The user may choose any program/software they are familiar with to quantify transcript abundance; however, for researchers without any prior bioinformatics analysis experience, we especially recommend Galaxy. It is a free web-based data analysis platform and its user-friendly interface is designed to make bioinformatic analysis more accessible to researchers without extensive experience in specialized software or programming. Salmon is a quick and accurate program for quantifying RNA transcript abundance and is available on the Galaxy platform. Note: Salmon quantification requires a reference transcriptome so use

of Salmon is only applicable to organisms with an assembled transcriptome (either *de novo* assembly or predicted from a sequenced genome).

## **Materials/Reagents/Equipment**

### **2.0 Materials**

#### **2.1 Consumables**

- 1) 0.2 ml thin-walled PCR tubes, nuclease-free
- 2) Syringe needles (needles should be less than 1" in length and any gauge between 25-31 G).
- 3) Pipette tips, nuclease-free
- 4) 1.5 ml microfuge tubes, nuclease-free
- 5) Nitrile or Latex gloves
- 6) 70% ethanol in a spray bottle
- 7) RNase decontaminating solution for wiping down surfaces and tools

#### **2.2 Reagents**

- 1) Molecular grade water, nuclease-free
- 2) Lysis buffer stock [25]
  - 20  $\mu$ l of 1M Tris-HCl pH 8.0
  - 20  $\mu$ l of 100% Triton X-100. (\*See Sec. 4 Note 1)
  - 200  $\mu$ l of 10% Tween 20
  - 2  $\mu$ l of 0.5 M EDTA

1.628 ml nuclease-free water

Total 1.871 ml

- 3) Proteinase K (QIAGEN, #19131)
- 4) RNasin ribonuclease inhibitor (Promega, #N2611)
- 5) dNTP (10 mM), (Thermo Fisher Scientific, #R0192)
- 6) Superscript II reverse transcriptase (Thermo Fisher Scientific, #18064014)
- 7) Betaine (BioUltra ≥ 99%, Sigma-Aldrich, #61962)
- 8) Magnesium chloride (Sigma-Aldrich, #M8266)
- 9) Phusion® High-Fidelity PCR Master Mix with HF Buffer (New England Biolabs, #M0531L)
- 10) Agencourt Ampure XP beads (Beckman Coulter, #A63881)
- 11) 80% ethanol in nuclease-free water
- 12) Elution Buffer of choice (10 mM Tris-Cl pH 8.5)
- 13) Nextera DNA Flex Library Prep Kit (Illumina, Inc. #20018704)

### **2.3 Oligonucleotides**

- 1) Oligo-dT<sub>30</sub>VN primer (ordered from idtdna.com)

**5'-AAGCAGTGGTATCAACGCAGAGTACT<sub>30</sub>VN-3'**

Oligonucleotide primer for annealing to the poly(A)-tail of mRNAs. V can be either A, C, or G. N can be any base. The primers should be solubilized in TE buffer to 100 µM. Store in aliquots at -20 °C for 6 months

2) LNA-modified TSO (Locked Nucleic Acid-modified Template Switching Oligonucleotide) (ordered from exiqon.com)

**5'-AAGCAGTGGTATCAACGCAGAGTACATrGrG+G-3'**

The two rG (riboguanosines) and +G (LNA-modified guanosine) help to facilitate template switching. Store in TE buffer at 100  $\mu$ M aliquots at -80 °C for up to 6 months. Minimize repeated free-thaw cycles.

3) IS PCR primers (ordered from idtdna.com)

**5'-AAGCAGTGGTATCAACGCAGAGT-3'**

Solubilize in TE buffer and store in 100  $\mu$ M aliquots at -20 °C for up to 6 months.

4) Table 2. Sequencing index primers [26].

Ad1_noMX	5'-AATGATACGGCGACCACCGAGATCTACACTCGTCGGCAGCGTCAGATGTG-3'
Ad2.1_TAAGGCGA	5'-CAAGCAGAAGACGGCATAACGAGATTCGCCTTAGTCTCGTGGGCTCGGAGATGT-3'
Ad2.2_CGTA TAG	5'-CAAGCAGAAGACGGCATAACGAGATCTAGTACGGTCTCGTGGGCTCGGAGATGT-3'
Ad2.3_AGGCAGAA	5'-CAAGCAGAAGACGGCATAACGAGATTTCTGCCTGTCTCGTGGGCTCGGAGATGT-3'
Ad2.4_TCCTGAGC	5'-CAAGCAGAAGACGGCATAACGAGATGCTCAGGAGTCTCGTGGGCTCGGAGATGT-3'
Ad2.5_GGACTCCT	5'-CAAGCAGAAGACGGCATAACGAGATAGGAGTCCGTCTCGTGGGCTCGGAGATGT-3'
Ad2.6_TAGGCATG	5'-CAAGCAGAAGACGGCATAACGAGATCATGCCTAGTCTCGTGGGCTCGGAGATGT-3'
Ad2.7_CTCTCTAC	5'-CAAGCAGAAGACGGCATAACGAGATGTAGAGAGGTCTCGTGGGCTCGGAGATGT-3'
Ad2.8_CAGAGAGG	5'-CAAGCAGAAGACGGCATAACGAGATCCTCTCTGGTCTCGTGGGCTCGGAGATGT-3'
Ad2.9_GCTACGCT	5'-CAAGCAGAAGACGGCATAACGAGATAGCGTAGCGTCTCGTGGGCTCGGAGATGT-3'
Ad2.10_CGAGGCTG	5'-CAAGCAGAAGACGGCATAACGAGATCAGCCTCGGTCTCGTGGGCTCGGAGATGT-3'
Ad2.11_AAGAGGCA	5'-CAAGCAGAAGACGGCATAACGAGATTGCCTCTTGTCTCGTGGGCTCGGAGATGT-3'
Ad2.12_GTAGAGGA	5'-CAAGCAGAAGACGGCATAACGAGATTCCTCTACGTCTCGTGGGCTCGGAGATGT-3'
Ad2.13_GTCGTGAT	5'-CAAGCAGAAGACGGCATAACGAGATATCACGACGTCTCGTGGGCTCGGAGATGT-3'
Ad2.14_ACCACTGT	5'-CAAGCAGAAGACGGCATAACGAGATACAGTGGTGTCTCGTGGGCTCGGAGATGT-3'
Ad2.15_TGGATCTG	5'-CAAGCAGAAGACGGCATAACGAGATCAGATCCAGTCTCGTGGGCTCGGAGATGT-3'
Ad2.16_CCGTTTGT	5'-CAAGCAGAAGACGGCATAACGAGATACAAACGGGTCTCGTGGGCTCGGAGATGT-3'
Ad2.17_TGCTGGGT	5'-CAAGCAGAAGACGGCATAACGAGATACCCAGCAGTCTCGTGGGCTCGGAGATGT-3'
Ad2.18_GAGGGGTT	5'-CAAGCAGAAGACGGCATAACGAGATAACCCCTCGTCTCGTGGGCTCGGAGATGT-3'
Ad2.19_AGGTTGGG	5'-CAAGCAGAAGACGGCATAACGAGATCCCAACCTGTCTCGTGGGCTCGGAGATGT-3'
Ad2.20_GTGTGGTG	5'-CAAGCAGAAGACGGCATAACGAGATCACCACACGTCTCGTGGGCTCGGAGATGT-3'
Ad2.21_TGGGTTTC	5'-CAAGCAGAAGACGGCATAACGAGATGAAACCCAGTCTCGTGGGCTCGGAGATGT-3'
Ad2.22_TGGTCACA	5'-CAAGCAGAAGACGGCATAACGAGATTGTGACCAGTCTCGTGGGCTCGGAGATGT-3'
Ad2.23_TTGACCTT	5'-CAAGCAGAAGACGGCATAACGAGATAGGGTCAAGTCTCGTGGGCTCGGAGATGT-3'
Ad2.24_CCACTCCT	5'-CAAGCAGAAGACGGCATAACGAGATAGGAGTGGGTCTCGTGGGCTCGGAGATGT-3'

\*Every sample will receive the Ad1\_noMX primer while each sample receives a different Ad2.# primer. Primers should be stored in TE buffer in 25 µM aliquots at -20 °C.

## 2.4 Equipment

- 1) Microcentrifuge
- 2) Dissecting microscope
- 2) Thermocycler

- 3) Magnetic separation stand (for 1.5 ml centrifuge tubes)
- 4) Heat Block
- 5) Access to a DNA fluorometric quantification device (i.e. Qubit fluorometer, Thermo Fisher Scientific Inc.) and its associated reagents.
- 6) Access to use or submit samples to a BioAnalyzer (Agilent Technologies, Inc)
- 7) Access to use or submit samples to a Next-Gen nucleic acid sequencer

### **3. Methods**

Clean all surface areas, pipettes, and equipment with 70% ethanol followed by an RNase decontaminant such as RNase away or RNaseZap. RNA can be extremely sensitive to degradation so after lysis of the nematode, do not let the mRNA samples simply sit on ice for more than an hour. Work hastily and always keep samples on ice. Be sure to change gloves frequently.

#### **3.1 Isolation and lysis of nematodes**

##### **1. Prepare incomplete lysis buffer**

46.8  $\mu$ l of lysis buffer stock

3.2  $\mu$ l of Proteinase K

50  $\mu$ l Total volume

##### **2. Prepare complete lysis buffer**

18  $\mu$ l of incomplete lysis buffer

2  $\mu$ l of RNase inhibitor

20  $\mu$ l Total volume

3. Add **2  $\mu$ l of complete lysis buffer** to the bottom of the 0.2 mL PCR tube(s). Briefly centrifuge to ensure the buffer is at the bottom of the tube and place the tubes on ice.
4. Wash the nematode 3 times in nuclease-free water.
5. Gently transfer the nematode in 2  $\mu$ l of nuclease-free water to the wall of the PCR tubes
6. Using the syringe needle to **cut the nematode into 3-4 pieces** while observing under a dissecting microscope (Fig 13). \*Use a new needle for every nematode.

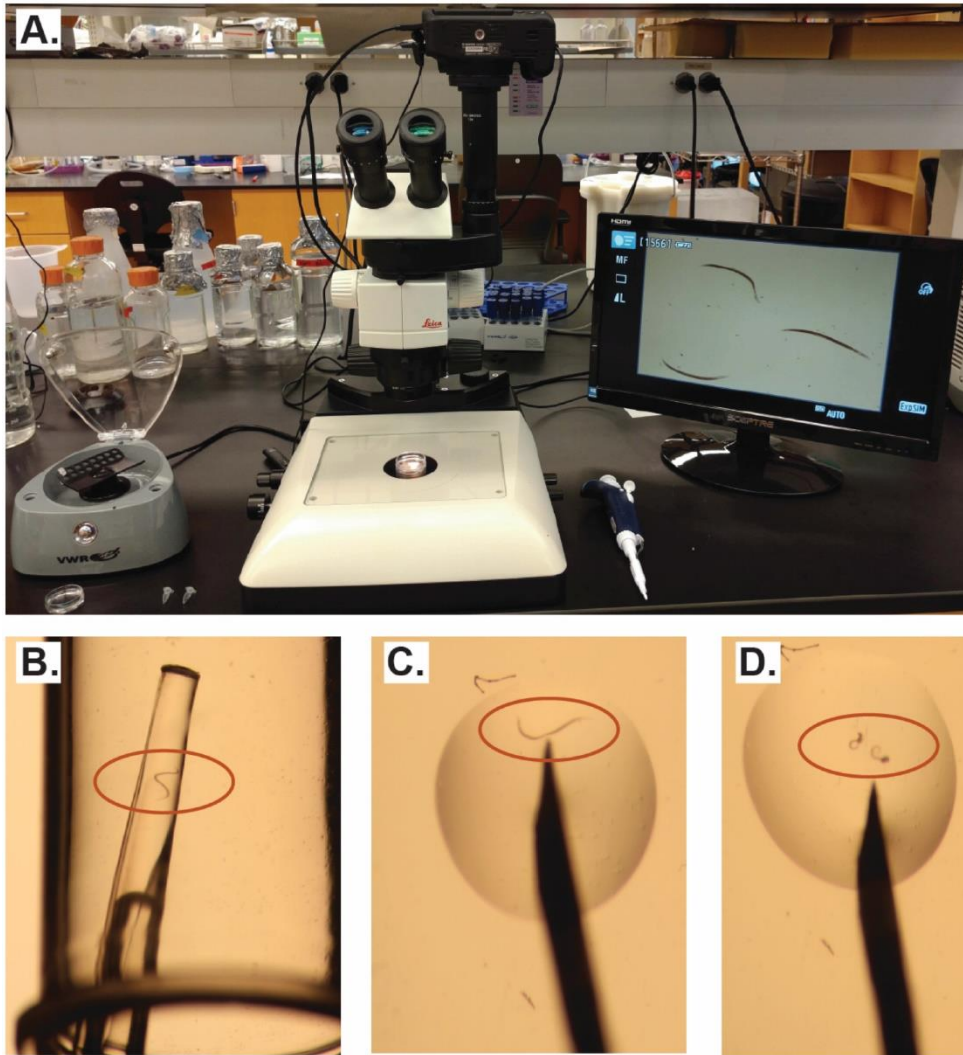


**Figure 13. Isolation and cutting of individual nematodes.** A) An example set up of a dissecting microscope station to cut nematodes. B) Transferring of a single nematode to the wall of a PCR tube. C) A nematode in 2  $\mu$ l of nuclease-free water before cutting. D) A nematode is cut with the tip of a 29 G syringe needle. Figure reproduced from Serra, L. et. al, 2018.

7. Quickly spin the nematode contents down into the lysis buffer at the bottom of the tube and place it on ice.

8. Incubate the samples in the thermocycler to digest nematode tissues with proteinase K at 65 °C for 10 min and inactivate the enzyme at 85 °C for 1 min.

Step	Temp	Time
1	65 °C	10 min
2	85 °C	1 min
3	4 °C	Continuous

9. Promptly remove the samples, briefly centrifuge, and place them back on ice.

### 3.2 First-strand cDNA synthesis with Smart-seq2

1. Add **1 µl of the oligo-dT VN primer** (10 µM) and **1 µl of dNTP** (10 mM) to the samples, mix by pipetting, briefly centrifuge, and place on ice.

2. Incubate the samples in a thermocycler at 72 °C for 3 min and promptly place them back on ice.

3. Prepare the reverse transcription master mix. DNase can be used however it is not required.

Reagent	Volume per sample (µl)	Final Concentration
Betaine (5M)	2	1 M
DTT (100 mM)	0.5	5 mM
MgCl <sub>2</sub> (1 M)	0.06	6 mM
TSO (100 µM)	0.1	1 µM
Superscript II first-strand buffer (5x)	2	1x
SuperScript II reverse transcriptase (200 U/µl)	0.5	100 U
RNasin ribonuclease inhibitor (40 U/µl)	0.25	10 U
Nuclease free water	0.29	--
<b>Total Volume</b>	<b>5.7</b>	<b>--</b>

4. Add **5.7 µl of the reverse transcription master mix** to each sample (now 10 µl total), mix by pipetting, briefly centrifuge, and place back on ice.

5. Run the First-Strand synthesis reaction in the thermocycler with the program below:

Step	Temp	Time
1	42 °C	90 min
2	50 °C	2 min
	42 °C	2 min
Go to step 2		14x
	70 °C	15 min
	4 °C	Continuous

This is a good stopping point and the samples can be stored at -20 °C.

### 3.3 PCR amplification

1. Place/thaw the first-strand samples on ice and prepare the PCR amplification master mix following the recipe below:

Reagent	Volume per sample (µl)	Final Concentration
KAPA HiFi HotStart ReadyMix (2x)	12.5	1x
IS PCR primer (10 µM)	0.25	0.1 µM
Nuclease free water	2.25	--
Total volume	15	

2. Add **15 µl of the PCR amplification master mix** to each First-strand synthesis sample (now 25 µl in total).

3. Run the samples with the PCR program below.

Step	Temp	Time
1	98 °C	3 min
2	98 °C	20 sec
	67 °C	15 sec
	72 °C	6 min
Go to step 2		17x
20	72 °C	5 min
21	4 °C	Continuous

This is a good stopping point and the samples can be stored at -20 °C

### 3.4 Cleanup of PCR amplicons

1. Thaw the PCR samples and allow them to come to room temperature, approx. 10 min.
2. Vortex the Ampure XP beads to thoroughly mix the beads in solution.
3. Aliquot **26 µl** of the beads into 1.5 mL microfuge tubes and allow them to warm up to room temperature (8 minutes).
4. Add the PCR sample (26 µL) to the beads at a 1:1 ratio. Mix thoroughly by pipetting up and down 10 times. Do NOT discard the old PCR tubes yet.
5. Incubate the sample at room temperature for **8 minutes**.
6. After incubation, place the samples on the magnetic separation stand for **5 minutes**. Ensure the solution becomes clear.
7. Be careful not to disturb the magnetized bead pellet and keeping the tube on the magnetic stand, transfer the supernatant to its previously associated PCR tube. (\*See Sec. 4 Note 1)

8. Quickly add **200 µl** of 80% ethanol to the bead pellet and incubate for **30 sec.**

(Do not mix)

9. Carefully remove the ethanol wash without disturbing the bead pellet.

10. Repeat steps 8 and 9 one more time.

11. Allow the beads to air dry on the magnetic rack for ~5 min or until the first signs of minor cracks. Observe under a microscope frequently for minor cracks.

(\*See Sec. 4 Note 2)

12. Quickly add **17.5 µl** of EB to the bead pellets for each sample, pipette to mix, and place on a **non-magnetic tube rack**. (\*See Sec. 4 Note 3)

13. Incubate the samples at room temperature for **2 min.**

14. Place the samples on the magnetic stand for 2-3 min until the beads pellet and the solution becomes clear.

15. Collect **15 µl** of the supernatant and place it on ice. If there are any visible remnants of the brown beads in the collected supernatant, transfer it back into the bead tube and repeat step 13.

### **3.5 Amplified DNA concentration and quality check (not detailed)**

The user should choose an appropriate method of DNA quantification.

Fluorometric quantification methods are more accurate than UV-based

(Nanodrop) methods and we recommend using the Qubit Fluorometer and its associated reagents. The quality of the amplified DNA should be checked with

the BioAnalyzer (Agilent Technologies). Figure 14 shows examples of

BioAnalyzer profiles of a high-quality DNA sample (Fig 14A) and a low-quality

DNA sample (Fig 14B). The distribution of the DNA lengths (correlating to mRNA transcript lengths) should show a strong group of peaks towards the 500-10,000 bp range for samples with minimal degradation (Fig 14A). Profiles without peaks or many smaller fragmented peaks indicate mRNA transcript degradation and should not be used (Fig 14B).

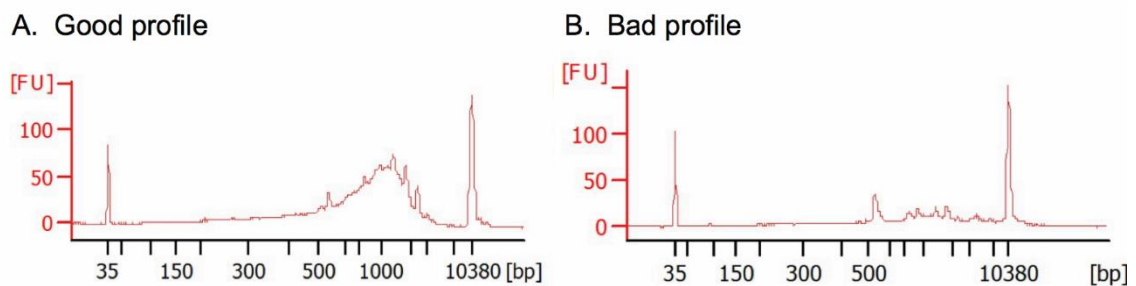


**Figure 14. Example bioanalyzer profiles of amplified DNA quality.** A) Profile of a DNA sample made from RNA with minimal degradation. The distribution of the large peaks is around 1,000 bp and peaks around 70 bp are not present, indicating no PCR primer contamination in the DNA. B) Profile of a low-quality DNA sample made from RNA that has been significantly degraded showing fragmented and small peaks. Figure reproduced from Serra, L. et. al, 2018.

### 3.6 Tagmentation of amplified DNA

The user can use their own Tagmentation kit of choice so long as the proper protocol for tagmentation and post tagmentation cleanup is followed. The protocol below details the use of the Nextera DNA Flex Library Prep kit (Illumina, Inc) and is adapted from its associated protocol.

1. Bring BLT and TB1 to room temperature (~8 min).

2. Set one heat block to **55 °C** and a second heat block to **37 °C**.
3. Transfer **20 ng** of DNA samples into 1.5 mL tubes and bring the volume to 8  $\mu$ l with nuclease-free water.
4. Vortex the BLT and TB1 for at least 10 seconds to thoroughly mix solutions. In a new PCR tube prepare the tagmentation master mix by combining **5.2  $\mu$ l** of **BLT** and **4.8  $\mu$ l** of **TB1** per sample. Vortex the mix one more time.
5. Add **10  $\mu$ l** of the tagmentation master mix into the DNA and pipette up and down at least 10 times.
6. Place sample for 15 minutes in the 55 °C heating block to initiate tagmentation. Remove samples immediately after 15 minutes.
7. Bring TSB and TWB to room temperature (~8 min). If TSB contains visible precipitates, it can be heated at 37°C for 10 minutes followed with some vortexing.
8. Add **5  $\mu$ l** of TSB to each tagmented sample and slowly mix by pipetting up and down 10 times.
9. Place sample for 15 minutes in the 37 °C heating block to stop tagmentation. Remove samples immediately after 15 minutes.
10. Place samples on the magnetic rack for 2-3 minutes until the solution is clear.
11. Carefully remove and discard the supernatant.
12. Remove the samples from the magnetic rack and wash the beads with **50  $\mu$ l** of TWB. Pipette up and down slowly to thoroughly mix the beads in solution.

13. Place the samples back on the magnetic rack and discard the solution.

**Repeat step 9-13** a 2<sup>nd</sup> time.

14. After removal of the TWB from the 2<sup>nd</sup> wash, add **50 µl** of TWB and pipette slowly to mix the beads.

15. Keep the samples on the magnetic stand without removing TWB until section 3.7 step 4.

### **3.7 Indexing tagmented DNA by PCR amplification**

1. Thaw EPM on ice and invert to mix. Then briefly centrifuge and place it back on ice.

2. Thaw index primers at room temperature, mix by flicking or pipetting, briefly centrifuge, then place them back on ice.

3. Prepare the Indexing PCR master mix by mixing **5 µl** EPM with **5 µl** of nuclease-free water and **2.5 µl** of Ad1\_nMX. Vortex and briefly centrifuge the master mix.

4. **Keeping the tubes on the magnetic rack**, carefully remove and discard the **50 µl** of TWB supernatant of the first sample.

5. Remove the first sample from the magnetic rack and resuspend beads in **12.5 µl** of the Indexing PCR master mix. Mix by pipetting up and down 10 times.

Transfer the mix **with beads** to a PCR tube. Repeat this for each sample.

6. Add **2.5 µl** of the Ad2.# to each sample (each sample receives a different Ad2.# primer, see Table 1)

7. Mix thoroughly and briefly centrifuge.

8. Run the indexing PCR with the following program:

Step	Temp	Time
1.	68 °C	3 min
2.	98 °C	3 min
3.	98 °C	45 sec
	62 °C	30 sec
	68 °C	2 min
Go to step 3		9 X
4.	68 °C	1 min
5.	10 °C	continuous

9. After PCR, centrifuge the samples at 280 x g for 1 minute.

\*This is a good stopping point and the samples can be stored at 2-8°C for up to 3 days.

### 3.8 DNA Library clean up

1. Bring Sample Purification Beads (SPB) and Resuspension Buffer (RSB) to room temperature (~ 8min). Vortex SPB frequently while using it, otherwise, the beads will settle in the bottom of the tube and samples won't be cleaned properly.
2. Transfer samples from PCR tubes to 1.5 mL microfuge tubes.
3. Place tubes in a magnetic stand and transfer **15 µl** of supernatant to a new 1.5 mL microfuge tube.
4. Add 20 µl of Nuclease-free water and **22.5 µl** of SPB to microfuge tube containing supernatant and pipette mixture 10 times.
5. Incubate samples at room temperature for 5 minutes.
6. While samples are incubating, vortex SPB and add **8 µl** to a **new** 1.5 mL microfuge tube.

7. Place samples from step 5 on a magnetic stand and wait 2-3 minutes for the solution to turn clear.
8. Transfer all the supernatant to the 1.5 mL microfuge tube prepared in step 6, mix thoroughly.
9. Incubate sample at room temperature for **5 minutes**.
10. Place sample from step 9 in a magnetic stand and wait for the solution to turn clear.
11. Without disturbing the beads, remove and discard the supernatant.
12. Quickly add **200  $\mu$ l** of 80% ethanol to the bead pellet (still on the magnetic stand) and incubate for 30 sec (Do not mix).
13. Carefully remove the 80% ethanol wash without disturbing the bead pellet.
14. Repeat steps 12 and 13 two more times.
15. Allow beads to air-dry on the magnetic stand for 5 minutes.
16. Remove samples from magnetic stand and resuspend beads in **17.5  $\mu$ l** of RSB.
17. Incubate at room temperature for 2 minutes on a tube rack.
18. Place tubes back in the magnetic stand and wait until the solution is clear.
19. Transfer **15  $\mu$ l** of supernatant containing the cDNA library to a new 1.5  $\mu$ l microfuge tube.

### **3.9 DNA library concentration and quality check**

The DNA library concentration should be measured as previously done, and the quality should be checked by BioAnalyzer. Figure 15 shows examples of a fully

tagmented library (Fig 15A) and partially tagmented library (Fig 15B). Most of the DNA that has been tagmented (along with fragmentation) should be around 200 bp long and that should be indicated by a central peak around 200 bp in the profile. A DNA library that has many partially- or un-tagmented DNA will result in varying sizes of DNA and is demonstrated by a broad peak or sometimes multiple smaller peaks across from 150-1000 bp.

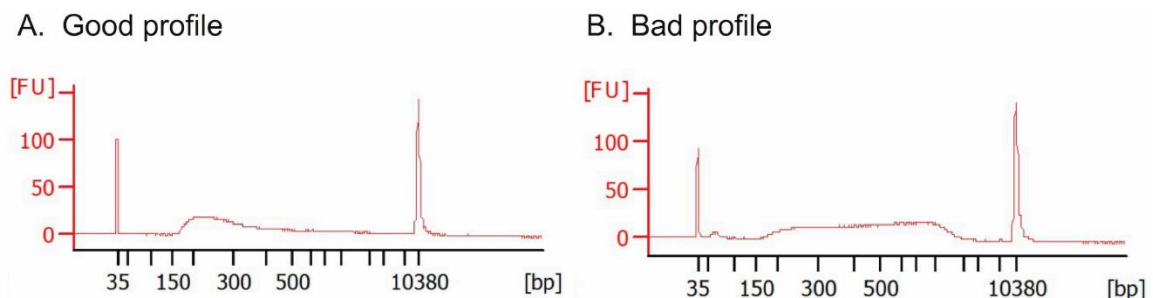


**Figure 15. Example BioAnalyzer profiles of DNA library quality.** A) Example profile of a tagmented DNA library with a central peak around 200 bp. B) Example profile of DNA library with deficient fragmentation and tagmentation resulting in a broad distribution of fragmented peaks from 150-1000 bp. Figure reproduced from Serra, L. et. al, 2018.

### 3.10 Sequencing of the DNA library (not detailed)

For RNA-seq data, sequence coverage/depth for each sample should be at least  $1 \times 10^7$  reads to reliably detect one transcript per million (TPM). Sequencing should be performed as paired-end, 43 bp reads. Sequencing with single-end reads is a viable alternative that is typically less expensive and quicker, however, paired-end sequencing allows for better alignment of reads to the reference genome resulting in a higher quality data set.

### **3.11 Use Galaxy to generate relative mRNA abundance data from raw sequencing data.**

Before beginning:

Log onto usegalaxy.org and create an account.

Download your reference transcriptome in the fasta/fastq file format.

Download your RNA-seq reads (raw sequencing files) in the fasta/fastq file format. If sequencing was performed as paired-end reads, you should have a 'read 1' file and a 'read 2' file for each sample.

1. On the Galaxy web-page on the left side under the 'Tools' menu, click on 'Get Data'.
2. In the new window, click 'Upload File'.
3. Click 'Choose local file' and choose your Transcriptome file, Read1 file, and Read2 file (the order does not matter).
4. Once your files are queued, you can change the file 'Type' box to their appropriate file type or leave the selection at 'Auto-detect'.
5. Click 'Start' and the files will begin to upload. The files will turn green when they are uploaded.
6. Close the upload window and you will see the files under the 'History' column on the right side of the web-page.
7. On the left side under the 'Tools' column, scroll down and click 'RNA-seq', then scroll down and click 'Salmon'.

8. In the middle of the page under the menu option ‘Select a reference transcriptome...’, click on the entry box and set it to ‘Use one from the history’.
9. Under ‘Select reference transcriptome’, click the entry box and select your transcriptome file.
10. Under ‘Is this library mate-paired?’, set the entry box to ‘Paired-end’ (or single-end instead, if that was part of the sequencing protocol).
11. Under ‘Mate pair 1’, select your RNA-seq read 1 file.
12. Under ‘Mate pair 2’, select your RNA-seq read 2 file.

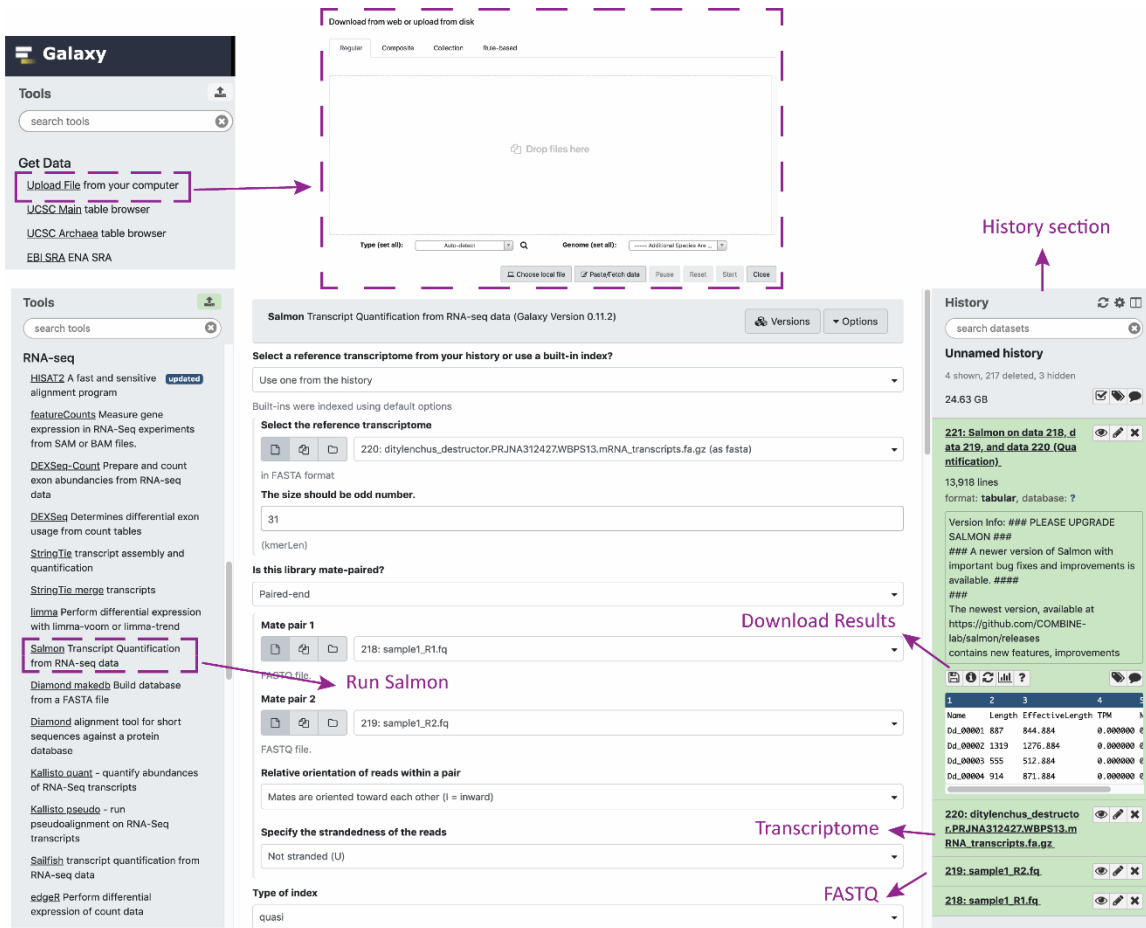


**Figure 16. Galaxy web-interface displaying RNA-seq analysis.** Upload the transcriptome and FASTQ RNA-seq files under “Get data”. Then under “RNA-seq” run Salmon to quantify gene expression. The results can be downloaded from the ‘History’ panel.

13. The other data menu options such as ‘Relative orientation of reads within a pair’ and ‘Specify the strandedness of the reads’ should be set according to your sequencing and library preparation protocol.

14. The options further below are parameters for running Salmon and can be left as their default options or adjusted as needed. Most of the parameters are supplemented with a description of their functions and effect on quantification.

More detailed descriptions can be found at

<https://salmon.readthedocs.io/en/latest/> and guidance can be found at

<https://combine-lab.github.io/salmon/faq/>

15. Important parameters such as ‘Perform sequence-specific bias correction’ and ‘Perform fragment GC bias correction’ should typically be set to ‘Yes’.

16. Once all parameters are set, click ‘Execute’. The analysis will be displayed in yellow under the ‘History’ panel to the right of the web-page and will turn green when completed.

17. After the analysis is completed, click on the file name and select the small floppy disk/save icon to download the file as a tab-delimited text file. The information in the file should be organized into columns: Transcript ID/Name, Transcript Length, Transcripts per Million (TPM), and Estimated number of reads. The TPM information can then be used for further analysis such as differential expression analysis.

#### **4. Notes:**

1. The final concentration of Triton X-100 in the lysis buffer is 1%, however, for nematode embryos, we have also used a final concentration of 0.3% Triton X-100 (see. Sec. 2.2 reagent #2)

2. Save the supernatant in case of insufficient DNA binding to the beads and repeating incubation of the supernatant with the beads is needed. (\*See Sec. 3.4 step 7)

3. Do not over-dry the beads as this will reduce DNA elution. The beads can sometimes dry in under 5 minutes, so we recommend frequently checking the bead pellet of each sample under the microscope and placing them back on the magnetic rack. At the very first sign of minor cracking, the bead pellet is dry enough. Other protocols do not recommend drying to the point of cracking however we found this degree of drying did not affect our DNA yield (\*See Sec. 3.4 step 11).
4. Pipette the EB solution up and down on the bead pellet until it breaks and dissolves. To minimize the over-drying of the beads we recommend a quick initial breaking of the pellet with the EB solution for each sample before returning to thoroughly mix and dissolve the beads for each sample. Ensure the solution is homogenously brown (\*See Step 3.4 step 12).
5. In our hands, 8/10 of the DNA samples typically pass the BioAnalyzer quality check.
6. Regarding sequencing, samples with less than  $1 \times 10^6$  reads are poor quality sequences and should not be used.
7. This protocol was optimized for handling a few samples at a time using individual PCR tubes and 1.5 mL microfuge tubes, however, the protocol can be re-optimized for a higher volume of samples using multi-well plates (Thermo Fisher Scientific, #AB-0859) with magnetic plates (Thermo Fisher Scientific, #AM10027)

## References

1. Gerard GF, Fox DK, Nathan M, Dalessio JM. Reverse transcriptase - The use of cloned moloney murine leukemia virus reverse transcriptase to synthesize DNA from RNA. *Mol Biotechnol.* 1997;8(1):61-77. doi: 10.1007/bf02762340. PubMed PMID: WOS:A1997XY27500007.
2. Zhu YY, Machleder EM, Chenchik A, Li R, Siebert PD. Reverse transcriptase template switching: A SMART (TM) approach for full-length cDNA library construction. *Biotechniques.* 2001;30(4):892-7. doi: 10.2144/01304pf02. PubMed PMID: WOS:000168024700023.
3. Chenchik A, Diachenko L, Moqadam F, Tarabykin V, Lukyanov S, Siebert PD. Full-length cDNA cloning and determination of mRNA 5' and 3' ends by amplification of adaptor-ligated cDNA. *Biotechniques.* 1996;21(3):526-34. PubMed PMID: WOS:A1996VG21200034.
4. Picelli S, Bjorklund AK, Faridani OR, Sagasser S, Winberg G, Sandberg R. Smart-seq2 for sensitive full-length transcriptome profiling in single cells. *Nat Methods.* 2013;10(11):1096-8. doi: 10.1038/nmeth.2639. PubMed PMID: WOS:000326507600024.
5. Picelli S, Faridani OR, Bjorklund AK, Winberg G, Sagasser S, Sandberg R. Full-length RNA-seq from single cells using Smart-seq2. *Nat Protoc.* 2014;9(1):171-81. doi: 10.1038/nprot.2014.006. PubMed PMID: WOS:000329186400016.
6. Kulpa D, Topping R, Telesnitsky A. Determination of the site of first strand transfer during Moloney murine leukemia virus reverse transcription and identification of strand transfer-associated reverse transcriptase errors. *Embo Journal.* 1997;16(4):856-65. doi: 10.1093/emboj/16.4.856. PubMed PMID: WOS:A1997WJ99200018.
7. Petersen M, Wengel J. LNA: a versatile tool for therapeutics and genomics. *Trends Biotechnol.* 2003;21(2):74-81. doi: 10.1016/s0167-7799(02)00038-0. PubMed PMID: WOS:000181154900007.
8. Picelli S. Single-cell RNA-sequencing: The future of genome biology is now. *RNA Biol.* 2017;14(5):637-50. doi: 10.1080/15476286.2016.1201618. PubMed PMID: WOS:000402095400017.
9. Gardner M, Dhroso A, Johnson N, Davis EL, Baum TJ, Korke D, et al. Novel global effector mining from the transcriptome of early life stages of the

- soybean cyst nematode *Heterodera glycines*. Sci Rep. 2018;8:15. doi: 10.1038/s41598-018-20536-5. PubMed PMID: WOS:000424189400021.
10. Kumar M, Gantasala NP, Roychowdhury T, Thakur PK, Banakar P, Shukla RN, et al. De Novo Transcriptome Sequencing and Analysis of the Cereal Cyst Nematode, *Heterodera avenae*. Plos One. 2014;9(5):16. doi: 10.1371/journal.pone.0096311. PubMed PMID: WOS:000338029800052.
  11. Cotton JA, Lilley CJ, Jones LM, Kikuchi T, Reid AJ, Thorpe P, et al. The genome and life-stage specific transcriptomes of *Globodera pallida* elucidate key aspects of plant parasitism by a cyst nematode. Genome Biol. 2014;15(3):17. doi: 10.1186/gb-2014-15-3-r43. PubMed PMID: WOS:000338981300004.
  12. Eves-van den Akker S, Lilley CJ, Danchin EGJ, Rancurel C, Cock PJA, Urwin PE, et al. The Transcriptome of *Nacobbus aberrans* Reveals Insights into the Evolution of Sedentary Endoparasitism in Plant-Parasitic Nematodes. Genome Biol Evol. 2014;6(9):2181-94. doi: 10.1093/gbe/evu171. PubMed PMID: WOS:000343249300001.
  13. Choi I, Subramanian P, Shim D, Oh BJ, Hahn BS. RNA-Seq of Plant-Parasitic Nematode *Meloidogyne incognita* at Various Stages of Its Development. Front Genet. 2017;8:3. doi: 10.3389/fgene.2017.00190. PubMed PMID: WOS:000416234000003.
  14. Perry RN, Moens M. Survival of Parasitic Nematodes outside the Host. In: Perry RN, Wharton DA, editors. Molecular and Physiological Basis of Nematode Survival. Wallingford: Cabi Publishing-C a B Int; 2011. p. 1-27.
  15. Grecis R, Harnett W. Survival of Animal-parasitic Nematodes inside the Animal Host. In: Perry RN, Wharton DA, editors. Molecular and Physiological Basis of Nematode Survival. Wallingford: Cabi Publishing-C a B Int; 2011. p. 66-85.
  16. Jones JT, Haegeman A, Danchin EGJ, Gaur HS, Helder J, Jones MGK, et al. Top 10 plant-parasitic nematodes in molecular plant pathology. Mol Plant Pathol. 2013;14(9):946-61. doi: 10.1111/mpp.12057. PubMed PMID: WOS:000326454500010.
  17. Moens M, Perry RN. Migratory Plant Endoparasitic Nematodes: A Group Rich in Contrasts and Divergence. Annual Review of Phytopathology. Annual Review of Phytopathology. 47. Palo Alto: Annual Reviews; 2009. p. 313-32.
  18. Bell CA, Lilley CJ, McCarthy J, Atkinson HJ, Urwin PE. Plant-parasitic nematodes respond to root exudate signals with host-specific gene expression

patterns. PLoS Pathog. 2019;15(2):19. doi: 10.1371/journal.ppat.1007503.  
PubMed PMID: WOS:000459972100009.

19. Trombetta JJ, Gennert D, Lu D, Satija R, Shalek AK, Regev A. Preparation of Single-Cell RNA-Seq Libraries for Next Generation Sequencing. *Current protocols in molecular biology*. 2014;107:4.22.1-17. Epub 2014/07/06. doi: 10.1002/0471142727.mb0422s107. PubMed PMID: 24984854; PubMed Central PMCID: PMC4338574.

20. Serra L, Chang D, Macchietto M, Williams K, Murad R, Lu D, et al. Adapting the Smart-seq2 Protocol for Robust Single Worm RNA-seq. *Bio-protocol*. 2018;8(4):e2729. doi: 10.21769/BioProtoc.2729.

21. Lu DH, Macchietto M, Chang D, Barros MM, Baldwin J, Mortazavi A, et al. Activated entomopathogenic nematode infective juveniles release lethal venom proteins. *PLoS Pathog*. 2017;13(4):31. doi: 10.1371/journal.ppat.1006302. PubMed PMID: WOS:000402555700018.

22. Macchietto M, Angdembe D, Heidarpour N, Serra L, Rodriguez B, El-Ali N, et al. Comparative Transcriptomics of *Steinernema* and *Caenorhabditis* Single Embryos Reveals Orthologous Gene Expression Convergence during Late Embryogenesis. *Genome Biol Evol*. 2017;9(10):2681-96. doi: 10.1093/gbe/evx195. PubMed PMID: WOS:000414778600017.

23. Afgan E, Baker D, Batut B, van den Beek M, Bouvier D, Cech M, et al. The Galaxy platform for accessible, reproducible and collaborative biomedical analyses: 2018 update. *Nucleic Acids Res*. 2018;46(W1):W537-W44. doi: 10.1093/nar/gky379. PubMed PMID: WOS:000438374100083.

24. Patro R, Duggal G, Love MI, Irizarry RA, Kingsford C. Salmon provides accurate, fast, and bias-aware transcript expression estimates using dual-phase inference. *bioRxiv*. 2016:021592. doi: 10.1101/021592.

25. Shaham (ed.) S. *Methods in cell biology*. WormBook. January 12, 2006. doi: 10.1895/wormbook.1.49.1.

26. Buenrostro JD, Wu B, Chang HY, Greenleaf WJ. ATAC-seq: A Method for Assaying Chromatin Accessibility Genome-Wide. *Current protocols in molecular biology*. 2015;109:21.9.1-9.9. doi: 10.1002/0471142727.mb2129s109. PubMed PMID: 25559105.

## CHAPTER 5

### Conclusions and Final Remarks

#### ***Steinernema* IJs actively contribute to host-killing**

My research has aimed to elucidate mechanisms of how the nematode, from the nematode-bacteria EPN duo complex, contributes to killing of the host insect.

Symbiotic bacteria have been traditionally thought of as the source of virulence [1-3] and the nematode served only as the vector, however my research along with others has demonstrated that this is not the case for EPNs in the genus *Steinernema* [4, 5]. *Steinernema* EPNs are capable and do in fact actively contribute to virulence against their host.

Chapter 2 details use of the *in vitro* activation EPN activation model that we developed to optimize activation of *Steinernema* IJs. This method increases the activation of IJs on average 20% [4] when compared to exposing the IJs to insect homogenate media alone. We suspect that this is due to better aeration for IJs and the sponge may act as a solid apparatus that better supports the IJs more similar to inside of an insect than the liquid solution of insect homogenate alone. The activation rates of IJs increase in a time-dependent manner (Chapter 2, Fig 2A). Gene expression profiling comparing to IJs activated *in vitro* to IJs activated *in vivo* showed that they were overall similar however timing played an important factor as we found that 6-hrs of *in vitro* activation was the most similar to 6-hrs of *in vivo* activation (Chapter 2, Fig3). This finding goes to show how important it is

to verify *in vitro* models as simple factors such as timing can affect well an *in vitro* model is relevant to what is happening *in vivo*. For the gene expression analysis, we adapted a single-cell RNA-seq method for single-worm RNA seq which is described in Chapter 4 [6].

We collected the ESPs of activated IJs from *S. feltiae* and *S. carpocapsae* and showed that they exhibited toxic properties when injected into insects (Chapter 2 Fig 3 [4, 5]. With as little as 20 ng of crude venom, these products were consistently toxic to *D. melanogaster* fruit flies and could either kill or cause paralysis in other insects such as the wax worm *G. mellonella* and the silkworm *B. mori* (with relatively larger amounts of venom) [4]. Venom collected from axenic IJs show similar levels of toxicity as symbiotic IJs supporting that the products from the nematode alone are capable of killing the insects [4, 5]. In all, these findings show that there is more to the interaction of host and EPN where the nematode was traditionally thought to simply vector in the symbiotic bacteria but rather, the nematode has an active role in virulence against the host and it is likely that nematode and bacteria have evolved to work synergistically to kill the host.

### **A core suite of ESP components shared by Steinernematids**

Although both *Steinernema* species that we studied utilized venom to contribute to killing of the host, they did so with some differences. *S. feltiae* IJs are capable

of producing ESPs without insect tissue stimulation, whereas *S. carpocapsae* did not do so under the same conditions (Chapter 2, Fig 3A & 3B). These ESPs were not toxic, and it would seem evolutionarily illogical to produce ESPs without proper stimulation, so we suspect that these ESPs play a role in *S. feltiae*'s strategy in surviving its physical environment or preparation for an encounter with a potential host. Furthermore, production and toxicity of venom from *S. feltiae* decreased drastically from the early hours (6-12 hours) after infecting a host to the later hours (18-30 hours) while *S. carpocapsae*'s venom production and toxicity stayed consistent (12-42 hours) (Chapter 2, Fig 3). Although there is some overlap between the insect species that *S. feltiae* and *S. carpocapsae* can infect and kill, these differences in their venom production and composition indicate their evolutionary adaptations to different hosts and niche partitioning. These two EPNs are related but not closely related as *S. feltiae* is from Clade III and *S. carpocapsae* is in Clade II [7]. With their differences in ecological niche and some differences in host specificity/efficacy [8, 9], it is expected that their venom composition would be different which we have touched on in the previous paragraph. An orthology analysis, on the other hand, showed that both species shared 52 common proteins in their venom (Chapter 2 Fig 6E). The molecules that are different between these two species may represent their adaptations to different hosts' physiology and immune response however this shared core set of proteins may represent the important molecules used against a wide array of insects hence a potential leeway into the physiology and immune response

shared between many insects. Additionally, many of the ESP components were found to be highly similar to proteins found in vertebrate-parasitic nematodes hence this pool of proteins may potentially be helpful in identifying homologous proteins among parasites in general.

### ***Steinernema* ESPs are both toxic and immunomodulatory**

Chapter 3 details our work to identify, produce, and characterize active protein components of *S. feltiae* ESPs. We fractionated crude EPN venom using anion-exchange FPLC and tested for fractions that maintained toxic activity (Chapter 3, Fig 1). From this fractionation we were able to separate proteins that showed properties indicative of melanization inhibition (Chapter 3, Fig 1C). Although our study did not focus on identifying these melanization inhibiting proteins, this observation demonstrates that the ESPs contains both toxic and immunomodulating proteins. We focused on toxic fractions that did not seem to contain melanization inhibitors and selected the proteins that were significantly enriched in abundance in the toxic fraction compared to crude venom (Chapter 3, Table 1). We and expressed these individual proteins in an *E. coli* system to test for activity and further characterization. For the scope of this dissertation, two proteins have been expressed (Sf-PLA2, a predicted phospholipase A2 protein, and Sf-GH, a predicted glycosyl hydrolase) while one (Sf-Tryp, a predicted trypsin-like serine protease) has been expressed and validated for proteolytic activity (Chapter 3, Fig A & B). It remains to be determined whether Sf-Tryp will

exhibit any toxic properties and further purification with testing by injection into fruit flies will be needed.

### **EPN virulence molecules and implications in agricultural pest control**

There are many factors to consider when using EPNs in biological control including efficacy against the target pest and tolerance in the environment. This coincides with selection of the species and even sub-strains of species that may be more efficacious than others [10]. My research has been a large part of the pool of research that establishes the capability of EPN IJs (*Steinernema* specifically) to produce virulent molecules against insects. This introduces a new pool of biological molecules to consider along with the genetics behind the biological molecules. One traditional approach to improving the efficacy of EPNs as biological control agents has been to breed and select for virulent strains based on virulence infection assays [11, 12]. However if we identify the genes responsible for virulence it would drastically improve the virulence selection process by allowing for screening/selection of those virulence genes or the use of genetic engineering technology to introduce or amplify expression of these virulence genes. Development of genetic tools for EPNs unfortunately, has been lacking and would require significant advances to take advantage of the discovery of important virulence genes. Additionally, the individual toxins can potentially be developed as part of a natural pesticide agent and expressed within the plant to deter foraging, similar to the widely adopted Bt toxins [13].

## References

1. Kaya HK, Gaugler R. Entomopathogenic Nematodes. *Annu Rev Entomol.* 1993;38:181-206. doi: 10.1146/annurev.en.38.010193.001145. PubMed PMID: WOS:A1993KF69700009.
2. Lewis EE, Clarke DJ. Nematode Parasites and Entomopathogens. In: Vega FE, Kaya HK, editors. *Insect Pathology*, 2nd Edition. San Diego: Elsevier Academic Press Inc; 2012. p. 395-424.
3. Goodrich-Blair H. They've got a ticket to ride: *Xenorhabdus nematophila-Steinernema carpocapsae* symbiosis. *Curr Opin Microbiol.* 2007;10(3):225-30. doi: 10.1016/j.mib.2007.05.006. PubMed PMID: WOS:000248036200005.
4. Lu DH, Macchietto M, Chang D, Barros MM, Baldwin J, Mortazavi A, et al. Activated entomopathogenic nematode infective juveniles release lethal venom proteins. *PLoS Pathog.* 2017;13(4):31. doi: 10.1371/journal.ppat.1006302. PubMed PMID: WOS:000402555700018.
5. Chang DZ, Serra L, Lu D, Mortazavi A, Dillman AR. A core set of venom proteins is released by entomopathogenic nematodes in the genus *Steinernema*. *PLoS Pathog.* 2019;15(5):e1007626. doi: 10.1371/journal.ppat.1007626.
6. Serra L, Chang D, Macchietto M, Williams K, Murad R, Lu D, et al. Adapting the Smart-seq2 Protocol for Robust Single Worm RNA-seq. *Bio-protocol.* 2018;8(4):e2729. doi: 10.21769/BioProtoc.2729.
7. Blaxter M, Koutsovoulos G. The evolution of parasitism in Nematoda. *Parasitology.* 2015;142:S26-S39. doi: 10.1017/s0031182014000791. PubMed PMID: WOS:000349552500004.
8. Shapiro-Ilan D. *Entomopathogenic nematology*: CABI; 2002. Available from: <https://www.cabi.org/cabebooks/ebook/20023023458>.
9. Shapiro-Ilan DI, Gaugler R. Rhabditida: *Steinernematidae* & *Heterorhabditidae* [Digital]. [cited 2019]. Available from: <https://biocontrol.entomology.cornell.edu/pathogens/nematodes.php>.
10. Gaugler R. Ecological considerations in the biological control of soil-inhabiting insects with entomopathogenic nematodes. *Agriculture, Ecosystems & Environment.* 1988;24(1):351-60. doi: [https://doi.org/10.1016/0167-8809\(88\)90078-3](https://doi.org/10.1016/0167-8809(88)90078-3).

11. Glazer I. Improvement of Entomopathogenic Nematodes: A Genetic Approach. In: Campos-Herrera R, editor. Nematode Pathogenesis of Insects and Other Pests: Ecology and Applied Technologies for Sustainable Plant and Crop Protection. Cham: Springer International Publishing; 2015. p. 29-55.
12. Glazer I, editor GENETIC IMPROVEMENT AND BREEDING OF EPN: THE RACE FOR THE " SUPER NEMATODE". J Nematol; 2014: SOC NEMATOLOGISTS PO BOX 311, MARCELINE, MO 64658 USA.
13. Vaeck M, Reynaerts A, Höfte H, Jansens S, De Beuckeleer M, Dean C, et. al. Transgenic plants protected from insect attack. Nature. 1987;328(6125):33-7. doi: 10.1038/32803